

Mohamed Khider University of Biskra
Faculty of exact sciences, natural
and life sciences
Department of Matter Sciences



جامعة محمد خيضر بسكرة
كلية العلوم الدقيقة وعلوم الطبيعة
والحياة
قسم علوم المادة

A thesis submitted to the graduate faculty
in partial fulfillment of the requirements for the degree of

DOCTOR OF SCIENCES: Chemistry

Specialty:

Materials Chemistry

TITLE

**MANUFACTURE AND CHARACTERIZATION OF POLYVINYL
CHLORIDE / POLYETHYLENE PVC / PE COMPOSITES FOR
STRUCTURAL APPLICATIONS**

Presented by:

MAOU Samira

On: Monday June 6th 2022

Board of Examiners

BEN MYA. O	Prof	University of El-Oued	Chairman
BENCHABANE. A	Prof	University of Biskra	Examiner
OUAHRANI. M. R	Prof	University of El-Oued	Examiner
MEGHEZZI. A	Prof	University of Biskra	Supervisor

DEDICATION

To my mom who passed away

ACKNOWLEDGEMENTS

At the very beginning, I would like to express my deepest gratitude to almighty Allah for giving me the strength and the composure to complete my work and prepare this thesis within the scheduled time. During the period of my scholarship work and coronavirus.

To Prof. **Ahmed MEGHEZZI**, thank you for your guidance and understanding for the past 7 years. Most importantly, I am forever grateful for the trust you had in me during the times I was barely considering pursuing my PhD and made it possible for me to further my studies at UBS University, France. You helped me to bring this journey to the finish line and I am deeply grateful for your advice and patience in the process.

To Prof. **Yves GROHENS**, thank you for all advice and confidence you had in me even during the times I was lost. Thank you for supporting and encouraging me all the way along. You did not only allow me to be a part of your team, but you also helped me in exploring new research areas.

I would also like to thank my committee members, Mr. **Omar Ben Mya**, professor of Process Engineering and Petrochemistry, Mr. **Mohammed Ridha OUAHRANI**, Professor of phytochemistry, University of El Oued, Algeria, and Mr. **Adel BENCHABANE**, Professor of Mechanical Engineering, University of Biskra, Algeria, for serving as my committee members. I also want to thank you for your brilliant comments and suggestions, thanks to you.

To Dr. **Antoine KERVOELEN**, I am so appreciative of not only the way you have given me your generosity with your time and resources, but I express my deepest gratitude for your guidance and support throughout this research in the last few years. You taught me a lot and showed me new perspectives on becoming a better researcher.

To the Ministry of Higher Education and Scientific Research, ALGERIA, thank you for giving me a scholarship of 10 months. To the Center of Christiaan Huygens (IRDL) for funding my research and allowing me to share the knowledge with many researchers and PHD students, thanks for the opportunity, guidance, and continuous motivation to make the Date Palm Fiber-bio composite a success story. To Dr. **Michael CASTRO**, **Françoise PERESSE**, **Anthony MAGUERESSE**, and **Hervé BELLEGOU**, thanks to you for sharing your knowledge and

ideas to be able to integrate the application of this research in the industry and for making my time at UBS university, Lorient, FRANCE a wonderful experience.

To **Dr. Yazid MAFTAH**, who was my biggest supporter, I could not have imagined how my study would have been without your support. Thank you for always being there even during all my life moments to get through difficult times, the past few years were not the same without you here. Thank you for always bringing joy and for being the best friend I could ever ask for.

I would especially like to thank my family, my sweet sister **MANEL**; the big piece of my heart brothers **AYOUB** and **YOUCEF** thank you for keeping me close to your hearts. I am so grateful to my family for their endless support all these years,

Thank you.

TABLE OF CONTENTS	Page
ABSTRACT	ii
ملخص	iii
RESUME	v
NOMENCLATURE	vii
LIST OF FIGURES	viii
LIST OF TABLES	xi
CHAPTER 1. GENERAL INTRODUCTION	1
1.1. BACKGROUND AND MOTIVATIONS	1
1.2. SCOPE AND OBJECTIVES	2
1.3. DISSERTATION OUTLINE	3
REFERENCES	5
CHAPTER 2. LITERATURE REVIEW	6
2.1. NATURAL LIGNOCELLULOSIC FIBER (NLCF _s)-BIOCOMPOSITES	6
2.2. POLYMERS AND BIOCOMPOSITES	7
2.3. NATURAL LIGNOCELLULOSIC FIBER COMPOSITION AND STRUCTURE	8
2.4. DATE PALM FIBERS (DPF _s)	11
2.4.1. Resources of DPFs	11
2.4.2. Characterization of Date Palm Fibers (DPFs)	14
2.4.3. Chemical Composition and Structure of Date Palm Fibers (DPFs)	15
2.4.4. Physical and Thermal Behaviors of Date Palm Fibers (DPFs)	15
2.4.5. Mechanical Properties of Date Palm Fibers (DPFs)	16
2.4.6. Surface Modification of DPFs	17
2.4.6.1. <i>Retting Water</i>	19
2.4.6.2. <i>Alkaline Modification</i>	19
2.4.6.3. <i>Soxhlet Extraction</i>	20
2.4.6.4. <i>Silane Coupling Agents Modification</i>	21
2.4.6.5. <i>Maleated Coupling Agents</i>	22
2.4.6.6. <i>Treatment with Peroxide</i>	22
2.4.7. DPFs Reinforced Polymeric Composites Processing Parameters	23
2.4.7.1. <i>Drying Parameters</i>	23
2.4.7.2. <i>Melt-Mixing</i>	24

2.4.7.3. <i>Extrusion</i>	24
2.4.7.4. <i>Hot Press/Compression Molding</i>	26
2.4.7.5. <i>Injection Molding</i>	28
REFERENCES	30
CHAPTER 3. SYNERGISTIC EFFECTS OF MIXED METAL STEARATE, CALCIUM CARBONATE PARTICLES AND LOW DENSITY POLYETHYLENE ON THE MECHANICAL, THERMAL AND STRUCTURAL PERFORMANCE OF POLYVINYL CHLORIDE MICROCOMPOSITE	
ABSTRACT	39
3.1. INTRODUCTION	40
3.2. EXPERIMENTAL	41
3.2.1. Materials	41
3.2.2. Fabrication of Microcomposites	42
3.2.3. Characterization	42
3.2.3.1. <i>Fourier Transform Infrared Spectroscopy (FTIR)</i>	42
3.2.3.2. <i>Mechanical Tests</i>	42
3.2.3.3. <i>Heat ageing Test</i>	42
3.2.3.4. <i>Investigation of Initial Thermal Stabilization for Microcomposites</i>	42
3.2.3.4.1. <i>Congo red Test</i>	42
3.2.3.4.2. <i>Discoloration Test</i>	42
3.2.3.5. <i>Thermogravimetric Analysis (TGA and DTG)</i>	43
3.2.3.6. <i>Scanning Electron Microscopy (SEM)</i>	44
3.2.3.7. <i>Calculation Details</i>	44
3.3. RESULTS AND DISCUSSION	44
3.3.1. FTIR analysis	44
3.3.2. Mechanical Properties	46
3.3.3. Thermal Stability of PVC and PVC/LDPE Microcomposites	49
3.3.4. Thermogravimetric Analysis (TGA, DTG)	50
3.3.5. Scanning Electron Microscopy (SEM) Results	53
3.3.6. The Results from DFT Calculations	54
3.4. CONCLUSIONS	56
ACKNOWLEDGEMENTS	56
REFERENCES	57

**CHAPTER 4. MECHANICAL AND THERMAL DEGRADATION OF PVC-LDPE
BLENDS REINFORCED BY DATE PALM LEAF FIBER**

ABSTRACT	62
4.1. INTRODUCTION	63
4.2. EXPERIMENTAL DETAILS	64
4.2.1. Materials	64
4.2.2. Date Palm Leaves Fibers Preparation	64
4.2.3. Blend and Composite Preparation	65
4.2.4. Ageing Conditions	65
4.2.5. Characterization	66
4.2.5.1. <i>Mechanical Characterization</i>	66
4.2.5.2. <i>Morphological Analysis</i>	66
4.2.5.3. <i>Thermal Properties</i>	66
4.3. RESULTS AND DISCUSSION	66
4.3.1. Mechanical Results	66
4.3.1.1. <i>Influence of LDPE Content on Mechanical Properties of Blends</i>	66
4.3.1.2. <i>The Mechanical Properties of the Composites</i>	67
4.3.2. Morphological Results	69
4.3.3. Thermal Analysis	70
4.3.3.1. <i>Thermal Analysis of Matrices</i>	70
4.3.3.2. <i>Thermal Analysis of Composites</i>	71
4.4. CONCLUSION	74
ACKNOWLEDGEMENTS	74
REFERENCES	75

**CHAPTER 5. EFFECT OF VARIOUS CHEMICAL MODIFICATIONS ON DATE
PALM FIBERS (DPFS)-PVC-HDPE BLEND COMPOSITES: STRUCTURAL,
MORPHOLOGICAL, THERMAL, MECHANICAL, MECHANICAL-DYNAMICAL,
AND RHEOLOGICAL PROPERTIES**

ABSTRACT	78
5.1. INTRODUCTION	79
5.2. EXPERIMENTAL	80
5.2.1. Raw Materials Used	80
5.2.2. Extraction Procedure of Date Palm Fibers (DPFs)	81

5.2.3. Chemical Composition of the Date Palm Fiber (DPF)	81
5.2.4. Surface Treatment of the Date Palm Fibers (DPFs)	81
5.2.4.1. Alkali Treatment of DPFs	81
5.2.4.2. Silane Treatment of DPFs	82
5.2.4.3. Combined Alkali-silane Treatment of DPFs	82
5.2.4.4. Sodium Chlorite Treatment of DPFs	82
5.2.4.5. Hydrogen Peroxide +Nitric Acid Treatment of DPFs	82
5.2.5. Processing of the Composites	83
5.2.6. Characterizations	84
5.2.6.1. Morphological Properties	84
5.2.6.2. Fourier Transform Infrared Spectroscopy (FTIR)	84
5.2.6.3. Thermogravimetric Analysis (TGA)	85
5.2.6.4. Diffraction Analysis (DRX)	85
5.2.6.5. Mechanical Properties	85
5.2.6.5.1. Tensile Properties	85
5.2.6.5.2. Flexural Properties	86
5.2.6.6. Dynamical Mechanical Analysis (DMA)	86
5.2.6.7. Rheological Measurements	86
5.2.6.8. Water Uptake Test	86
5.3. RESULTS AND DISCUSSIONS	87
5.3.1. Date Palm Fibers (DPFs) Characterization	87
5.3.1.1. Morphological Properties of DPFs	87
5.3.1.2. FTIR Analysis of DPFs	88
5.3.1.3. Thermogravimetric Analysis of DPFs	89
5.3.1.4. X-ray Diffraction Analysis of DPFs	91
5.3.2. Characterization of PVC-HDPE-DPFs Composites	92
5.3.2.1. Morphological Investigation of the PVC-HDPE-DPFs Composites	92
5.3.2.2. Thermal Properties of PVC-HDPE-DPFs Composites	94
5.3.2.3. Mechanical Properties of PVC-HDPE-DPFs Composites	96
5.3.2.4. Rheological Measurements of PVC-HDPE- DPFs Composites	98
5.3.2.5. Dynamic Mechanical Analysis (DMA) of PVC-HDPE-DPFs Composites	100
5.3.2.6. Water Uptake Behavior of PVC-HDPE-DPFs Composites	103
5.4. CONCLUSIONS	106

ACKNOWLEDGEMENTS	106
REFERENCES	107
CHAPTER 6. GENERAL CONCLUSION	
6.1. Conclusion	115
6.2. Future Work	116

ABSTRACT

The research initially studied a safe recycling process that decreases the accumulation of thermoplastic wastes and prevents pollution of the environment. Obtained all composites in these works were analyzed for mechanical, thermal, and morphological dynamical- mechanical and rheological characteristics. This research aims to develop a new polyvinylchloride (PVC) microcomposite that incorporates low density polyethylene (LDPE), calcium carbonate (CaCO_3), and calcium/zinc stearate ($\text{CaSt}_2/\text{ZnSt}_2$). The addition of 5 phr of $\text{CaSt}_2: \text{ZnSt}_2 = 9:1$ into PVC appears to yield an optimal mechanical result and shows high thermal stability. Moreover, when a heat stabilizer rich in calcium is mixed with CaCO_3 and LDPE, an excellent synergistic effect is demonstrated.

The properties of polyvinyl chloride (PVC) and low density polyethylene (LDPE) blends, at three different ratios (20, 50, and 80 wt.%) of renewable LDPE were studied. Besides, Biobased composite with PVC-LDPE blend and date palm fiber as reinforcement at different loading levels (0-30 wt.%) were also investigated. The matrix in which PVC-LDPE (20 wt.%-80 wt.%) had the optimum mechanical and thermal properties. The modulus of the composites is enhanced with increasing DPLF content. Scanning electron microscopic micrographs revealed that morphological properties of fracture surfaces are following the tensile properties of these blends and composites. Thermal analysis showed that the thermal degradation of PVC-LDPE (20 wt.%/80 wt.%) blend and PVC-LDPE-DPLF (10 and 30 wt.%) composites took place in two steps: in the first step, the blend was more stable than the composites. In the second step, the composites showed slightly better stability than the PVC-LDPE (20 wt.%-80 wt.%) blend.

Leaflets and rachis fibers (DPFs) were used as a sustainable reinforcement material to strengthen PVC-HDPE (20:80) biocomposites to further study the feasibility of compounding date palm fiber. As this renewable material used in this project work are crop wastes, the fibers had to be pre-treated to eliminate lignin and impurities for enhancing the interfacial adhesion between matrix and fiber, composites with untreated and treated DPFs containing 30 wt% were produced. Infrared spectroscopy (FTIR), scanning electron microscopy (SEM), and thermogravimetric analysis (TGA) have confirmed the enhancement of surface modification of DPFs from the delignification process to the extraction of cellulose microcrystals (CMCs). Furthermore, structural, morphological, thermal, mechanical, dynamic-mechanical, rheological, and water absorption all improved the biocomposites characteristic performances as a function of the modified DPFs. Hence, the PVC HDPE- HNO_3 F composite reveals a selective advantage to be a good potential candidate for several structural applications.

ملخص

يدرس البحث في البداية عملية إعادة تدوير أمنة تقلل من تراكم مخلفات اللدائن الحرارية وتمنع تلوث البيئة. تم تحليل جميع المركبات التي تم الحصول عليها في هذه الاعمال من حيث الخصائص الميكانيكية، الحرارية، الديناميكية الحرارية و الريولوجية . إن الهدف من هذا البحث هو تطوير مركب جديد من البولي فينيل كلوريد (PVC) يحتوي على البولي إيثيلين منخفض الكثافة (LDPE)، و كربونات الكالسيوم ($CaCO_3$)، وستيرات الكالسيوم / الزنك ($CaSt_2 / ZnSt_2$). يبدو أن إضافة 5 بالمئة من $CaSt_2 : ZnSt_2 = 9 : 1$ في PVC يعطي نتائج ميكانيكية مثالية ويظهر ثباتاً حرارياً عالياً. علاوة على ذلك، عندما يتم خلط مثبت الحرارة الغني بالكالسيوم مع $CaCO_3$ و LDPE، يظهر تأثير تآزري ممتاز.

تمت دراسة خواص مزيج البولي فينيل كلوريد (PVC) والبولي إيثيلين منخفض الكثافة (LDPE) بثلاث نسب مختلفة (20، 50 و 80 % من وزن العينة) من البولي إيثيلين منخفض الكثافة. بالإضافة إلى ذلك، تم اختبار المركب الأخضر مع مزيج PVC-LDPE المعزز بألياف نخيل التمر بنسب مختلفة (10، 20 و 30 بالمئة من وزن العينة). مصفوفة PVC-LDPE (20 % - 80 % من وزن العينة) لها الخواص الميكانيكية والحرارية المثلى. تم تحسين معامل الصلابة للمركبات بزيادة محتوى DPLF. كشف المسح الميكروسكوبي الإلكتروني أن الخصائص المورفولوجية لأسطح الكسر تتوافق مع خصائص الشد لهذه المصفوفات والمركبات. أظهر التحليل الحراري أن التحلل الحراري لمزيج PVC-LDPE (20 % - 80 % من وزن العينة) و (10 و 30 % من وزن العينة) لمزيج PVC-LDPE - DPLF حدث في خطوتين: في المرحلة الأولى، كان مزيج المماكبات أكثر استقراراً من المركبات. في المرحلة الثانية، أظهرت المركبات ثباتاً أفضل قليلاً من مزيج المماكبات PVC-LDPE (20 % - 80 % من وزن العينة).

تم استخدام أوراق وغصن النخيل (الجريد) (DPFs) كمادة تقوية مستدامة لتعزيز المركبات الخضراء (PVC-HDPE 20) (80 % - 20 % من وزن العينة) لمزيد من دراسة قابلية استخدام ألياف نخيل التمر. نظرًا لأن هذه المادة المتجددة المستخدمة في هذا المشروع هي نفايات المحاصيل، فقد كان لابد من معالجة الألياف مسبقاً للتخلص من اللجنين والشوائب لتعزيز الالتصاق البيئي بين المصفوفة والألياف، تم تحضير المواد المركبة مع DPFs غير المعالجة والمعالجة التي تحتوي على 30% من وزن العينة. للتحقيق في أسطح الألياف المعدلة من DPFs. أكد التحليل الطيفي بالأشعة تحت الحمراء (FTIR)، والفحص المجهر الإلكتروني (SEM)، والتحليل الحراري الوزني (TGA) تحسن سطح DPFs ناتج عن عملية إزالة اللجنين حتى إلى استخراج بلورات السليلوز الدقيقة (CMCs). علاوة على ذلك، فإن الخصائص الهيكلية، والمورفولوجيا، والحرارية، والميكانيكية، والديناميك- الميكانيكية، والريولوجية، وامتصاص الماء كلها أظهرت تحسن الأداء للمركبات الحيوية المعززة

ب DPFs المعالجة. ومن ثم، يكشف مركب PVC-HDPE-HNO₃F عن ميزة انتقائية ليكون مرشحاً جيداً للعديد من التطبيقات الهيكلية.

RESUME

Notre recherche a étudiée un processus de recyclage qui diminue l'accumulation de déchets thermoplastiques et empêche la pollution de l'environnement. Tous les composites obtenus dans ces travaux ont été analysés pour leurs caractéristiques mécaniques, thermiques et morphologiques dynamiques mécaniques et rhéologiques. Le but de ce travail est de développer un nouveau micro composite de polychlorure de vinyle (PVC) qui incorpore du polyéthylène à basse densité (LDPE), carbonate de calcium (CaCO_3) et stéarate de calcium / zinc ($\text{CaSt}_2 / \text{ZnSt}_2$). L'ajout de 5 phr de $\text{CaSt}_2 : \text{ZnSt}_2 = 9 : 1$ dans le PVC semble donner un résultat mécanique optimal et montre une stabilité thermique élevée. De plus, lorsqu'un stabilisant thermique riche en calcium est mélangé avec du CaCO_3 et LDPE, un excellent effet synergique est démontré.

Les propriétés des mélanges de polychlorure de vinyle (PVC) et polyéthylène à basse densité (LDPE), à trois rapports différents (20, 50 et 80% en poids) de la partie renouvelable LDPE ont été étudiées. En outre, des composites biosourcés d'un mélange de PVC-LDPE sont renforcés par la fibre de palmier dattier à différents pourcentages de charge (0-30% en poids) ont également été étudiés. La matrice dans laquelle PVC-LDPE (20% en poids - 80% en poids) avait les propriétés mécaniques et thermiques optimales. La contrainte des composites est améliorée avec l'augmentation du contenu de la DPLF. Des micrographies au microscope électronique à balayage ont révélé que les propriétés morphologiques de la surface fracturée sont en accord avec les propriétés de traction de ces mélanges et ces composites. L'analyse thermique a montré que la dégradation thermique du mélange PVC-LDPE (20% en poids / 80% en poids) et des composites PVC-LDPE-DPLF (10 et 30% en poids) se sont déroulés en deux étapes : dans la première étape, le mélange était plus stable que les composites. Dans la seconde étape, les composites ont montré une stabilité légèrement meilleure que le mélange PVC-LDPE (20% en poids - 80% en poids). Sur la base des résultats de cette recherche.

Des folioles et rachis de la palme (FPDs) ont été utilisés comme matériaux de renforcement durables pour renforcer les biocomposites à base de PVC-HDPE (20 :80) afin d'étudier plus profondément la faisabilité du renforcement de la fibre de palmier dattier, comme ce matériau renouvelable utilisé dans ce projet, a été traité pour éliminer la lignine et les impuretés à fin d'améliorer l'adhérence inter faciale entre la matrice et la fibre. Les composites avec les FPDs non traités et traités contenant 30% en poids ont été produits. La spectroscopie infrarouge (FTIR), la microscopie électronique à balayage (MEB) et l'analyse thermogravimétrique (ATG)

ont confirmé l'amélioration de la surface modifiée après le processus de la délignification jusqu'au l'extraction de microcristaux de cellulose (CMC). De plus, les résultats structurelles, morphologiques, thermiques, mécaniques, dynamique-mécaniques, rhéologiques et l'absorption d'eau ont amélioré les performances des biocomposites en fonction des FPDs traités. Par conséquent, le composite PVC-HDPE-HNO₃F se révèle avantageux pour être un candidat potentiel pour plusieurs applications structurelles.

NOMENCLATURE

CMC	Cellulose M icro- C ristal
CMF	Cellulose M icro- F ibril
CNC	Computer Numerical Control milling machine
DPLF	D ate P alm L eaf F iber
DPFs	D ate P alm F ibers
DMA	D ynamical M echanical A nalysis
DFT	D ensity F unctional T heory
DOP	B is (2-ethylhexyl) T erephthalate
FTIR	F ourier T ransform I nfra- R ed Spectroscopy
HDPE	H igh D ensity P olyethylene
LDPE-g-PVC	L ow D ensity P olyethylene G rafted P olyvinyl C hloride
LDPE	L ow D ensity P olyethylene
NLCF	N atural L ignocellulosic F iber
PVC	P olyvinyl C hloride
SEM	S canning E lectron M icroscopy
TGA	T hermo G ravimetric A nalysis
WF	W ood F lour

LIST OF FIGURES	page
CHAPTER 2. LITERATURE REVIEW	
Fig 2.1. The life cycle of biodegradable, NLCFs reinforced composites [8].	7
Fig 2.2. Natural Lignocellulosic fibers (NLCFs), biopolymers and biocomposites [10].	9
Fig 2.3. Structural hierarchy in leaflets and rachis parts of date palm tree (modified from [16]).	10
Fig 2.4. Prices of DPFs compared to other NLCFs [22].	14
Fig 2.5. World production of DPFs compared to other NLCFs [22, 25].	14
Fig 2.6. Chemical bonding of maleated coupling agents with WF [68].	22
Fig 2.7. Extrusion machine.	25
Fig 2.8. Hot Press/Compression Molding.	28
Fig 2.9. Injection Molding machine.	29
CHAPTER 3. APPLICATION 1	
Fig 3.1. FTIR spectra of PVC microcomposites exposed to thermal ageing for t= 360 h under temperature T=100°C:(a) OH water group superposed region, (b) CO carbonyl group superposed region.	45
Fig 3.2. FTIR spectra of PVC-LDPE microcomposites exposed to thermal ageing for 360 h under temperature T=100°C: (a) OH water group region, (b) CO carbonyl group region.	46
Fig 3.3(a). Evolution of the mechanical properties of PVC microcomposites before and after heat ageing.	47
Fig 3.3(b). Evolution of the mechanical properties of PVC-LDPE microcomposites before and after heat ageing.	48
Fig 3.4. (a) Thermal stability time (Congo red test) of PVC microcomposites at 180°C.	50
(b)Discoloration photos of PVC and PVC-LDPE microcomposites at 180°C for 110 min.	
Fig 3.5(a).TGA curves of PVC microcomposites.	51
Fig 3.5(b). DTG curves of PVC microcomposites.	51

Fig 3.5(c). TGA curves of PVC-LDPE blend microcomposites.	52
Fig 3.5(d). DTG curves of PVC-LDPE blend microcomposites.	52
Fig 3.6. SEM images of the fracture surfaces of (a, c) MC4 and (b, d) MC10 microcomposite.	54
Fig 3.7. (a) Optimized geometries of reactants, transition states and products for the thermal dehydrochlorination of PVC with different thermal stabilizers. Distance given in Å. Atom color code: H in white, C in grey, Cl in green, O in red, Ca in yellow and Zn in blue and (b) Relative free energies of the dehydrochlorination process with (blue) CaSt ₂ and (red) ZnSt ₂ at the M06-2X/6-31++G (p, d) level.	55

CHAPTER 4. APPLICATION 2

Fig 4.1. The geometry of the notched specimens for mechanical test.	65
Fig 4.2. Evolution of the tensile strength, the elongation at break, and the modulus of PVC-LDPE with various LDPE content.	67
Fig 4.3. Evolution of the tensile strength, the elongation at break, and the modulus of PVC-LDPE (20/80) with various DPLF content (a) before and (b) after ageing.	68
Fig 4.4. SEM photo micrographs of (a) PVC-LDPE (20/80) C0, (b) PVC-LDPE (50/50), (c) PVC-LDPE (80/20), (d) PVC-LDPE-DPLF (C10), (e) PVC-LDPE-DPLF (C20), and (f) PVC-LDPE-DPLF (C30).	69
Fig 4.5. Effect of LDPE content on (a) TGA and (b) DTG (b) of PVC-LDPE blend.	70
Fig 4.6. Effect of fiber loading on (a) TGA and (b) DTG of PVC-LDPE-DPLF composite.	72

CHAPTER 5. APPLICATION 3

Fig 5.1. The steps of fabrication process of DPFs fibers reinforced PVC-HDPE composites.	83
Fig 5.2. SEM micrograph of (a) raw DPFs, (b) NaOH treated DPFs (c) Silane treated DPFs (d) alkali-Silane treated DPFs (e) Cellulose microfibers (CMFs) (f) Cellulose microcrystals (CMCs).	87
Fig 5.3. FTIR spectra of DPFs before and after various surface fiber modifications.	89
Fig 5.4. Thermal stability of DPFs before and after various surface fiber modifications determined by (a) TGA, (b) DTG.	90

Fig 5.5. X-ray diffraction patterns of DPFs before and after various surface modifications of fibers.	92
Fig 5.6. Scanning electron micrographs of (A) HDPE-PVC, (B) HDPE-PVC-UntF, (C) HDPE-PVC-AlF (D) HDPE-PVC-SiF (E) HDPE-PVC-(Al-Si) F, (F) HDPE-PVC-NaClO ₂ F, and (G) HDPE-PVC-HNO ₃ F.	93
Fig 5.7. Thermal stability of PVC-HDPE and PVC-HDPE-DPFs composites determined by (a) TGA, (b) DTG.	95
Fig 5.8. (a) Tensile results, (b) Flexural results of PVC-HDPE and PVC-HDPE-DPFs composites.	97
Fig 5.9. Complex viscosity, η^* vs frequency, curves of PVC-HDPE and PVC-HDPE- DPFs composites at 170 °C.	99
Fig 5.10. Storage moduli G' vs frequency, curves of PVC-HDPE and PVC-HDPE-DPFs composites at 170 °C.	99
Fig 5.11. Loss moduli G'' vs frequency, curves of PVC-HDPE and PVC-HDPE-DPFs composites at 170 °C.	100
Fig 5.12. (a) Storage modulus (E') curves of PVC-HDPE and PVC-HDPE-DPFs composites as a function of temperature.	102
Fig 5.12. (b) Loss modulus (E'') curves of PVC-HDPE and PVC-HDPE-DPFs composites as a function of temperature.	102
Fig 5.12. (c) Damping factor ($\text{Tan } \delta$) curves of PVC-HDPE and PVC-HDPE-DPFs composites as a function of temperature.	103
Fig 5.13. Water uptake properties of pure blend matrix and DPFs reinforced composites with and without various treatments.	104

LIST OF TABLES **Page**

CHAPTER 2. LITERATURE REVIEW

Table 2.1. Six general types of NLCFs [10].	9
Table 2.2. Chemical composition of some common NLCFs.	11
Table 2.3. Number of DPTs cultivated in the North Africa and Middle East countries [21].	12
Table 2.4. The amount of agricultural waste from DPTs in the Middle East & North Africa region.	13
Table 2.5. Average physical properties of DPFs and other NLCFs adopted from [22,37-39].	16
Table 2.6. Mechanical properties of date palm fiber and other lignocellulosic fibers. [8, 64, 86].	17
Table 2.7. Surface modification conditions for DPFs.	18
Table 2.8. Influence of alkaline modification of date palm fibers and its composites.	20
Table 2.9. Drying parameters of DPFs.	24
Table 2.10. Melt-mixing parameters of DPFs.	24
Table 2.11. Extrusion processing parameters of DPFs.	25
Table 2.12. Hot press/ compression molding processing parameters of DPFs.	27

CHAPTER 3. APPLICATION 1

Table 3.1. Different composition of the PVC and PVC/LDPE microcomposites.	42
Table 3.2. The mechanical results before and after heat ageing of PVC and PVC/LDPE microcomposites.	49
Table 3.3. Interested decomposition temperatures and weight loss levels of PVC and PVC-LDPE microcomposites.	53

CHAPTER 4. APPLICATION 2

Table 4.1. Properties of PVC.	64
Table 4.2. Additives of PVC.	64
Table 4.3. Different compositions and codes of polymer samples.	65
Table 4.4. The temperature of decomposition of PVC-LDPE Samples with different ratio.	71
Table 4.5. The temperature of decomposition of PVC-LDPE-DPLF samples with different ratio.	73

CHAPTER 5. APPLICATION 3

Table 5.1. Some published research studies on treated date palm fibers reinforced Polymer.	80
Table 5.2. Amount of various chemical compounds in untreated and various chemically treated date palm fibers (leaflets and rachis).	83
Table 5.3. The sample code and composition of PVC-HDPE-DPFs composites.	84
Table 5.4. Values of T_{onset} , $T_{10\%}$, $T_{20\%}$, $T_{\text{MAX}1,2,3}$, and % char yield of DPFs surface modifications.	91
Table 5.5. Thermal degradation temperatures, T_{Onset} ($^{\circ}\text{C}$), $T_{10\%}$, $T_{50\%}$, $T_{\text{MAX}1,2}$, and % char yield of PVC-HDPE and its composites.	96
Table 5.6. Mechanical properties of PVC-HDPE and its composites.	98
Table 5.7. Dynamical mechanical properties of PVC-HDPE and its composites.	103

CHAPTER 1. GENERAL INTRODUCTION

1.1. BACKGROUND AND MOTIVATIONS

During the last few years, the quest to make more environmentally safe products has been accelerated as a result of an increase of plastic wastes in nature, landfill site shortage, and overexploitation of fossil fuels. From an environmental point of view, most countries support green and sustainable material research. The government policy in these countries has motivated industry and academia to find and invest in new technology derived from more renewable sources to serve the needs of these markets for biobased materials. Lignocellulosic fibers, by description, represent environmentally raw materials and have evolved as a feasible alternative to synthetic fibers, as well as other inorganic fillers for various applications in the automotive and aerospace industry, building, and packaging materials. Polymer biocomposites are now a large and rapidly developing field of materials engineering, thanks to their significant benefits that make them interesting as a potential replacement for conventional synthetic fibers. Besides, lignocellulosic fibers have benefits of lower cost and energy compared with synthetic fillers such as glass and carbon fibers. In particular, when compared to synthetic fibers, lignocellulosic fibers provide optimally specific physical behaviors, low density, considerably non-abrasive characteristics, CO₂ capture, reusability, and biodegradability.

These characteristics, therefore, make lignocellulosic fibers beneficial as a reinforcement product in a plastic matrix for several applications. The biocomposite industry focuses on finding alternative renewable and biodegradable products such as lignocellulosic fibers that could minimize the weight of products, reduce the use of petrochemicals and reduce the total environmental effect of plastic products [1]. The biocomposite industry focuses on finding alternative renewable and biodegradable products such as lignocellulosic fibers that could minimize the weight of products, reduce the use of petrochemicals and reduce the total environmental effect of plastic products. Lignocellulosic fibers filled polymer plastics have become particularly popular in the industry, where optimal mechanical and physical characteristics should be coupled with lightweight. Simultaneously, these biocomposites will lead to reducing the cost and weight of industrial products. Most of the effective applications in different areas involve sisal, jute, kenaf, aloe vera, cellulose, sawdust wood, date palm fiber, and rice hull [2, 3]. The date palm grove, the pivot of the oasis ecosystem is commonly cultivated in all Saharan countries. Date fruits are considered to be the most important Saharan fruit available commercially in the Middle East. Date palm fiber (DPF) is one of the waste materials in crop production; rachis and leaflets are known as waste materials of date trees and are commonly used for manufacturing lignocellulosic fibers [4-6]. Recovering natural waste

CHAPTER 1. GENERAL INTRODUCTION

requires the investigation of the mechanical, morphological, and thermal performances of these natural wastes to produce sustainable new green composites. This often prevents the risks of burning or allowing the fibers to deteriorate in the process. Moreover, there are concerns about the impact of fiber and low thermal stability which reduces the higher processing temperature (200 °C). Furthermore, the use of natural fibers has weakly interfacial adhesion with polymer matrices. Usually, these limitations may be solved by sufficient fiber chemical modifications and optimization of process conditions. It is therefore important to optimize the method of producing eco-friendly composites with high performance.

This dissertation discusses the feasibility of using this cheap and biodegradable waste material, abundantly present in Algeria, in particular date palm fiber, as a reinforcement of new biocomposites.

1.2. SCOPE AND OBJECTIVES

This project is a sub-part of the PRFU project entitled “Development of composite materials based thermoplastic matrix: Natural renewable resources (date palm fiber) reinforced polyvinyl chloride (PVC) and polystyrene (PS)”, funded by the ministry of higher education and scientific research from Algeria.

The main aims of this work were to develop the expertise to enhance the adoption of lignocellulosic fiber composites from agricultural residues, to supply innovation and advice to several industry applications by increasing the use of durable materials and designing new materials based on polymer matrices.

The thermoplastic thermo-mechanical recycling process is the cheapest way to recover plastic wastes such as PVC and LDPE with lower ecological impact. In the quest for improved PVC microcomposites, the optimization of different additives, such as mixed calcium/zinc stearate, CaCO₃ particles, and LDPE was investigated. On the other side, we carefully studied the dehydrochlorination mechanism using density functional theory and obtained a nice agreement with the experimental findings. To determine the effect of natural waste in the production of green composites. We used this cheap and biodegradable waste material, abundantly present in Algeria, in particular date palm leaf fiber, as a naturally renewable resource and reinforcement of new composites. In particular, the mechanical and thermal properties of Polyvinyl chloride (PVC)/low-density polyethylene (LDPE) blends with varied LDPE concentrations are described. Besides, composite samples that were prepared from PVC/LDPE blend reinforced with date palm leaf fiber (DPLF) were also studied and characterized.

CHAPTER 1. GENERAL INTRODUCTION

To examine the optimization of the influence of DPLF fiber surface treatment, such as alkaline treatment, silane treatment, combined alkaline-silane treatment, sodium chlorite bleaching treatment, and hydrogen peroxide as well as nitric acid treatment, on the morphological, thermal, mechanical, rheological, dynamical mechanical, and water uptake properties of PVC-HDPE- DPFs green composites reinforced with 30 wt.% of date palm fiber. We found that cellulose concentration increases after the aforementioned various treatments leading to good interfacial adhesion between fiber and matrix.

1.3. DISSERTATION OUTLINE

This thesis is organized into six chapters:

Chapter 1 " General Introduction" shows the general context and describes the particular concerns that need to be discussed to extend the use of date palm fiber biocomposites in several industrial applications. It also defines the scope and the key goals of the study.

Chapter 2 " Literature Review" presents an overview of the previous work on lignocellulosic composites, focusing on the characteristics of eco-friendly composites. A review of the current state-of-the-art lignocellulosic composites in several applications is also presented. The following three chapters consist of three manuscripts prepared for publication in high-impact journals. The first paper has been published in the journal of vinyl and additives technology in October 2018, while the second paper was submitted to the Journal of Material Cycles and Waste Management in September 2021. The third has been published in the Journal of Industrial Crops and Products in August 2021.

Chapter 3 " Synergistic effects of mixed metal stearate, calcium carbonate particles and low density polyethylene on the mechanical, thermal and structural performance of polyvinylchloride microcomposite." examines the introduction of heat stabilizers (Ca/Zn) and calcium carbonate (CaCO_3) into the polymer blends composite of polyvinyl chloride (PVC) and Low-density polyethylene (LDPE) for many applications. This chapter also evaluates the loading level optimization of the additives to improve mechanical and thermal performances.

Chapter 4 " Mechanical, Morphological, and Thermal Properties of Polyvinyl chloride/Low density polyethylene composites filled with Date palm leaf fiber" evaluates the influence of date palm leaf fibers to design new green composites that can be used in a range of applications, in a particular construction [5].

CHAPTER 1. GENERAL INTRODUCTION

Chapter 5 " A new study on the effect of various chemical modifications on date palm fiber-filled PVC-HDPE blend composites: Structural, morphological, thermal, mechanical, mechanical dynamical, and rheological properties" reports on studies of the effects of surface treatments on date palm fiber to enhance the interfacial adhesion between fiber and matrix [6].

Finally, **Chapter 6** " General conclusions & Future Work" lists the main findings of the thesis, and suggestions for future studies for the development of date palm fiber eco-friendly composites for other applications are provided.

CHAPTER 1. GENERAL INTRODUCTION

REFERENCES

1. U.S. Environmental Protection Agency. Recycling and Reuse: End-of Life-Vehicles and Extended Producer Responsibility: *European Union Directive*. 2016. Available online: https://archive.epa.gov/oswer/international/web/html/200811_elv_directive.ht (Accessed on 20 February 2018).
2. Holbery, J.; Houston, D. Natural-fibre-reinforced polymer composites in automotive applications. *J. Miner. Met. Mater. Soc.*58, 80–86 (2006).
3. Huiqin, W. 2011 engineering plastics sector to see increase of 10.93%. 2012. Available Online: http://en.ce.cn/Insight/201202/01/t20120201_23034917. (Accessed on 18 February 2018).
4. Ahmad, F.; Choi, H.S.; Park, M.K. A review: Natural fiber composites selection in view of mechanical, lightweight, and economic properties. *Macromol. Mater. Eng.* 300, 10–24 (2015).
5. Maou, S.; Meghezzi, A.; Nebbache, N.; Meftah, Y. Mechanical, morphological, and thermal properties of poly (vinyl chloride)/low-density polyethylene composites filled with date palm leaf fiber. *J Vinyl Addit Technol.* 25: E8–E93. [https:// doi. org/ 10. 1002/ vnl. 21687](https://doi.org/10.1002/vnl.21687) (2019).
6. Maou, S. ; Meghezzi, A. ; Grohens, Y. ; et al. Effect of various chemical modifications of date palm fibers (DPFs) on the thermo-physical properties of polyvinyl chloride (PVC) – high-density polyethylene (HDPE) composites. *Ind Crop Prod.* 171 :113974. [https:// doi. org/ 10. 1016/j. ind crop. 2021. 113974](https://doi.org/10.1016/j.indcrop.2021.113974)(2021).

CHAPTER 2. LITERATURE REVIEW

2.1. NATURAL LIGNOCELLULOSIC FIBERS (NLCFS)-COMPOSITES

The use of natural fiber with another product to form composite materials is not a recent development and has been used for decades, like clay filled with straw for applications in ancient Egypt around 4000 B.C [1]. Natural wastes have also been used to produce doors, ropes, beds, packaging for decades. With the rapid growth of fossil fuel products in the 19th and 20th centuries and the manufacturing of more resilient substances i.e., metals, the usage of natural materials disappeared as man-made products were easier to design, biodegradable, high yield and even low cost [2]. Besides that, growing environmental consciousness, industrial pollution issues, the implementation of environmental policies and legislation are interested in increasing demand for sustainable power in numerous sectors. Composites reinforced natural wastes are becoming a rapidly growing field of materials science.

The abundant natural resources, as well as other abundantly available crop production residues, offer impetus for new research into sustainable technology in polymer science and engineering. Agricultural materials are the basis for new manufacturing products to be produced from renewable technology. Agricultural wastes have traditionally been used for different purposes, based on their nature. Examples include leather, ropes, wool fibers, textile products and geotextiles, insulation fabrics, nonwoven products and, more recently, plastic reinforcements [3-7].

The main objective of the introduction of natural wastes would be to incorporate low-cost and lightweight products by replacing conventional high-density additives. Natural Lignocellulosic fibers (NLCFs) have a lower density ($1.2\text{--}1.6\text{ g/cm}^3$) than synthetic fibers ($2.4\text{--}2.7\text{ g/cm}^3$) that enable the development of lightweight composite materials while retaining higher specific mechanical properties comparison with synthetic fiber. These polymer composites display several more benefits compared with synthetic fibers, such as flexibility during the manufacturing process, low equipment wear, low prices, suitability, and renewability [9]. The objective of this report is to provide a global overview and to incorporate NLCFs composites, in particular, date palm fiber, which is the key focus of this project. The life cycle of these fibers in all walks of life is seen in Figure 2.1.

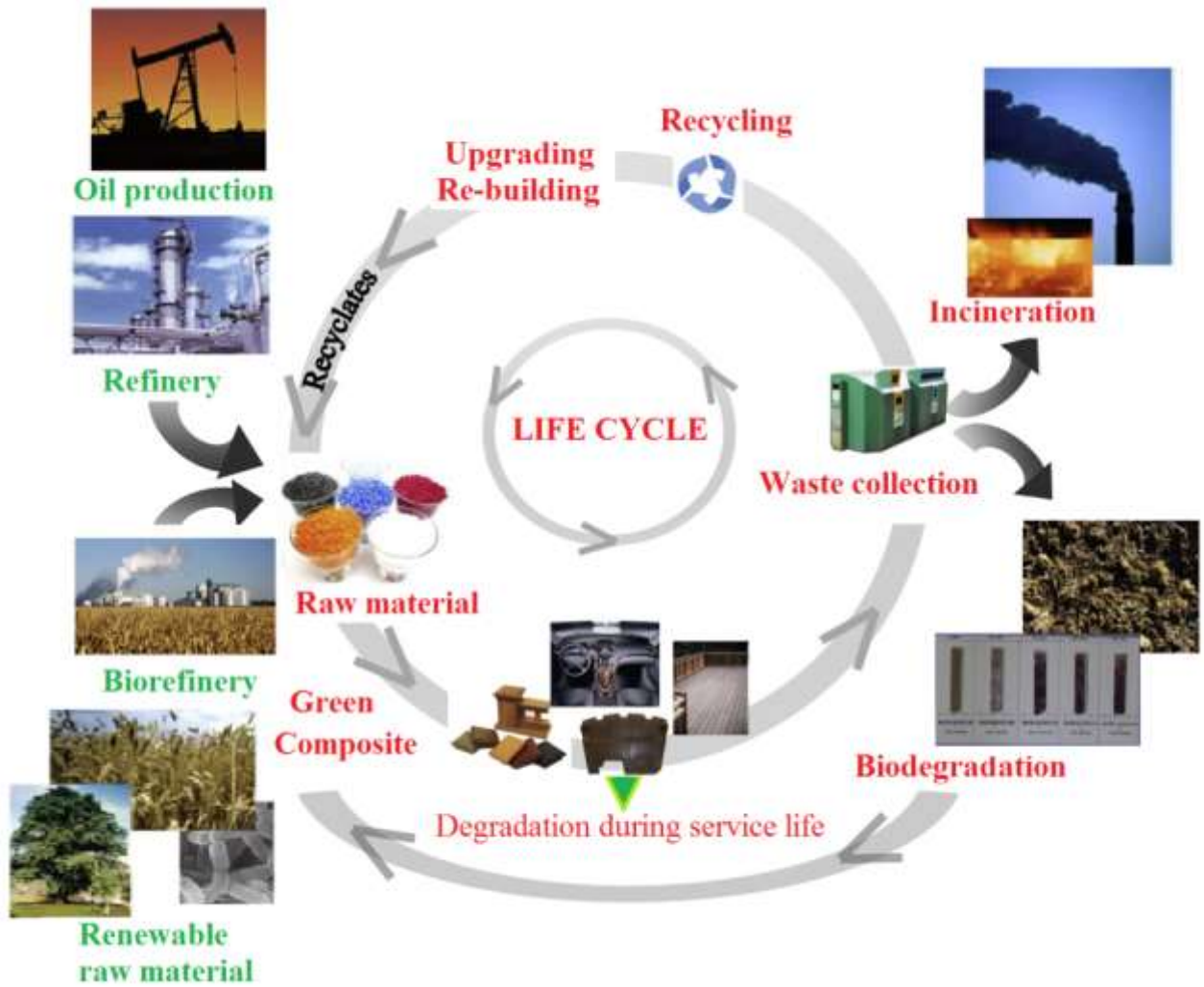


Fig 2.1. The life cycle of biodegradable, NLCFs reinforced composites [8].

2.2. POLYMERS AND BIOCOMPOSITES

Biopolymers and fossil fuel polymers are popular matrices for biocomposite systems. Fossil fuel materials represent the overwhelming majority of matrices used for natural waste bio-products including commodity thermoplastics (polyethylene, polystyrene, polyvinyl chloride) and thermosets (polyester, epoxy, vinyl esters) widely used in modern applications. Biopolymers widely include using cellulose polymeric materials, starch polymers, and protein as well as vegetable oil materials. Biocomposites are commonly classified as composite products composed of a mixture of agricultural waste and fossil fuel polymers such as polystyrene (PS), low-density polyethylene (LDPE), high-density (HDPE), polyethylene, polyvinyl chloride (PVC), or biomaterials such as Polyhydroxybutyrate (PHB), polyhydroxyalkanoate (PHA) and polylactic acid (PLA). Products produced by biobased

CHAPTER 2. LITERATURE REVIEW

polymers and glass or carbon fibers, also incorporate elements of biocomposites [7]. Biocomposites generated through biobased plastics and natural fibers are typically referred to as environmentally friendly or "green composites." It is significant to mention that not every biopolymer is decomposable and also some fossil fuel polymers can indeed be decomposable through microorganisms, photodegradation, oxo-degradation and hydrolysis.

Biodegradable plastics are generally described as plastics that conduct a method of decomposition generated by microorganisms in the anaerobic process of digestion. The system of decomposition is strongly connected to the molecular polymer structure and is separated from the origin of the substance. Soy oil-based resins and biopolymers are non-biodegradable materials. In comparison, poly(ϵ -caprolactone) and aliphatic polyesters are typical types of fossil fuel materials as biodegradable matrices [10]

Hybrid biocomposites involve a mixture of natural fibers and a polymer matrix. Thermoplastic polymer or a mixture of both seems to be of specific importance to the synergistic system of polymer matrices as they can provide exciting low prices and provide a balance between petroleum plastic matrices and fully biomaterials by reducing the moisture and/or water uptake and enhancing the mechanical behaviors [6]. An overview of the composites based natural fibers types and their linked compounds are presented in Figure 2.2.

2.3. NATURAL LIGNOCELLULOSIC FIBERS COMPOSITION AND STRUCTURE

NLCFs are classified on the principle of their nature, whether they are generated from crops, animals, and minerals. The most important category of natural fibers is the botanical kind, which includes stems, branches, seeds, fruits, wood, and trunks, as seen in Table 2.1. The composition and properties of the fibers are influenced by different conditions, i.e., through the ecosystem, aging, and chemical modification. Real fibers consist mainly of cellulose chains, hemicelluloses, lignin, pectin, and waxes [12–15]. Cellulose chains are considered to be a linear homopolymer of D-glucopyranose ($C_6H_{11}O_5$) which are linked by α -1, 4 glycosidic with high crystallinity degree, which is also the essential design part of the walls of cells (Figure 2.3). Hemicelluloses are composed of hexoses and pentoses (from five to six carbon sugars). Hemicellulose compounds are bound together through the glycosidic and hydrogen bonding system of fiber cellulose and are attainable to chemical and physical treatments. Lignin

CHAPTER 2. LITERATURE REVIEW

is an amorphous part of NLCFs structure and a strong constituent that penetrates the fibrils during growth [11].

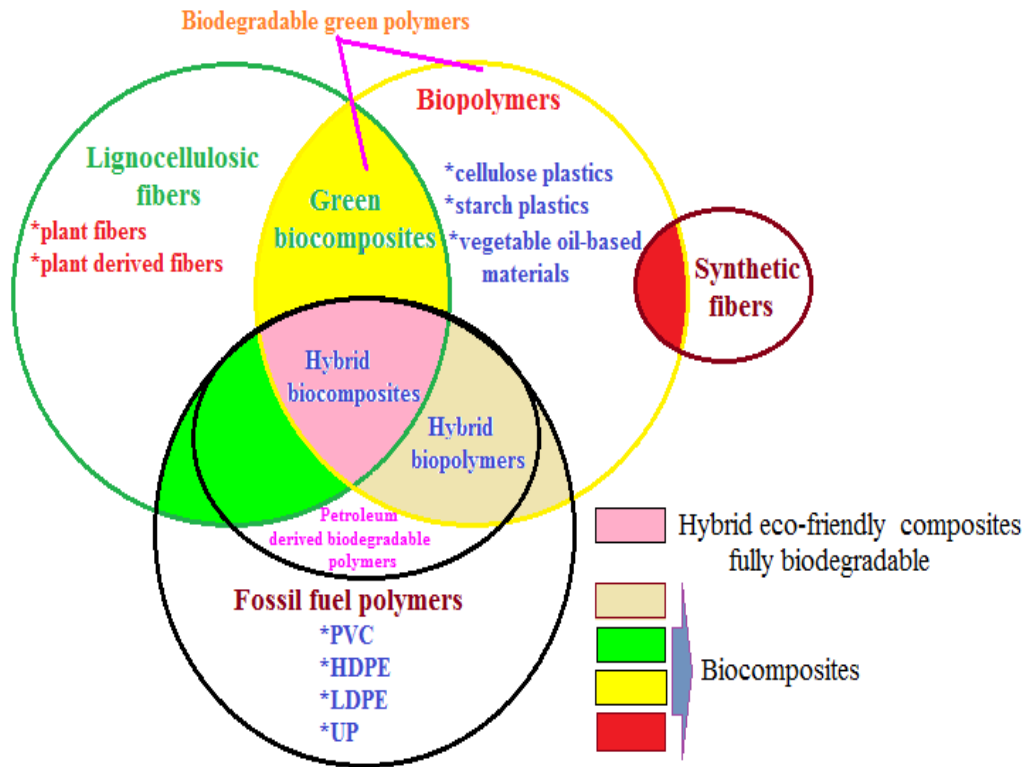


Fig 2.2. Natural Lignocellulosic fibers (NLCFs), biopolymers and biocomposites [10].

Table 2.1. Six general types of NLCFs [10].

Bast	Leaf	Seed				Hulls	Core	Grass	Others		
		Fibers	Pod	Husk	Fruit						
Hemp	Pineapple	Cotton	Kapok	Coir	Oil palm	Rice	Kenaf	Wheat	Wood		
Ramie	Sisal		Loofah			Oat		Jute		Oat	Roots
Flax	Date palm		Milk weed			Wheat		Hemp		Barley	Date palm
Kenaf	Agave					Rye		Flax		Rice	
Jute	Henequen					Wheat				Bamboo	
Mesta	Curaua									Bagasse	
Urena	Banana					Corn					
Roselle	Ababca					Rape					
Flax	Palm					Rye					
	Cabuja					Esparto					
	Albardine		Sabai								
	Raphia		Canary								

CHAPTER 2. LITERATURE REVIEW

The chemical composition of the natural fibers varies from different plant species and in various areas of the same plant. Table 2.2 lists the chemical composition and also the configuration of natural lignocellulosic and synthetic fibers.

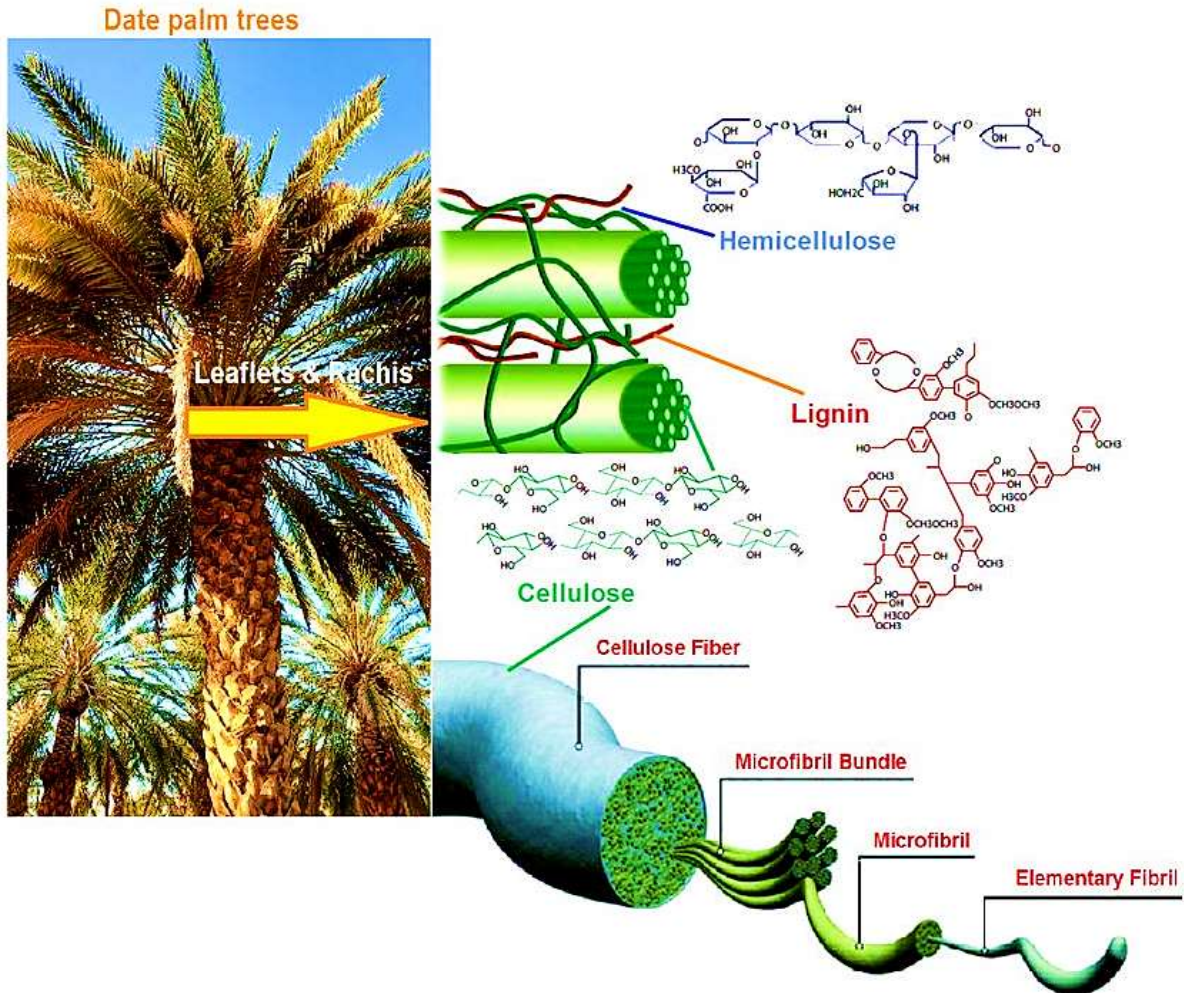


Fig 2.3. Structural hierarchy in leaflets and rachis parts of date palm tree (modified from [16]).

Table 2.2 indicates the range of chemical compositions for a wide range of NLCFs types that are typically non-abrasive while blended in industrial blending and molding instruments, which might lead to considerable machine repair cost reductions. They still provide safer processing and working conditions in comparison with synthetic fillers, such as glass fibers. During the manufacturing of natural fibers, these latter provide safer working conditions than glass fibers and thus decrease the risk of subcutaneous or breathing complications and a significant feature of natural fibers is their favorable environmental impact in comparison to synthetic fillers.

CHAPTER 2. LITERATURE REVIEW

Natural fibers are green products where they are eco-friendly materials and where their processing needs minimal energy.

Table 2.2. Chemical composition of some common NLCFs.

Fiber	Cellulose (wt%)	Hemicellulose (wt%)	Lignin (wt%)	Waxes (wt%)
Abaca	56-63	20-25	7-9	3
Bamboo	55.2	30	21-31	-
Coir	32-43	0.15-0.25	40-45	-
Date palm fiber	41.1	24.66	26.91	14.61
Mesh	43.71	18.66	29.43	11.11
Rachis	39.93	26.48	25.20	14.81
Leaflets	40.21	20.05	25.19	13.99
Midribs	45.66	25.65	28.85	5.27
Trunk	36.02	32.45	25.90	20.2
Bagasse	55.2	16.8	25.3	-
Flax	71	18.6-20.6	2.2	1.5
Oil palm	65	-	29	-
Pineapple	81	-	12.7	-
Rice husk	35-45	19.25	20	14-17
ramie	68.6-76.2	13-16	0.6-0.7	0.3

2.4. DATE PALM FIBERS (DPFs)

2.4.1. Resources of DPFs

The date palm trees (DPTs) which refer to the Palmae (Arecaceae) family have been planted in tropical and subtropical regions since prehistoric times for their nutritious sweet fruits recognized as dates. While its exact country of origin is unknown, it is believed that it originated in important points between Egypt and Western Asia [17–20], this type is grown in five continents but extensively around North Africa and Middle East countries such as Algeria, Tunisia, Sudan, Saudi Arabia, Iraq, Pakistan, United Arab Emirates (UAE) and Iran. The total

CHAPTER 2. LITERATURE REVIEW

number of date palm trees planted in the Arab countries according to the count of the Arab Organization for Agricultural exports in 2015 is seen in table 2.3.

Table 2.3. Number of DPTs cultivated in the North Africa and Middle East countries [21-22].

Country	Number of trees ($\times 1000$)	Country	Number of trees ($\times 1000$)
Egypt	14.96	Libya	2100.00
Algeria	15508.59	Morocco	4954.13
Saudi Arabia	12000.00	Kuwait	312.21
Iraq	10475.00	Yemen	4623.00
UAE	16757.94	Sudan	2646.00
Oman	6383.00	Qatar	517.16
Tunisia	3335.80	Jordan	332.64
Bahrain	376.70	Mauritania	600.00
Syria	68.60	Palestine territories	301.20

Phoenix dactylifera L, is known to become the most planted kind of the date palm tree and is known to become the tallest of its type with a length of much more than 30 m and a fruit dimension about of 10 mm \times 40 mm [16]. DPTs develop in the sand and salinity soil where water is near the surface caused by air gaps in their roots. In addition, these trees do not need a significant amount of water [18,23].

In fact, humidity significantly influences the value of the fruit, as high moisture contributes to fracturing and throwing away of fruit, the proportion of waste materials generated by different sections of the date palm tree per country can be determined in Table 2.4. It could be found that the overall quantity of crop waste generated yearly in the Middle East and South Africa region can range between 2.6 and 2.8 million tonnes. It is also important to find creative ways of valuing this available green resource [24]. One of these innovations that has already been applied on a fundamental research study is to produce novel products from date palm fiber wastes using various extraction techniques such as biological, chemical, or physical methods and then for using these extracted fibers in the reinforcement of thermoplastic and thermoset composites that are able to be implemented for several industrial innovations.

CHAPTER 2. LITERATURE REVIEW

Table 2.4. The amount of agricultural waste from DPTs in the Middle East & North Africa region.

Country	Amount of agricultural waste from DPT (tons)				
	Midribs	Leaflets	Spadix stems	Mesh	Date palm pits
Egypt	146.6	119.7	104.7	19.4	2202.9
Algeria	151984.2	124068.7	108560.1	20161.2	15941.4
Saudi Arabia	117600.0	96000.0	84000.0	15600.0	105855.9
Iraq	102655.0	83800.0	73325.0	13617.5	75476.1
UAE	164227.8	134063.5	117305.6	21785.3	61881.8
Oman	62553.4	51064.0	44681.0	8297.9	47528.6
Tunisia	32690.8	26686.4	23350.6	4336.5	36091.7
Bahrain	3691.7	3013.6	2636.9	489.7	26000.0
Syria	672.3	548.8	480.2	89.2	1050.1
Libya	20580.0	16800.0	14700.0	2730.0	430.9
Morocco	48550.5	39633.0	34678.9	640.4	210.0
Kuwait	3059.7	2497.7	2185.5	405.9	12956.2
Yemen	45305.4	36984.0	32361.0	6009.9	8739.1
Sudan	25930.8	21168.0	18522.0	3439.8	4761.5
Qatar	5068.2	4137.3	3620.1	672.3	43935.5
Mauritania	5880.0	4800.0	4200.0	780.0	2522.2
Palestine territories	2951.8	2409.6	2108.4	391.6	4396.7
Total	796807.9	650455.4	569148.5	105699.0	596021

Besides that, the low price per kilogram (kg) of DPFs and their availability widely are known to be important factors for their uses in various industries. DPFs are known as one of the lowest price natural fibers and most available caused by a significant percentage of date palm trees available in the world According to AL-Oqla and Sapuan, and Asim et al. Figures 2.4 and 2.5 presented the difference in cost and availability of DPFs and other NLCFs respectively [22, 25].

CHAPTER 2. LITERATURE REVIEW

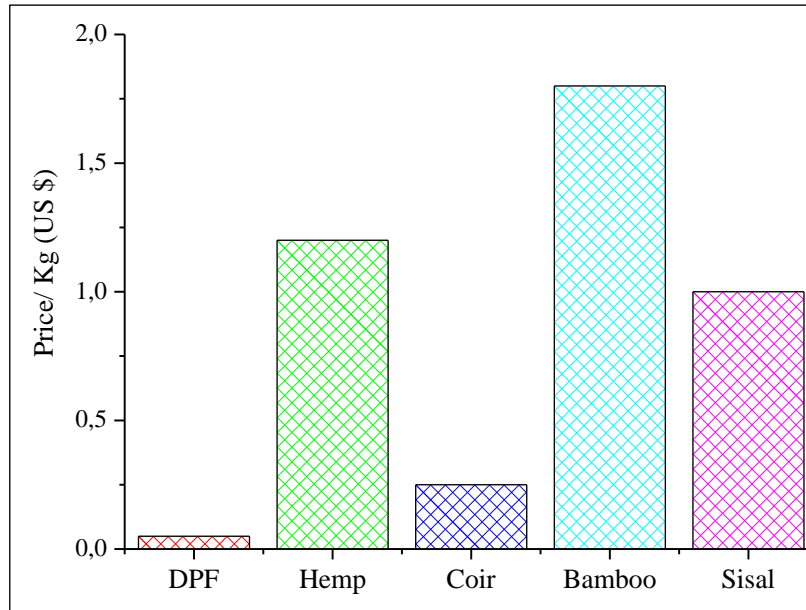


Fig 2.4. Prices of DPFs compared to other NLCFs [22].

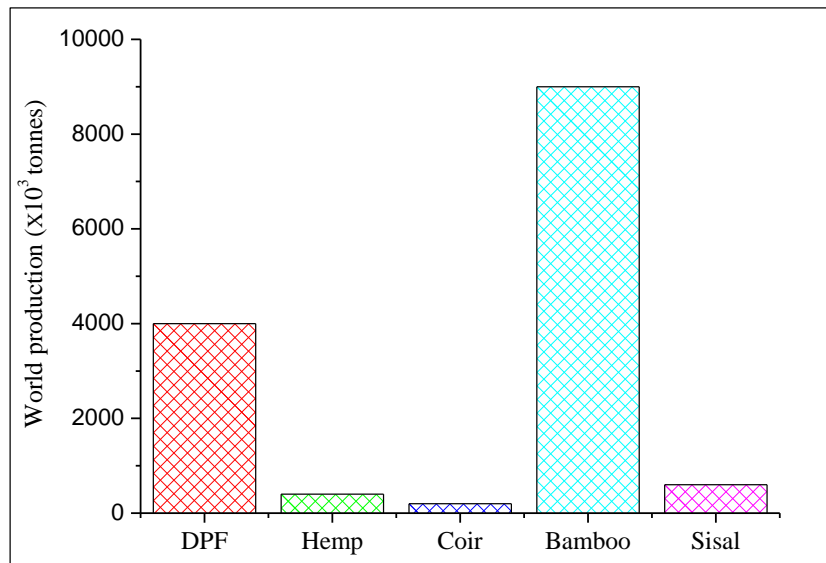


Fig 2.5. World production of DPFs compared to other NLCFs [22, 25].

2.4.2 Characterizations of Date Palm Fibers (DPFs)

The use of date palm fibers (DPFs) for industry sectors as a filler in polymeric matrices is a significant novel technology. Therefore, in order to consider the drawbacks and benefits of date palm fiber composite materials, it is important to understand the chemical, electrical, mechanical and thermal properties of DPFs. The study on DPFs and their composite materials

CHAPTER 2. LITERATURE REVIEW

began in 2004, but these characteristics are not yet strongly defined. Many researchers were carried out and published on DPFs chemical, physical, mechanical and thermal characteristics is therefore evaluated and mentioned by several reports [26, 28, 29].

2.4.3 Chemical Composition and Structure of Date Palm Fibers (DPFs)

Worldwide, each region has varying climates and geographical environments that have an effect on the composition and properties of NLCFs [28]. It is also often revealed that the percentage sum of chemical components cannot be up to 100%. This is demonstrated by the fact that there are many components inside the fibers that have not been identified to a measurable amount. In addition, comprehending the chemical structure of DPFs is important for determining their potential application to diverse applications, especially in the development of date palm fiber composite materials. DPFs compose of micro cellulose fibrils incorporated in the lignin molecular chains which are identified to be the most significant elements in the fiber structure with high mechanical properties and stability [29-31].

The aspect and crystalline nature of cellulose established by the hydrogen bonding in it controls the physical behaviors of date palm fiber. Cellulose is resistant to chemical treatments such as acid hydrolysis by acid, bleaching, and also alkaline solutions. It deteriorates to some degree when applied various chemical modifications for a long time [29, 46, 55]. In addition, hemicelluloses are polysaccharides connected together through comparatively short branching chains that are deeply connected to microfibrils of cellulose (CMFs). They have got hydrophilic nature, with an average molecular weight smaller than cellulose structure [28]. On the other hand, lignin is an aromatic material that offers stiffness to agricultural materials and helps move water. It is hydrophobic in nature, withstands most assaults by microorganisms and also hydrolysis, it is normally dissolvable in alkaline solution, quickly oxidized, and readily condensed with phenol [30]. Lignin, proteins, and waxes can be eliminated by several treatments such as retting to enhance interfacial adhesion (fiber/matrix) [26].

2.4.4. Physical and Thermal Behaviors of Date Palm Fibers (DPFs)

Physical characteristics of DPFs are important in achieving their qualification for diverse applications in relation to the growth of DPFs-composites which depending on the type of fiber. The dimensions, density and aspect ratio of date palm fiber are known to be essential physical characteristics [22, 32, 33]. Date palm fiber density was estimated by a number of experts and

CHAPTER 2. LITERATURE REVIEW

it was lower than most other NLCFs such as sisal, cotton, hemp, and coir, this may contribute positively in the sector of biocomposites development [22, 23, 32, 34], which may be ideal for aerospace and automotive applications [1]. Table 2.5. showed physical characteristics of date palm fibers, and comparison between DPFs and other NLCFs with respect to their physical characteristics [22].

Table 2.5. Average physical properties of DPFs and other NLCFs adopted from [22,37-39]

Fiber type	Density (g/cm ³)	Length (mm)	Diameter (μm)	Specific modulus (approx)	Thermal conductivity (W/mK)
DPF	0.93	20-150	100-1000	7.00	0.083
Rachis	0.75	1.9	600-750	70.00	-
Leaflets	0.83	4.70	435.2-900	10-93	-
Mesh	0.79	15-60	200-800	10.80	-
Petiole	0.86	1.00	400-1000	18.75-300	-
Hemp	1.45	5-55	25-500	40.00	0.115
Coir	1.20	20-150	10-650	4.00	0.047
Sisal	1.40	1-900	8-200	17.00	0.070

The thermal behaviors of date palm fibers are important in evaluating their qualification for insulating materials provided by their inherent Physico-chemical characteristics. Al-Juruf et al. investigated that date palm fibers can establish composites with a low thermal conductivity that might be used to improving thermal insulation products to enhance comfort thermal conditions [36].

2.4.5. Mechanical Properties of Date Palm Fibers (DPFs)

The mechanical characteristics of date palm fibers are influenced by a range of factors, such as microstructure and dimensions, chemical composition and microfibrillar angle. This latter must be highlighted for its influence on the mechanical characteristics of date palm fibers [35, 26, 27, 29, 40]. Many researchers investigated that the narrower the angle, the hardness of the date

CHAPTER 2. LITERATURE REVIEW

palm fiber increases. Typically, date palm characteristics such as (tensile, flexural) strength, and modulus, increase dramatically as cellulose content and/ or cell microfibril length increase [31, 41]. The mechanical characteristics of DPFs and some LCFs are seen in Table 2.6.

Table 2.6. Mechanical properties of DPFs and other NLCFs [42, 39, 43].

Fibre type	Tensile Strength (MPa)	Elongation at break (%)	Young's Modulus (GPa)
DPF	58–309	5.0–19.0	2.0–7.5
Coir	106–220	15.0–47.0	4.0–6.0
Kenaf	250–930	1.2–7.5	4.3–53.0
Cotton	287–800	7.0–8.0	5.5–12.6
Hemp	350–1,100	1.6–8.1	30.0–70.0
Bamboo	140–740	2.0	11.0–50.0
Abaca	400	3.0–10.0	12.0
Sisal	300–700	2.0–15.0	9.0–38.0
Flax	600–2,000	1.0–4.0	12.0–85.0

2.4.6. Surface Modification of Date Palm Fibers (DPFs)

DPFs are susceptible to moisture because of the existence of hydroxyl groups inside their molecular structure [32]. In order to improve the properties of DPFs-composites, it is also important to transmit hydrophobicity to date palm fibers by modifying the fiber surface chemically, physically and/or mechanically for enhancing the interfacial adhesion between fibers and matrix material [35]. It is interesting to note that only one research has been reported on the physical modification of DPFs surface used corona modification [44]. The surface modifications of DPFs investigated by many researchers were presented in Table 2.7.

CHAPTER 2. LITERATURE REVIEW

Table 2.7. Surface modification conditions for DPFs.

Fiber type	Treatment type	Additives	Solution wt%	Drying dur (h)-temp (°C)	Soaking temp (°C)-time (h)	Ref
Leaf-Rachis	Alkali	NaOH	8, 12	-, -	100, 2-3	[45]
		Ca(OH) ₂	12			
Leaf	Soxhlet extraction	Ethanol/ Toluene	1 :2 (v/v)	24,105	-,24	[46]
		Commercial detergent	N. S			
Mesh	Alkali	NaOH	5	NS, NS	100, 2	[47]
		Dioxin solution	N.S			
Leaf	Soxhlet extraction	Acetone/ Ethanol	75:25	2, 8	-, 24	[48]
		Acetic anhydride & maleic anhydride	-			
Mesh	Soxhlet extraction	Toluene:Methanol:Acetone	4:1:1	24, 60	NS, 24	[49]
N.S	Chlorination	Carbon tetrachloride	N.S	24, 60	25, 1	[50,56]
	Alkali	NaOH	2			
	Silane	Silane	1			
Leaf	Retting	Water	2, 5			[51]
Spadix stems	Alkali	NaOH	2.5	24, Room temp	23, 2-4-6-24	[52]
	Acid	Acetic acid	N. S			
Leaf	Soxhlet-extraction	-Acetone/Methanol	75 :25	N.S, N. S	NS, 24	[53]
	Catalytic-oxidation	-TEMPO, NaBr-2H ₂ O, NaClO ₂	0.3, 0.9, 1.6			
Midribs	Acid	NaCl	-	-, -	-, 48	[57]
	Water	Cold water	-			
		Boiling water	5			
Mesh	Water	Hot water	1	24,70	50, 0.5	[54]

CHAPTER 2. LITERATURE REVIEW

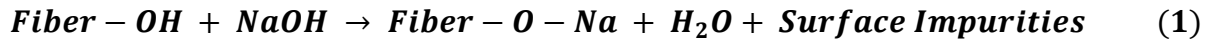
2.4.6.1. Retting Water

The water retting technique is a technique of extracting cellular tissues and impurities from the surface of natural fibers using moisture and microorganisms [58]. Besides that, as a treatment or pre-treatment process for natural fibers, it has not been commonly used. This may be due to the lengthy treatment duration (7–14 days) needed to facilitate water penetration into the plant and crack the outer coating layer, allowing a bacterial colony to form and improve water uptake [59]. In addition, the length of treatment is dependent on a number of factors, including the type of microorganism colony, the type of water, and the temperature of the bath. Even so, as opposed to other treatment methods, such as chemical and physical modifications, water retting is both environmentally sustainable and cheaper [58, 60]. Few researchers have documented immersing DPFs in water for a few days as a pre-treatment before any kind of chemical modification. Partially extracting lignin, hemicelluloses, and other constituents from DPFs was made possible by the water retting process [61-62]. More study on the water retting process, however, is needed because the impact of this process on DPFs physical, mechanical, and chemical properties has yet to be studied.

2.4.6.2. Alkaline Modification

Alkaline modification of the DPFs is among the most commonly used chemical treatment methods due to its simplicity, efficiency in surface modification, and even its low cost. Alkaline modification extracts lignin partially and removes waxes and other substances that coat the external surface of the fiber and reveals the hollocellulose. Furthermore, some quantity of hemicelluloses is eliminated which provides the opportunity for the fibrils to reorganize themselves in the position of tensile strain. On the other hand, alkaline modification decreases the hydrogen bonding in the date palm fiber structure which enhances the ionization of the hydroxyl group and transforms it into Alkoxide [63, 64]. Therefore, the surface roughness of the fiber increases, producing many holes on the surface topography of the fibers, which enhances the interfacial bonding between fiber and matrix. Nevertheless, as DPFs are subjected to the high concentration of sodium hydroxide for a long time period, the fibers begin to deteriorate, resulting in weakened and destabilized fiber, leading to a reduction in the mechanical and thermal properties of the composite. The main disadvantage to using alkaline treatment is it's not an ecological procedure. Equation 1 reveals chemical reaction between NaOH and DPFs.

CHAPTER 2. LITERATURE REVIEW



The treatment parameters and effect of NaOH treatment on various part of DPT fibers is summarized in Table 2.8.

2.4.6.3. Soxhlet Extraction

Soxhlet extraction is an ancient technique of solid materials extraction in which different solvents, like dichloromethane and hexane, or their mixtures with various percentages, including hexane with acetone and/or dichloromethane.

Table 2.8. Influence of alkaline modification of date palm fibers and its composites.

Fibre	NaOH (wt%)	Soaking time (h)	Soaking Temp (°C)	Results	Ref
Leaf	8- 12	2- 3	100	12wt% alkaline concentration with 3(h) immersion time easily enhanced the removal partially of lignin and other residues.	[45]
Mesh	5	2	100	NaOH treatment enhanced the flexural strength by 24% and the impact resulted by 71% of the advanced composite.	[47]
Mesh	2	24	N.S	The Young's Modulus, tensile strength and elongation at break enhanced by 32%, 47% and 25% respectively.	[49]
N.S	2	1	25	Alkaline treatment flowed silane coupling agent, enhance the dynamical mechanical properties	[50]
Spadix stems	2.5	2- 4- 6 - 24	23	Optimal mechanical values were resulted at 2 h and 4 h at Alkali solution concentrations of 2% and 5% respectively.	[52]
Mesh	0.5- 1- 1.5- 2.5- 5	1	100	Alkaline modification gave a positive effect on the mechanical properties of date palm fiber.	[43]
Mesh	3- 6- 9	24	R.T	6 w% was the optimum concentration, whereas 9% alkaline treatment destabilized and deteriorate the fibers.	[65]

CHAPTER 2. LITERATURE REVIEW

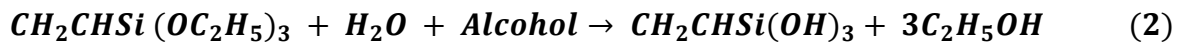
Mesh	6	24	R.T	6 w% decreased of the porosity and improved the interfacial adhesion between the matrix and fibers	[66]
------	---	----	-----	--	------

Table 2.8.(continued)

The main drawbacks of the Soxhlet extraction process are the substantial volumes of solvents that are used usually long process times, more than 24 h [37, 49]. The previous researches indicate that few works of Soxhlet extraction were used to modify date palm fiber surface. The process occurred for up to 24 hours without determining the solution temperature. Fibers modified by the Soxhlet treatment using toluene, methanol and acetone with a 4:1:1 ratio respectively yields optimal results for the mechanical properties of DPF-composites compared to others [49].

2.4.6.4. Silane Coupling Agents Modification

Silane is a chemical molecule with the formula SiH_4 that is used as a bonding agent to enhance interfacial adhesion between natural fiber and matrix. The number of cellulose hydroxyl groups in the DPF/matrix interface is reduced by silane bonding agents [50, 67]. The hydrolysis of the alkyl group bonded to an oxygen atom in water and alcohol results in the formation of silanols, which react with the hydroxyl groups of natural fiber to form stable covalent bonds to the cell wall. As a result of the covalent bonding between DPF and the matrix, the hydrocarbon chains formed by the silane treatment inhibit DPFs swelling by forming a cross linked network [63, 64]. Equations 2 and 3 can be used to give reaction schemes.



Wazzan has described the first silane modification of Date Palm Fibers [50]. He compared the results of alkali treatment using 2 % NaOH aqueous solution and silane treatment using 1.0 % w/w silane and 0.5 percent w/w Dicumyl peroxide (DCP), both dissolved in a 90/10 w/w methanol/water mixture. His study found that silane coupling agent improves tensile strength and interfacial adhesion more than alkaline treatment. As compared to both alkaline and silane treatments performed separately, treating Date Palm Fiber with an alkaline solution followed by treatment with silane solution resulted in higher tensile strength (up to 52% increase) and interfacial shear stress (up to 40% increase). Oushabi et al. have investigated the impact of various silane concentrations on alkaline-treated DPFs. When DPFs filled epoxy and

CHAPTER 2. LITERATURE REVIEW

polyurethane matrices, their findings showed that the alkaline treated DPFs, 5% NaOH with 1% silane treatment, produced the optimum results [67].

2.4.6.5. Maleated Coupling Agents

Maleic anhydride (MA) is now the most commonly applied coupling agent to be grafted to some polymers such as polyethylene or polypropylene to create maleic anhydride-g-polymer. Structural reports by Whitney and others indicate that the grafting uses the unsaturated carbon-carbon of MA to make a connection to the molecular chains, rendering the anhydride group ready to interact as an anhydride in the recently created polymer [68, 69].

Figure 2.6 demonstrated the chemical reaction between maleic anhydride coupling agents and lignocellulosic fiber. The experiment conditions are known to be of considerable significance for the use of polymer matrices reinforced lignocellulosic fibers. Whereas there is not enough study on optimal parameters for composite manufacturing conditions.

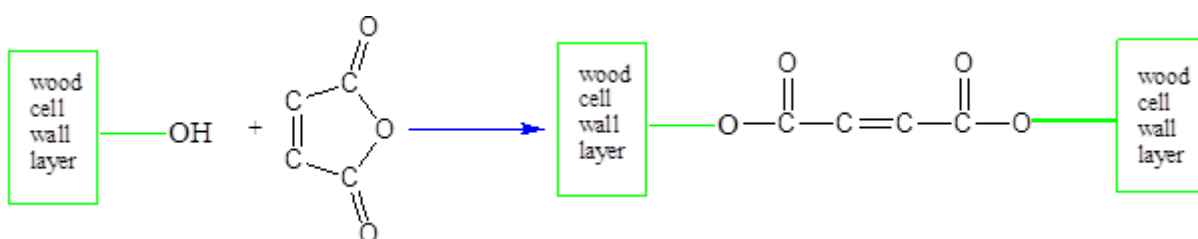
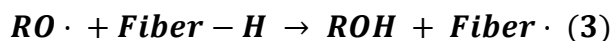
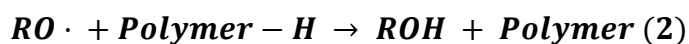
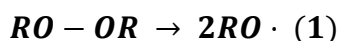


Fig 2.6. Chemical bonding of maleated coupling agents with WF [68] .

2.4.6.6. Treatment with Peroxide

Peroxide is an organic molecule that has the functional group RO–OR. Organic peroxides are easily decomposed to RO. radicals, which react with the matrix's hydrogen group and natural fibers. The following equations 1-4, for example, demonstrate the peroxide-initiated free radical reaction between polymer matrix and natural fibers [68].



CHAPTER 2. LITERATURE REVIEW

Polymer + Fiber · → *Polymer – Fiber* (4)

Dicumyl peroxide (DCP) is an organic peroxide that has been used as a compatibilizer by AlMaadeed et al. [70]. The result of adding 1%, 2%, and 3% DCP (wt.%) to various formulations of date palm wood (DPW) reinforced recycled linear low-density polyethylene (RLLDPE) was explored by the authors. DCP was added after both DPW and RLLDPE had been melt mixed together. The addition of a small percentage of DCP to the composite samples enhanced their mechanical behaviors [70].

2.4.7. DPFs Reinforced Polymeric Composites Processing Parameters

Since NLCFs and polymer matrices have different properties, the processing conditions are extremely critical when using them. Although there is insufficient research on optimal parameters for DPFs-composites processing conditions, the principal purpose of this review part is to clarify the latest available techniques of processing DPFs reinforced polymer matrices, as well as analyze their processing parameters.

2.4.7.1. Drying parameters

Previous to date palm fibers composite production, fibers should be adequately dried to avoid hydrolysis, which can result in lower physical performances such as tensile and flexural strength according to previous applications and studies; it is proposed that DPFs have humidity content between 1 and 2%. This can be accomplished by using a vacuum oven and then collecting the dried DPFs and polymers in a zip-lock plastic bag ready for more processing. The drying conditions for DPFs used in the design of DPFs-composite are described in Table 2.9. Nevertheless, using a higher temperature of more than 95 °C, for 24 hours can deteriorate the fiber, so it is necessary to dry it for a limited time at high temperatures [71, 72].

Table 2.9. Drying parameters of DPFs.

DPF type	Temperature (°C)	Duration (h)	References
Mesh	60	24	[47]
DPWF	65	24	[73]

CHAPTER 2. LITERATURE REVIEW

N.S	70	24	[74]
Leaf	60	24	[75,78]
Mesh	100	1.5	[71]
Leaflet & rachis	100	24	[38]
Leaf	80	1	[72]
Leaf	70	24	[76]
Leaf	50	24	[77]

2.4.7.2. Melt-Mixing

Until manufacturing date palm fibers composite, the polymer material and DPFs are typically melt-mixed to ensure a homogeneous mixture of the composite system and to improve interfacial adhesion between fiber/matrix. At that point, compounds such as plasticizers and coupling agents are introduced. Following that, the component is powdered and prepared to be included in various manufacturing processes such as extrusion, injection molding, hydraulic hot press, or compression molding. Table 2.10 presents the melt-mixing conditions for DPFs-reinforced polymer matrices and their additives for manufacturing.

Table 2.10. Melt-mixing parameters of DPFs.

Polymer blend	Additives	Mixing temperature (°C)	Mixing speed (rpm)	Mixing time (min)	References
PP/Rachis	MAPP	N.S	40	10	[79]
LLDPE/DPW	DCP	140	35	10	[70]
PVP/Leaf fiber	N.S	160	100	5	[76]

2.4.7.3. Extrusion

Extrusion is a fundamental method of composites manufacturing that changes polymer pieces from the solid to the liquid level in an extrusion process. The temperature at various locations of the extrusion and die is important in extruding composites. This is due to the fact that polymer and fibers degrade at high temperatures and shear with weak homogeneity at low temperatures.

CHAPTER 2. LITERATURE REVIEW

The maximum temperature is usually used at the extruder's inlet to ensure that the polymer melts without deteriorating. The extrusion parameters of DPFs-composites investigated by different researchers are shown in table 2.11.

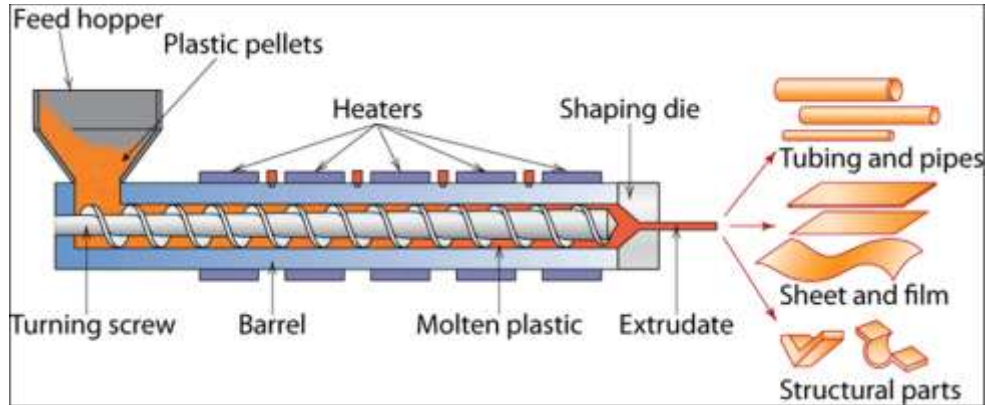


Fig 2.7. Extrusion machine.

Table 2.11. Extrusion processing parameters of DPFs.

Polymer blend	Additives	Zones temp (°C)	Screw speed (rpm)	Screw length (mm)	L/D ratio	Refe- rences
HDPE/Petiole	MAPE	170	30	N.S		[34]
HDPE/Rachis						
HDPE/Trunk						
RPP/DPWF	-	190-230		N.S		[73]
PP-EPDM/	MAPP	160-200	60	N.S		[74]
PLA/N.S DPF	-	175-200	63	N.S		[44]
PC/Leaf		120-240	25-55	750	30	[80]
PVC/Leaf		100-220	25-50			
PS/Leaf		120-180	70			
RPET/Leaf	-	225-245	55	N.S		[75]
LDPE/ Leaf & rachis	MAPE	145-150	7	N.S	21	[38]

CHAPTER 2. LITERATURE REVIEW

RHDPE/RLDPE /RPP/Leaf	MAPE	180-220	60	N.S		[78]
PP/N.S	MAPP	100-200	N.S		40	[81]
PCL/Mesh	-	-	100&400	1.018	36	[82]

Table 2.11.(continued)

Although the lowest temperature should be at the die point, where the composite is resulted, in order to obtain an optimal melt viscosity and guarantee that all of the crystalline regions of the semi-crystalline polymers are melted, on the other hand, the temperature of the extruder zones is increased near the melting temperature of the mixture.

The shear and residence configuration time of the polymer melting is determined by the screw's flight length to its external diameter, known as the L/D ratio. Screws with a large L/D ratio have a longer melting time, and perfect mixing in the extruder. The speed of the screw defines how easily the polymer is collected from the extruder.

2.4.7.4. Hot Press/Compression Molding

Compression molding is a process that involves compressing a preheated polymer into a heated mold cavity at a specific pressure for a specified period of time, typically a few minutes. Depending on the mold parameters, this method will create samples of varying lengths, thicknesses, and complexities (Figure 2.8). The compression pressure, temperature, and time of compressions are all essential factors that affect the composite's properties. Finally, the cooling stage following the heating compression is an important parameter that many researchers neglect and do not investigate.

The most important parameter to note is the initial calculation of the necessary quantity of material needed to fill the mold, as well as the appropriate temperature to melt the polymer without degrading the Date Palm Fiber processed. Besides that, the minimum time needed to heat the material is important in order to prevent material deterioration. Table 2.12 lists the compression molding processing conditions described by previous researchers.

CHAPTER 2. LITERATURE REVIEW

Table 2.12. Hot press/ compression molding processing parameters of DPFs.

Composite	Temperature (°C)	Pressure	Duration (min)	Thickness (mm)	Ref
HDPE/Petiole	170	150 kg/cm ²	N.S	N.S	[34]
HDPE/Rachis					
HDPE/Trunk					
PC/Leaf	185	118 tons	N.S	10±0.5	[80]
PVC/Leaf	185	119 tons			
PS/Leaf	160	119 tons			
PLA/N.S DPF	165	3 bar	N.S	N.S	[44]
Rachis	130	5 tons	8	N.S	[79]
LLDPE/DPW	140	N.S	1	1	[83]
TPS/Spadix stems	160	5MPa	30	N.S	[61]
Leaflet Flour	160	30-35 bar	6	5	[38]
Rachis Flour					
TPS/Spadix stems	160	5MPa	30	2	[62]
TPS/Mesh	130	5 tons	60	3	[84]
EPS/Leaflet	NS	10 bar	10	30.4	[85]
RLLDPE/Mesh	190	N.S	N.S	N.S	[86]
Bio-phenolic resin/N.S DPF	140	N.S	8	N.S	[87]



Fig 2.8. Hot Press/Compression Molding.

2.4.7.5. Injection Molding

Injection molding, also known as infusion shaping, is the most widely used process, as evidenced by specifically dimensioned products and high production rates. The screw choices and injection nozzle are the only differences between an extruder and an injection molding machine. In injection molding, the composite is softened by an extruder with a reciprocating screw that turns and pushes forward and backward to infuse the liquid composite into a mold.

The process is as follows: first, the polymer particles are extruded by injecting them into the inlet and heating them until they exceed their liquefying melting temperature in the container. The molds are then closed, the nozzle is opened, and the screw is moved by inserting the molten composite into the mold through the nozzle. The mold has a cooling framework that allows for controlled stiffening and cooling of the composite, and the screw is retained in the infusion position by ensuring constant pressure so the composite shrinks during cooling. At last, as the

CHAPTER 2. LITERATURE REVIEW

composite cools in the mold, the nozzle is turned off, and the screw begins to reverse backward under a regulated back pressure to ensure that it is dimensionally stable enough to resist the molds opening stroke as shown in Figure 2.9.

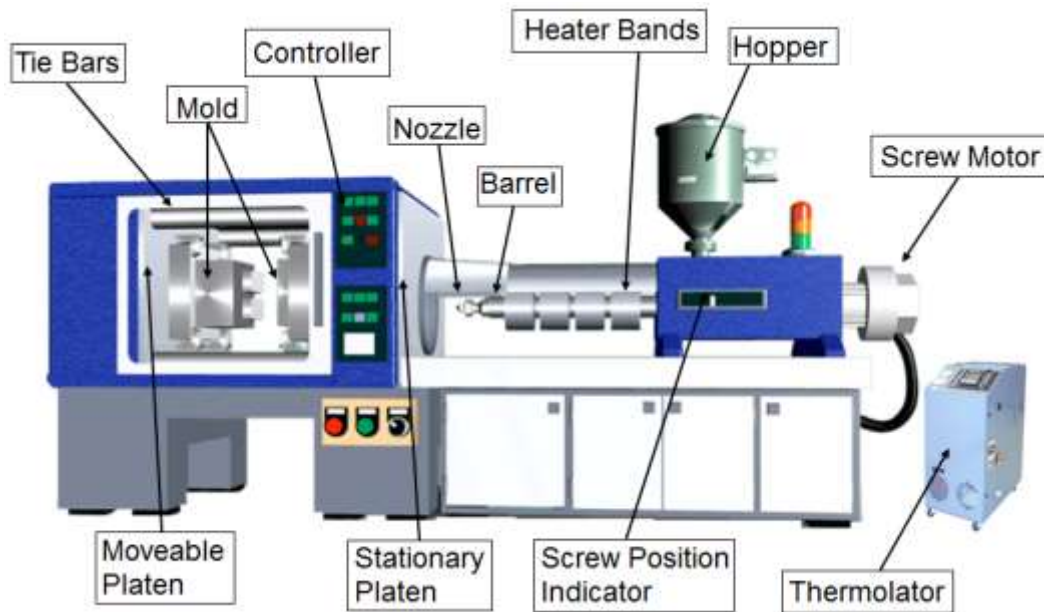


Fig 2.9. Injection Molding machine.

CHAPTER 2. LITERATURE REVIEW

REFERENCES

1. Kiziltas, A.; Erbas Kiziltas, E.; Boran, S.; Gardner, D.J.: Micro-and nanocellulose composites for automotive applications, In Society of Plastics Engineers-13th Annual Automotive Composites Conference and Exhibition, ACCE.1, 402–414 (2013).
2. Njuguna, J.; Wambua, P.; Pielichowski, K.; Kayvantash, K.: Natural Fibre-Reinforced Polymer Composites and Nanocomposites for Automotive Applications. In Cellulose Fibers: Bio- and Nano-Polymer Composites.70, 661–700 (2011).
3. Saba, N.; Tahir, P.M.; Jawaid, M.: A review on potentiality of nano filler/natural fiber filled polymer hybrid composites. *Polymers*. 6, 2247–2273 (2014).
4. Ahmad, F.; Choi, H.S.; Park, M.K.: A review: Natural fiber composites selection in view of mechanical, light weight, and economic properties. *Macromol. Mater. Eng.* 300, 10–24 (2015).
5. Yashas Gowda, T.G.; Sanjay, M.R.; Subrahmanya Bhat, K.; Madhu, P.; Senthamarai kannan,P.; Yogesha, B. Polymer matrix-natural fiber composites: An overview. *Cogent Eng. Cogent OA*. 5, (2018).
6. Mishra, S.; Mohanty, A.K.; Drzal, L.T.; Misra, M.; Parija, S.; Nayak, S.K.; Tripathy, S.S.: Studies on mechanical performance of bio fibre/glass reinforced polyester hybrid composites, *Compos.Sci. Technol.* 63, 1377–1385 (2003).
7. Kalaprasad, G.; Joseph, K.; Thomas, S.: Influence of Short Glass Fiber Addition on the Mechanical Properties of Sisal Reinforced Low Density Polyethylene Composites. *J. Compos. Mater.* 31, 509–527 (1997)
8. Khan, M.Z.; Srivastava, S.K.; Gupta, M.: Tensile and flexural properties of natural fiber reinforced polymer composites: A review. *J. Reinf. Plast. Compos.* 37, 1435–1455 (2018)
9. Langhorst, A.E.; Burkholder, J.; Long, J.; Thomas, R.; Kiziltas, A.; Mielewski, D. Blue-agave fiber-reinforced polypropylene composites for automotive applications. *Bio Resources* 13, 820–835 (2018)

CHAPTER 2. LITERATURE REVIEW

10. Kahl, C.; Feldmann, M.; Salzer, P.; Heim, H.P.: Advanced short fiber composites with hybrid reinforcement and selective fiber-matrix-adhesion based on polypropylene. *Compos. Part A Appl. Sci. Manuf.* 111, 54–61 (2018)
11. Santos, P.A.; Spinace, M.A.S.; Feroselli, K.K.G.; De Paoli, M.A.: Polyamide-6/vegetal fiber composite prepared by extrusion and injection molding. *Compos. Part A Appl. Sci. Manuf.* 38, 2404–2411 (2007)
12. Chandramohan. D.; Marimuthu. K.: A REVIEW ON NATURAL FIBERS. *IJRRAS.* 8, (2011).
13. Plastics Europe.: Automotive. The world moves with plastics. Plastics Europe AISBL Avenue, Belgium. 1–24, (2013).
14. Dittenber, D. B., Gangarao, H. V. S.: Critical review of recent publications on use of natural composites in infrastructure. *Composites Part A: Applied Science and Manufacturing.* 43, 1419–1429 (2012)
15. Ramli, N.: Natural fiber for green technology in automotive industry: A brief review. (2018).
16. tak Lau, K., yan Hung, P., Zhu, M. H., Hui, D.: Properties of natural fibre composites for structural engineering applications. *Compos. Part B Eng.* 136, 222–233 (2018).
17. Abd Rabou, A.F.N., Radwan, E.S.: The current status of the date palm (*Phoenix dactylifera*) and its uses in the Gaza Strip Palestine. *Biodiversitas* 18, 1047–1061 (2017).
18. Al-Alawi, R. A., Al-Mashiqri, J. H., Al-Nadabi, J. S. M., Al-Shihi, B. I., Baqi, Y. Date Palm Tree (*Phoenix dactylifera* L.): Natural Products and Therapeutic Options. *Frontiers in Plant Science.* 8, (2017).
19. Ghori, W., Saba, N., Jawaid, M., Asim, M.: A review on date palm (*Phoenix dactylifera*) fibers and its polymer composites. *IOP Conf. Ser. Mater. Sci. Eng.* 368, (2018).
20. Jaradat, A.A., Zaid, A.: Quality traits of date palm fruits in a center of origin and center of diversity. *Food Agric. Environ.* 2, 208–217 (2004).

CHAPTER 2. LITERATURE REVIEW

21. Arab Agricultural Statistics Yearbook. 2016, (2016).
22. Al-Oqla, F.M., Sapuan, S.M.: Natural fiber reinforced polymer composites in industrial applications: feasibility of date palm fibers for sustainable automotive industry. *J. Clean. Prod.* 66, 347–354 (2014).
23. Elseify, L.A., Midani, M., Shihata, L.A., El-Mously, H.: Review on cellulosic fibers extracted from date palms (*Phoenix dactylifera* L.) and their applications. *Cellulose*. 26, 2209–2232 (2019).
24. Chandrasekaran, M., Bahkali, A.H.: Valorization of date palm (*Phoenix dactylifera*) fruit processing by-products and wastes using bioprocess technology—review. *Saudi J. Biol. Sci.* 20, 105–120 (2013).
25. Asim, M., Abdan, K., Jawaid, M., Nasir, M., Dashtizadeh, Z., Ishak, M.R., et al.: A review on pineapple leaves fibre and its composites. *Int. J. Polym. Sci.* 2015, 1-17 (2015).
26. Dittenber, D.B., Gangarao, H.V.S.: Critical review of recent publications on use of natural composites in infrastructure. *Compos. A*. 43, 1419–1429 (2012).
27. Saba, N., Alothman, O.Y., Almutairi, Z., Jawaid, M., Ghori, W.: Date palm reinforced epoxy composites: tensile, impact and morphological properties. *J. Mater. Res. Technol.* 8, 3959–3969 (2019).
28. Komuraiah, A., Kumar, N.S., Prasad, B.D.: Chemical composition of natural fibers and its influence on their mechanical properties. *Mech. Compos. Mater.* 50, 359–376 (2014).
29. Azwa, Z.N., Yousif, B.F., Manalo, A.C., Karunasena, W.: A review on the degradability of polymeric composites based on natural fibres. *Mater. Des.* 47, 424–442 (2013).
30. John, M.J., Anandjiwala, R.D., Pothan, L.A., Thomas, S.: Cellulosic fibre-reinforced green composites. *Compos. Interfaces*. 14, 733–751 (2007).
31. John, M.J., Thomas, S.: Biofibres and biocomposites. *Carbohydr. Polym.* 71, 343–364 (2008).

CHAPTER 2. LITERATURE REVIEW

32. Al-Khanbashi, A., Al-Kaabi, K., Hammami, A.: Date palm fibers as polymeric matrix reinforcement: fiber characterization. *Polym. Compos.* 26, 486–497 (2005).
33. Alves, C., Ferrão, P.M.C., Silva, A.J., Reis, L.G., Freitas, M., Rodrigues, L.B., et al.: Eco design of automotive components making use of natural jute fiber composites. *J. Clean. Prod.* 18, 313–327 (2010).
34. Mahdavi, S., Kermanian, H., Varshoei, A.: Comparison of mechanical properties of date palm fiber-polyethylene composite. *Bio Resources.* 4, 2391–2403 (2010).
35. Al-Oqla, F.M., Alothman, O.Y., Jawaid, M., Sapuan, S.M., Es-Saheb, M.H.: Processing and properties of date palm fibers and its composites. *Biomass Bioenergy Process. Prop.* 6, 1-25 (2014).
36. Al-Juruf, R.S., Ahmed, F.A., Alam, I.A., Abdel-Rahman, H.H.: Determination of the thermal conductivity of date palm leaves. *J. Therm. Envel. Build. Sci.* 11, 152–157 (1988).
37. Abu-Sharkh, B.F., Hamid, H.: Degradation study of date palm fibre/polypropylene composites in natural and artificial weathering: mechanical and thermal analysis. *Polym. Degrad. Stab.* 85, 967–973 (2004).
38. Mirmehdi, S.M., Zeinaly, F., Dabbagh, F.: Date palm wood flour as filler of linear low-density polyethylene. *Compos. B.* 56, 137–141 (2014).
39. Almi, K., Benchabane, A., Lakel, S., Kriker, A.: Potential utilization of date palm wood as composite reinforcement. *J. Reinf. Plast. Compos.* 34, 1231–1240 (2015).
40. Wong, K.J., Yousif, B.F., Low, K.O.: The effects of alkali treatment on the interfacial adhesion of bamboo fibres. *Proc. Inst. Mech. Eng. L.* 224, 139–148 (2010).
41. Methacanon, P., Weerawatsophon, U., Sumransin, N., Prahsarn, C., Bergado, D.T.: Properties and potential application of the selected natural fibers as limited life geotextiles. *Carbohydr. Polym.* 82, 1090–1096 (2010).

CHAPTER 2. LITERATURE REVIEW

42. Kriker, A., Bali, A., Debicki, G., Bouziane, M., Chabannet, M.: Durability of date palm fibres and their use as reinforcement in hot dry climates. *Cem. Concr. Compos.* 30, 639–648 (2008).
43. Alawar, A., Hamed, A.M., Al-Kaabi, K.: Characterization of treated date palm tree fiber as composite reinforcement. *Compos. B* 40, 601–606 (2009).
44. Amirou, S., Zerizer, A., Haddadou, I., Merlin, A.: Effects of corona discharge treatment on the mechanical properties of biocomposites from polylactic acid and Algerian date palm fibres. *Sci. Res. Essays.* 8, 946–952 (2013).
45. El-Morsy, M.: Studies on the rachises of the Egyptian date palm leaves for hardboard production. *Fibre Sci. Technol.* 13, 317–323 (1980).
46. Pandey, S.N., Ghosh, S.K.: The chemical nature of date-palm (*Phoenix dactylifera* L.) leaf fibre. *J. Text. Inst.* 86, 487–489 (1995).
47. Al-Kaabi, K., Al-Khanbashi, A., Hammami, A.: Date palm fibers as polymeric matrix reinforcement: DPF/polyester composite properties. *Polym. Compos.* 26, 604–613 (2005).
48. Kaddami, H., Dufresne, A., Khelifi, B., Bendahou, A., Taourirte, M., Raihane, M.: Short palm tree fibers—thermoset matrices composites. *Compos. A* 37, 1413–1422 (2006).
49. Taha, I., Steuernagel, L., Ziegmann, G.: Chemical modification of date palm mesh fibres for reinforcement of polymeric materials. Part I examination of different cleaning methods. *Polym. Polym. Compos.* 14, 767–778 (2006).
50. Wazzan, A.A.: The effect of surface treatment on the strength and adhesion characteristics of phoenix dactylifera-L (date palm) fibers. *Int. J. Polym. Mater. Polym. Biomater.* 55, 485–499 (2006).
51. Rao, K.M.M., Rao, K.M.: Extraction and tensile properties of natural fibers: vakka, date and bamboo. *Compos. Struct.* 77, 288–295 (2007).
52. Taha, I., Steuernagel, L., Ziegmann, G.: Optimization of the alkali treatment process of date palm fibres for polymeric composites. *Compos. Interfaces* 14, 669–684 (2007).

CHAPTER 2. LITERATURE REVIEW

53. Sbiai, A., Kaddami, H., Fleury, E., Maazouz, A., Erchiqui, F., Koubaa, A., et al.: Effect of the fiber size on the physicochemical and mechanical properties of composites of epoxy and date palm tree fibers. *Macromol. Mater. Eng.* 293, 684–691 (2008).
54. Abdal-Hay, A., Suardana, N.P.G., Jung, D.Y., Choi, K.S., Lim, J.K.: Effect of diameters and alkali treatment on the tensile properties of date palm fiber reinforced epoxy composites. *Int. J. Precis. Eng. Manuf.* 13, 1199–1206 (2012).
55. Tioua, T., Kriker, A., Barluenga, G., Palomar, I.: Influence of date palm fiber and shrinkage reducing admixture on self-compacting concrete performance at early age in hot-dry environment. *Constr. Build. Mater.* 154, 721–733 (2017).
56. Aldousiri, B., Alajmi, M., Shalwan, A.: Mechanical properties of palm fibre reinforced recycled HDPE. *Adv. Mater. Sci. Eng.* (2013).
57. Nasser, R.A., Al-Mefarrej, H.A.: Midribs of date palm as a raw material for wood-cement composite industry in Saudi Arabia. *World Appl. Sci. J.* 15, 1651–1658 (2011).
58. Sisti, L., Totaro, G., Vannini, M., Celli, A.: Retting process as a pretreatment of natural fibers for the development of polymer composites. *Lignocellulosic Composite Materials*, pp. 97–135. Springer, Cham (2017).
59. Donaghy, J., Levett, P., Haylock, R.: Changes in microbial populations during anaerobic flax retting. *J. Appl. Bacteriol.* 69, 634–641 (1980).
60. Mohanty, A.K., Misra, M., Drzal, L.T. (eds.): *Natural fibers, biopolymers, and biocomposites*. CRC press (2005).
61. Ibrahim, H., Farag, M., Megahed, H., Mehanny, S.: Characteristics of starch-based biodegradable composites reinforced with date palm and flax fibers. *Carbohydr. Polym.* 101, 11–19 (2014).
62. Ibrahim, H., Mehanny, S., Darwish, L., Farag, M.: A comparative study on the mechanical and biodegradation characteristics of starch-based composites reinforced with different lignocellulosic fibers. *J. Polym. Environ.* 26, 2434–2447 (2017).

CHAPTER 2. LITERATURE REVIEW

63. Li, X., Tabil, L.G., Panigrahi, S.: Chemical treatments of natural fiber for use in natural fiber-reinforced composites: a review. *J. Polym. Environ.* 15, 25–33 (2007).
64. Agrawal, R., Saxena, N., Sharma, K., Thomas, S., Sreekala, M.: Activation energy and crystallization kinetics of untreated and treated oil palm fibre reinforced phenol formaldehyde composites. *Materials Science and Engineering: A.* 277, 77-82 (2000)
65. Alsaeed, T., Yousif, B.F., Ku, H.: The potential of using date palm fibres as reinforcement for polymeric composites. *Mater. Des.* 43, 177–184 (2013).
66. Shalwan, A., Yousif, B.F.: Influence of date palm fibre and graphite filler on mechanical and wear characteristics of epoxy composites. *Mater. Des.* 59, 264–273 (2014).
67. Oushabi, A., Sair, S., Oudrhiri Hassani, F., Abboud, Y., Tanane, O., El Bouari, A.: The effect of alkali treatment on mechanical, study of the interface of DPF–polyurethane composite. *S. Afr. J.Chem. Eng.* 23, 116–123 (2017).
68. Zhou, Y., Fan, M., Chen, L.: Interface and bonding mechanisms of plant fibre composites: an overview. *Compos. B.* 101, 31–45 (2016).
69. Keener, T.J., Stuart, R.K., Brown, T.K.: Maleated coupling agents for natural fibre composites. *Compos. A* 35, 357–362 (2004).
70. Al-Maadeed, M.A., Nógellová, Z., Janigová, I., Krupa, I.: Improved mechanical properties of recycled linear low-density polyethylene composites filled with date palm wood powder. *Mater. Des.* 58, 209–216 (2014).
71. El-badry, E.A.: Agro-residues: surface treatment and characterization of date palm tree fiber as composite reinforcement. *J. Compos.* 2014, 1–8 (2014).
72. Mahdi, E., Hernández, D.R., Eltai, E.O.: Effect of water absorption on the mechanical properties of long date palm leaf fiber reinforced epoxy composites. *J. Biobased Mater. Bioenergy* 9, 173–181 (2015).

CHAPTER 2. LITERATURE REVIEW

73. Al-Maadeed, M.A., Kahraman, R., Noorunnisa Khanam, P., Madi, N.: Date palm wood flour/glass fibre reinforced hybrid composites of recycled polypropylene: mechanical and thermal properties. *Mater. Des.* 42, 289–294 (2012).
74. Asadzadeh, M., Khalili, S., Eslami Farsani, R., Rafizadeh, S.: Bending properties of date palm fiber and jute fiber reinforced polymeric composite. *ADMT J.* 5, (2012).
75. Dehghani, A., Madadi Ardekani, S., Al-Maadeed, M.A., Hassan, A., Wahit, M.U.: Mechanical and thermal properties of date palm leaf fiber reinforced recycled poly (ethylene terephthalate) composites. *Mater. Des.* 52, 841–848 (2013).
76. Mohanty, J.R., Das, S.N., Das, H.C., Swain, S.K.: Effect of chemically modified date palm leaf fiber on mechanical, thermal and rheological properties of polyvinylpyrrolidone. *Fibers Polym.* 15, 1062–1070 (2014).
77. Rao, K.M.M., Rao, K.M.: Extraction and tensile properties of natural fibers: vakka, date and bamboo. *Compos. Struct.* 77, 288–295 (2007).
78. Zadeh, K.M., Inuwa, I.M., Arjmandi, R., Hassan, A., Al maadeed, M., Mohamad, Z., et al.: Effects of date palm leaf fiber on the thermal and tensile properties of recycled ternary polyolefin blend composites. *Fibers Polym.* 18, 1330–1335 (2017).
79. Mahmoudi, N.: Use of date palm fibers as reinforcement for thermoplastic-based composites. *Mech. Ind.* 14, 71–77 (2013).
80. Binhussain, M.A., El-Tonsy, M.M.: Palm leave and plastic waste wood composite for outdoor structures. *Constr. Build. Mater.* 47, 1431–1435 (2013).
81. Boukettaya, S., Alawar, A., Almaskari, F., Ben Daly, H., Abdala, A., Chatti, S.: Modeling of water diffusion mechanism in polypropylene/ date palm fiber composite materials. *J. Compos. Mater.* 52, 2651–2659 (2018).
82. Dhakal, H., Bourmaud, A., Berzin, F., Almansour, F., Zhang, Z., Shah, D.U., et al.: Mechanical properties of leaf sheath date palm fibre waste biomass reinforced polycaprolactone (PCL) biocomposites. *Ind. Crops Prod.* 126, 394–402 (2018).

CHAPTER 2. LITERATURE REVIEW

83. Al-Maadeed, M.A., Nógellová, Z., Mičušík, M., Novák, I., Krupa, I.: Mechanical, sorption and adhesive properties of composites based on low density polyethylene filled with date palm wood powder. *Mater. Des.* 53, 29–37 (2014).
84. Saleh, M.A., Al Haron, M.H., Saleh, A.A., Farag, M.: Fatigue behavior and life prediction of biodegradable composites of starch reinforced with date palm fibers. *Int. J. Fatigue* 103, 216–222 (2017).
85. Masri, T., Ounis, H., Sedira, L., Kaci, A., Benchabane, A.: Characterization of new composite material based on date palm leaflets and expanded polystyrene wastes. *Constr. Build. Mater.* 164, 410–418 (2018).
86. Al shabanat, M.: Morphological, thermal, and biodegradation properties of LLDPE/treated date palm waste composite buried in a soil environment. *J. Saudi Chem. Soc.* 23, 355–364 (2019).
87. Asim, M., Jawaid, M., Khan, A., Asiri, A.M., Malik, M.A.: Effects of date palm fibres loading on mechanical, and thermal properties of date palm reinforced phenolic composites. *J. Mater. Res. Technol.* 9, 3614-3621 (2020).

CHAPTER 3. APPLICATION 1

SYNERGISTIC EFFECTS OF MIXED METAL STEARATE, CALCIUM CARBONATE PARTICLES AND LOW DENSITY POLYETHYLENE ON THE MECHANICAL, THERMAL AND STRUCTURAL PERFORMANCE OF POLYVINYLCHLORIDE MICROCOMPOSITE.

ABSTRACT

To reduce the accumulation of thermoplastic wastes and to prevent the pollution environment through safe recycling procedures. Thus, the target in this work is to achieve a new strong polyvinyl chloride (PVC) microcomposite combined with low density polyethylene (LDPE), calcium carbonate (CaCO_3) and Calcium/Zinc stearate ($\text{CaSt}_2/\text{ZnSt}_2$). The effects of two ratios of ($\text{CaSt}_2: \text{ZnSt}_2 = 9 : 1$ and $\text{CaSt}_2: \text{ZnSt}_2 = 1 : 9$) with different concentrations (2, 5 and 10) parts per hundred (phr), on the mechanical properties and thermal stability of PVC and PVC-LDPE (1:1) blend were studied. The samples were prepared by a twin screw extruder at 175°C with speed rotor 60 tr/min and were characterized using infrared spectroscopy (FTIR), mechanical tests, thermal analysis and scanning electron microscopy (SEM). The addition of 5 phr of $\text{CaSt}_2: \text{ZnSt}_2 = 9 : 1$ into PVC (MC4) seems to produce an optimum tensile strength and elongation at break values. In addition, it is highlighted that MC4 showed high thermal stability. Moreover, the incorporation of LDPE into PVC makes the PVC matrix stronger and more stable than pure PVC which yields high mechanical and thermal performances. Furthermore, an outstanding synergistic effect can be shown when a heat stabilizer rich in calcium combined with CaCO_3 and LDPE. This PVC-LDPE blend as waste composite can be used in several industrial fields. Finally, we used DFT calculation to elucidate the dehydrochlorination mechanism of PVC in presence of Ca and Zn stearate.

Keywords: PVC, LDPE, Thermal stabilizer, CaCO_3 , Density functional theory.

CHAPTER 3. APPLICATION 1

3.1. INTRODUCTION

The Novel industry technology influences positively on the performance of composite materials in the economic sector, especially thermoplastic polymers, blends and their composites [1]. For fast economic development and significant protection of the environment, recycled waste technology is known as a clean energy source and plays a very important role in solid waste disposal. Thermoplastic garbage is more difficult to biodegrade than any other organic matter in landfill sites [2]. Polyvinylchloride (PVC) is one of the most important thermoplastic polymers used in industrial products, such as pipes, cables, food product containers, construction applications, medical and electronic devices, due to high mechanical properties [3–5]. Lower thermal stabilization was observed for the PVC compared with other thermoplastic polymers such as : low density polyethylene (LDPE), high density polyethylene (HDPE), polypropylene (PP), polystyrene (PS) and polyethylene terephthalate (PET) due to dehydrochlorination reaction of PVC around 100 °C [6]. The pyrolysis of PVC characterizes two interesting steps : (1) initial degradation of PVC due to the first dehydrochlorination of PVC at low temperature, (2) final degradation due to strongly cracking and decomposition of the PVC at higher temperatures [7]. To decrease the pure PVC degradation, it should be mixed with thermal stabilizers to produce plastic with high thermal performance used in several applications [8, 9]. Incorporation of thermal stabilizer into PVC can make the zipper decomposition more difficult at both low and high temperatures, in which the chlorine atom can be absorbed by heat stabilizer [10]. The combination of commercial calcium stearate (CaSt_2) and zinc stearate (ZnSt_2) has attracted the attention of several researchers, in which ZnSt_2 can substitute labile chlorine atom of PVC chain forming a strong Lewis acid, ZnCl_2 , which in turn can react with HCl to perform dehydrochlorination reaction. On the other side, HCl is absorbed by CaSt_2 to generate CaCl_2 and fatty acid [11]. Moreover, calcium/zinc compounds can be considered as environmentally friendly thermal stabilizers compared with organo tin and lead compounds [12]. It is significant to develop new heat stabilizer of PVC that exhibited synergistic effect with commercial thermal stabilizers $\text{CaSt}_2/\text{ZnSt}_2$ [9, 13]. Li et al. found that new mixed Ca/Zn synthesized from tung oil fatty acid improved the thermal proprieties of PVC [14]. Moreover, Wang et al. studied the synergistic effect of tung-oil-based Ca/Zn and polyol in stabilizing polyvinylchloride [15]. The results show that the positive synergistic effect can be attributed to the hydroxyl and nitrogen groups of the heat stabilizers. In addition, Ye et al. reported the zinc urate (Zn_3Ur_2) is a good thermal stabilizer of PVC compared with ZnSt_2 [16]. Recently, the synergistic effects of traditional heat stabilizer ($\text{CaSt}_2/\text{ZnSt}_2$) and Tung-oil-derived imide epoxidized ester (GEABTMI) on the thermal stabilization of PVC were

CHAPTER 3. APPLICATION 1

successfully investigated by Wang et al. they found that the imide and epoxy functions of GEABTMI compound can scavenge free radicals and absorb HCl generated from PVC pyrolysis [17]. Li et al. studied the interesting performance of mechanical properties of the PVC composite reinforced with CaCO₃ nano-particles, which these particles considered as good dispersion agents in the PVC polymer system, and it can be an effective approach to resist the migration of plasticizer from the PVC [18]. It is well known that the addition of CaCO₃ fillers increase thermal stability of PVC polymer. The results appeared that the CaCO₃ can absorb HCl to generate CaCl₂, CO₂ and H₂O [19]. Ahmad et al. investigated the synergistic effect of calcium carbonate (CaCO₃)/ layered double hydroxides (LDHs) on the thermal degradation of PVC [20]. Many researchers reported the incorporation of different polymers in PVC induced high thermal and mechanical performance [21, 22]. Our previous experimental results revealed that thermal stability of the PVC-LDPE blend was improved significantly by increasing the LDPE loading to values above 50 wt.% [23]. To the best of our knowledge there are no reports of degradation behavior of PVC, considering the synergistic effects of mixed metal stabilizers (CaSt₂/ZnSt₂) with different concentrations and different ratios of calcium/zinc stearates, Calcium carbonate (CaCO₃) as micro-filler and low-density polyethylene (LDPE). In this paper, two ratios of calcium/zinc stearates metal Stabilizers, CaCO₃ particles and LDPE were added into PVC. This study investigates a new microcomposite based PVC with high mechanical, thermal and morphological performance which can provide sufficient information to reveal the degradation process of PVC. Furthermore, we conducted density functional theory (DFT) calculations to elucidate the role of Ca-Zn in the thermal stability of PVC.

3.2. EXPERIMENTAL

3.2.1. Materials

An amorphous PVC white powder (4000M, K-value = 67-72), and a semi crystalline LDPE, white transparent, with melting point = 129 °C, and the specific enthalpy of melting =106 J/g were purchased from the “Enterprise National de Pétrochimie (ENIP)”, Skikda, Algeria. Calcium stearate (CaSt₂, Ca content: 6.6–7.4%), zinc stearate (ZnSt₂, Zn content: 10–12%), and calcium carbonate (CaCO₃,2500 mesh) were obtained from Nanjing OMYA Fine Chemical Ind. Co. Ltd. (Nanjing China). Bis (2-ethylhexyl) terephthalate (DOP) was obtained from Shanxi Sanwei Group Co, Ltd. Mixed Metal Stabilizers Calcium / Zinc stearate were prepared in the form of (CaSt₂: ZnSt₂ =9 :1 and CaSt₂: ZnSt₂ =1 :9).

CHAPTER 3. APPLICATION 1

3.2.2. Fabrication of Microcomposites

All materials were dried in an oven at 80°C for 12 hours before blending to remove humidity. PVC and PVC: LDPE (1:1) microcomposites using different concentrations of mixed metal stabilizers and calcium carbonate were extruded using the twin screw extruder, type MSH, at a processing temperature of 175°C, screw speed of 50 rpm for 10 min from the feed zone to die zone. All different samples are summarized in Table 3.1, the samples obtained after extruding were cooled at room temperature and then it was pressed into a square mold of thick of 2 mm and 20 mm long using a heated hydraulic press for 7 min at 170°C with 200 bar pressure. After cooling with water system to room temperature, the sample was cut off in altered form by the (Computer numerical control) CNC milling machine, before carrying out different characterizations.

Table 3.1. Different composition of the PVC and PVC/LDPE microcomposites.

Sample	PVC (phr)	LDPE (phr)	CaCO ₃ (phr)	Heat stabilizer ^(a) & ^(b) of PVC (phr)	Bis(2-ethylhexyl) terephthalate (DOP, 98%) (phr)
MC0	100	-	20	-	25
MC1	100	-	20	2 ^a	25
MC2	100	-	20	2 ^b	25
MC3	100	-	20	5 ^a	25
MC4	100	-	20	5 ^b	25
MC5	100	-	20	10 ^a	25
MC6	100	-	20	10 ^b	25
MC7	100	100	20	2 ^a	25
MC8	100	100	20	2 ^b	25
MC9	100	100	20	5 ^a	25
MC10	100	100	20	5 ^b	25
MC11	100	100	20	10 ^a	25
MC12	100	100	20	10 ^b	25

(a) Attribute to the CaSt₂: ZnSt₂= 1:9 and (b) Attribute to the CaSt₂: ZnSt₂= 9:1 heat stabilizer.

CHAPTER 3. APPLICATION 1

3.2.3. Characterization

3.2.3.1. *Fourier Transform Infrared Spectroscopy (FTIR)*

The structural analysis of the PVC and PVC-LDPE microcomposite samples was carried out by Fourier Transform Infrared Spectroscopy Vertex 70v FTIR (Bruker Company, Billerica, MA, USA) coupled with ATR Golden Gate Diamond. The Samples were measured from 4000 to 400 cm^{-1} with a 4 cm^{-1} spectrum resolution to obtain FTIR spectra.

3.2.3.2. *Mechanical Tests*

The mechanical tests in the tensile mode were measured at room temperature using a mechanical testing machine (Zwick / Roell, ISO 527, Germany). Each tensile sample was performed five times to report the average value.

3.2.3.3. *Heat Ageing Test*

The samples were heated in air oven at 100 ± 1 °C for 360 h (15 days), the mechanical results were compared with unaged samples.

3.2.3.4. *Investigation of Initial Thermal Stabilization for Microcomposites*

3.2.3.4.1. *Congo Red Test*

10.0 g of each PVC sample was put into an airtight tube and immersed in an oil bath at 180 °C refer to the GB/T 2917.1-2002 standard, furthermore, the PVC samples were controlled by Congo red paper and the thermal stability time was recorded when the color of the paper turned blue. The Congo red test was executed three times and an average value was reported.

3.2.3.4.2. *Discoloration Test*

PVC and PVC-LDPE samples were cut into sheets having dimensions of 15.0 mm×15.0 mm ×2.0 mm according to the GB/T 9349-2002 standard. The samples were moved onto the ceramic plate in temperature-controlled oven (V 50 e, Prolabo) at 180 °C, after that the samples were scanned every 10 min using (Epson Perfection V19) to evaluate the PVC discoloration during heating.

3.2.3.5. *Thermogravimetric Analysis (TGA and DTG)*

The TGA and DTG results of the microcomposites were obtained by using SDT Q600 (TGA/DSC simultaneous thermo gravimetric analyzer and differential scanning calorimeter) from TA Instruments under N_2 atmosphere with a heating rate of 10 °C/min using 3 to 5 mg of the sample was analyzed.

CHAPTER 3. APPLICATION 1

3.2.3.6. Scanning Electron Microscopy (SEM)

The morphology of the microcomposites was examined using scanning electron microscope (SEM) (JEOL JSM 6460LV) with an accelerating voltage of 20 kv. The samples were soaked in liquid nitrogen before fracturing and then were covered with a thin gold layer by sputtering using EDWARDS scan-coat on the surface and the cross-sections.

3.2.3.7. Calculation Details

All the calculations were conducted by using the Gaussian 09 program package, we used hybrid functional M06-2X [24], because several theoretical studies of polymer pyrolysis reported that this functional is more viable in comparison with B3LYP [25–27], to reduce the computational cost, a 4-carbon PVC molecule and the polar part of thermal stabilizers CaSt₂ and ZnSt₂, were employed as a model reactants. Geometries of the reactants (R1, R2), transition states (TS1, TS2), and products (P1, P2) were optimized at M06-2X/6-31++G (d,p) level of theory. Frequencies were computed for all stationary points and used to compute the free energies at 298 K and 1 bar. Finally, we performed IRC calculation to confirm the connection between products and reactants.

3.3. RESULTS AND DISCUSSION

3.3.1. FTIR Analysis

FTIR tests were conducted to investigate and clarify the modifications in the functional groups of the microcomposites with different heat stabilizer ratios after the heat ageing at 100°C for 168 hours. From the FTIR spectra depicted in Figure 3.1 and Figure 3.2, the characteristic bands of PVC and PVC-LDPE microcomposites are well shown and the assignments of these bands are in line with those provided by several researchers corresponding with composites based PVC [28–31].

The peaks in the region 2940-2960 cm⁻¹ correspond to symmetric stretching C-H in the adjacent CH-Cl, but the peak at 2849 cm⁻¹ in PVC-LDPE microcomposites is attributed to the asymmetric stretching, of C-H in -CH₃ groups and in -CH₂- groups. The peaks in the range 800-870 cm⁻¹ can be attributed to the calcium carbonate group CaCO₃. Moreover, the asymmetric stretching of C-Cl can be related to the peaks in the range of 610-730 cm⁻¹. Furthermore, the weak bands around 3620 and 3660 cm⁻¹ in Figure 3.1(a) and Figure 3.2(a), attributed to the hydroxyl group OH stretch of the water phase may result from adsorption of HCl by CaCO₃ particles.

CHAPTER 3. APPLICATION 1

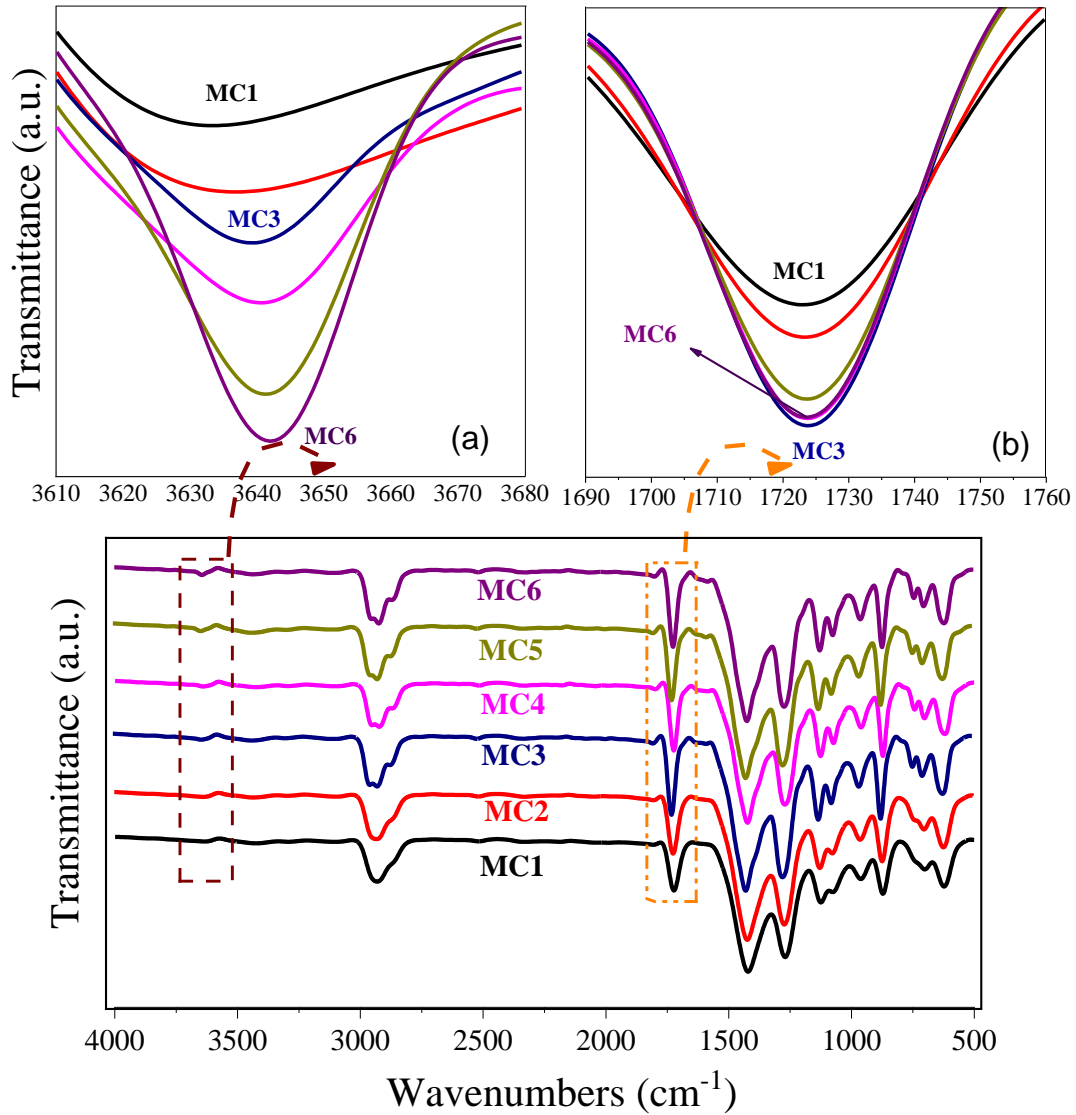


Fig 3.1. FTIR spectra of PVC microcomposites exposed to thermal ageing for $t=360$ h under temperature $T=100^{\circ}\text{C}$:(a) OH water group superposed region, (b) CO carbonyl group superposed region.

A strong peak at 1732 cm^{-1} in Figure 3.1(b) and Figure 3.2(b) is attributed to C=O stretch presented in DOP structure and also it is probably due to the oxidation process during heat ageing test. The difference of FTIR peaks between PVC and PVC-LDPE micro composites are visible in the superposed intensity and shape of characteristic bands represented above.

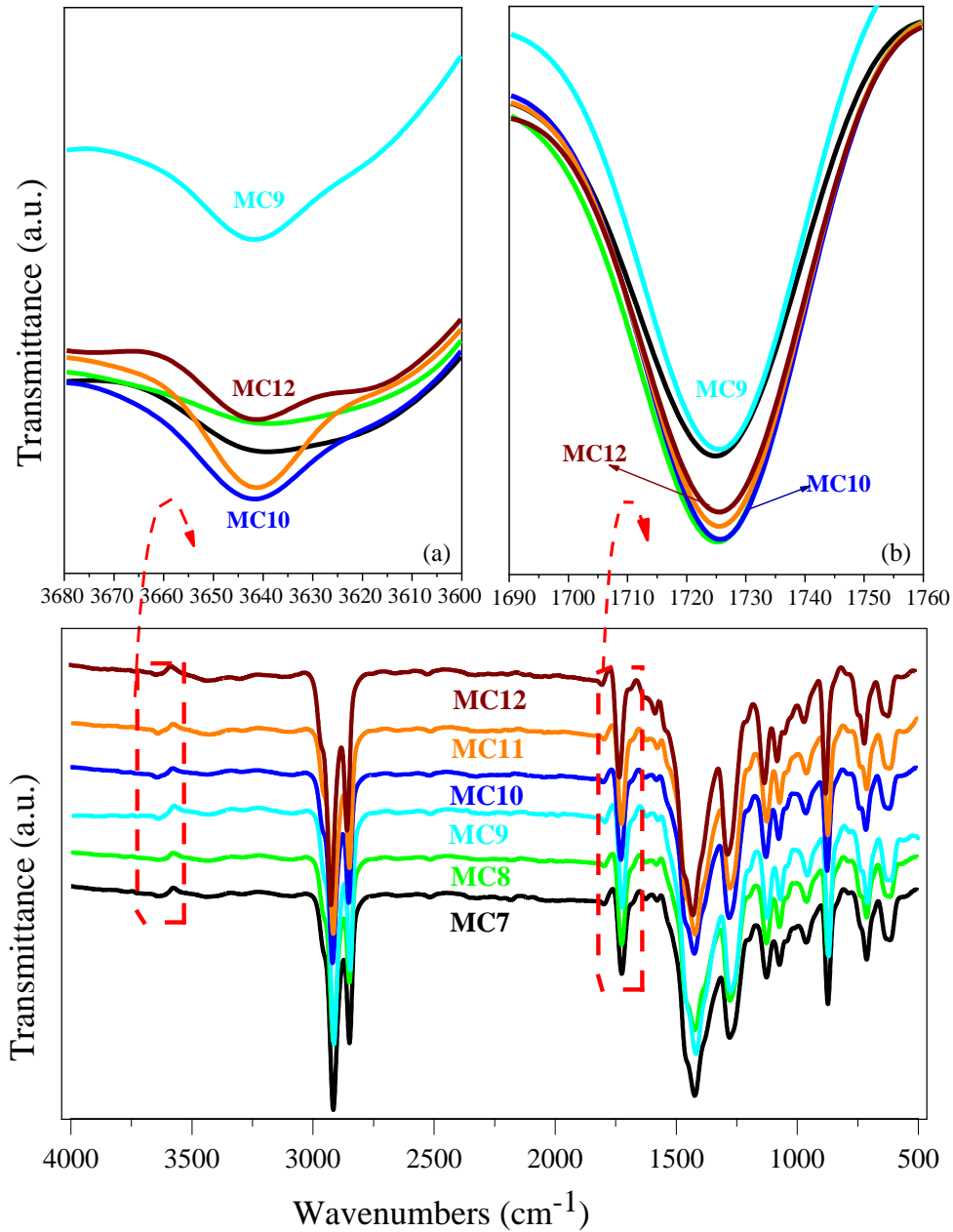


Fig 3.2. FTIR spectra of PVC-LDPE microcomposites exposed to thermal ageing for 360 h under temperature $T=100^{\circ}\text{C}$: (a) OH water group region, (b) CO carbonyl group region.

3.3.2. Mechanical Properties

The Tensile strength, Elongation at break and Young's modulus results of PVC and PVC-LDPE microcomposites before and after ageing are displayed in Figure 3.3(a, b) and Table 3.2. In fact, pure PVC gets more brittle as a thermoplastic polymer, but in general, with the incorporation of heat stabilizers, CaCO_3 , and LDPE into PVC matrix, the material can be more mechanically strong.

CHAPTER 3. APPLICATION 1

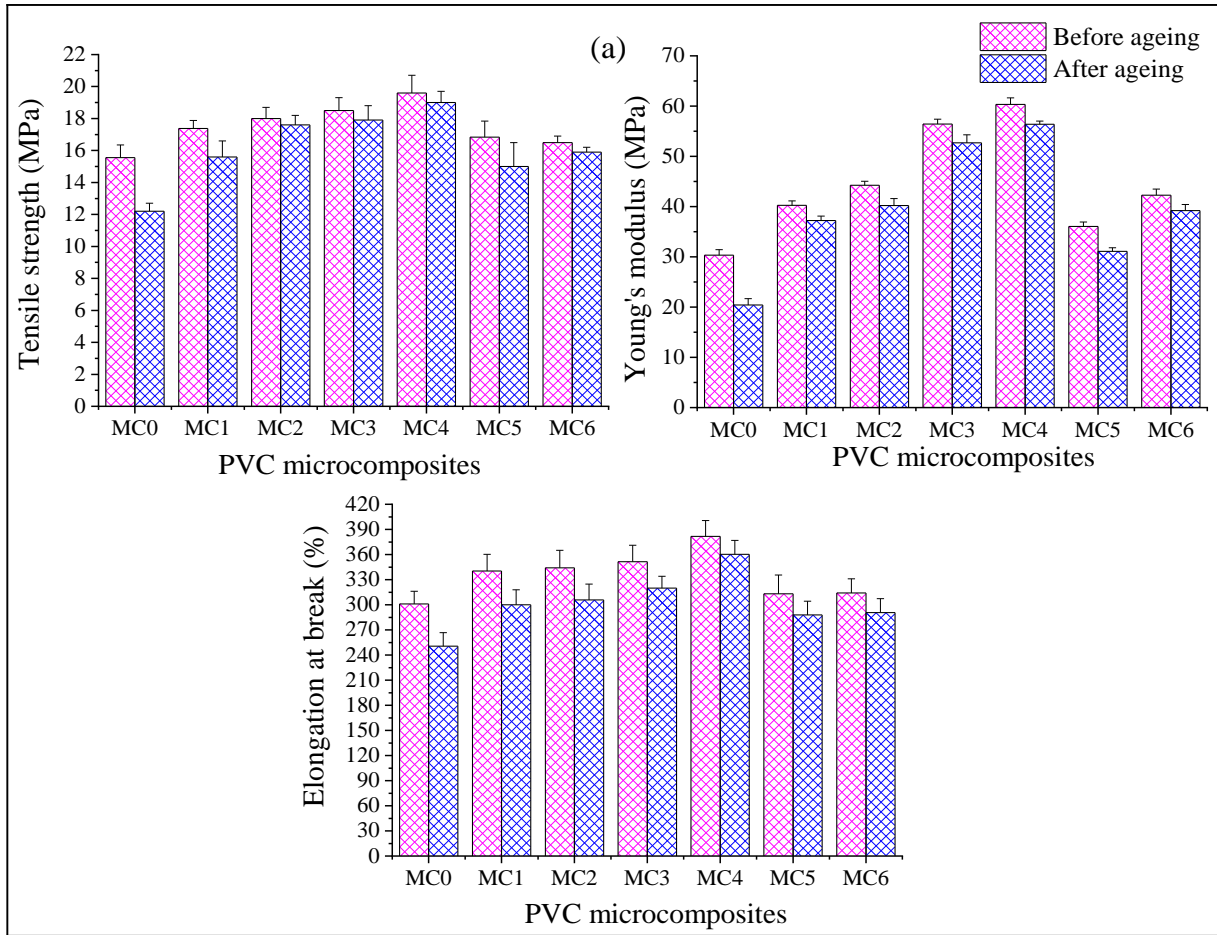


Fig 3.3(a). Evolution of the mechanical properties of PVC microcomposites before and after heat ageing.

Figure 3.3(a) shows the variation of tensile behaviors of PVC microcomposites at different heat stabilizers with different ratios. The mechanical performance is remarkably decreased in the sample without thermal stabilizer MC0 after ageing. In addition, the sample MC4 exhibits better mechanical performance than the pure PVC and other samples, before and after ageing. It revealed that the optimum concentration of mixed stearate $\text{CaSt}_2 : \text{ZnSt}_2 = 9 : 1$ for the highest tensile strength, elongation at break and young's modulus is 5 phr, this concentration probably leads to the good dispersion of CaSt_2 particles in PVC and also the increasing of the flexibility of the PVC. From a mechanical point of view, we can also see that 2 phr of thermal stabilizers MC1 and MC2 are slightly better than 10 phr, MC5 and MC6 with little favor of heat stabilizer with a high concentration of calcium, due to the interaction between the polar ends of Calcium stearate and the somewhat polar PVC chains [32].

CHAPTER 3. APPLICATION 1

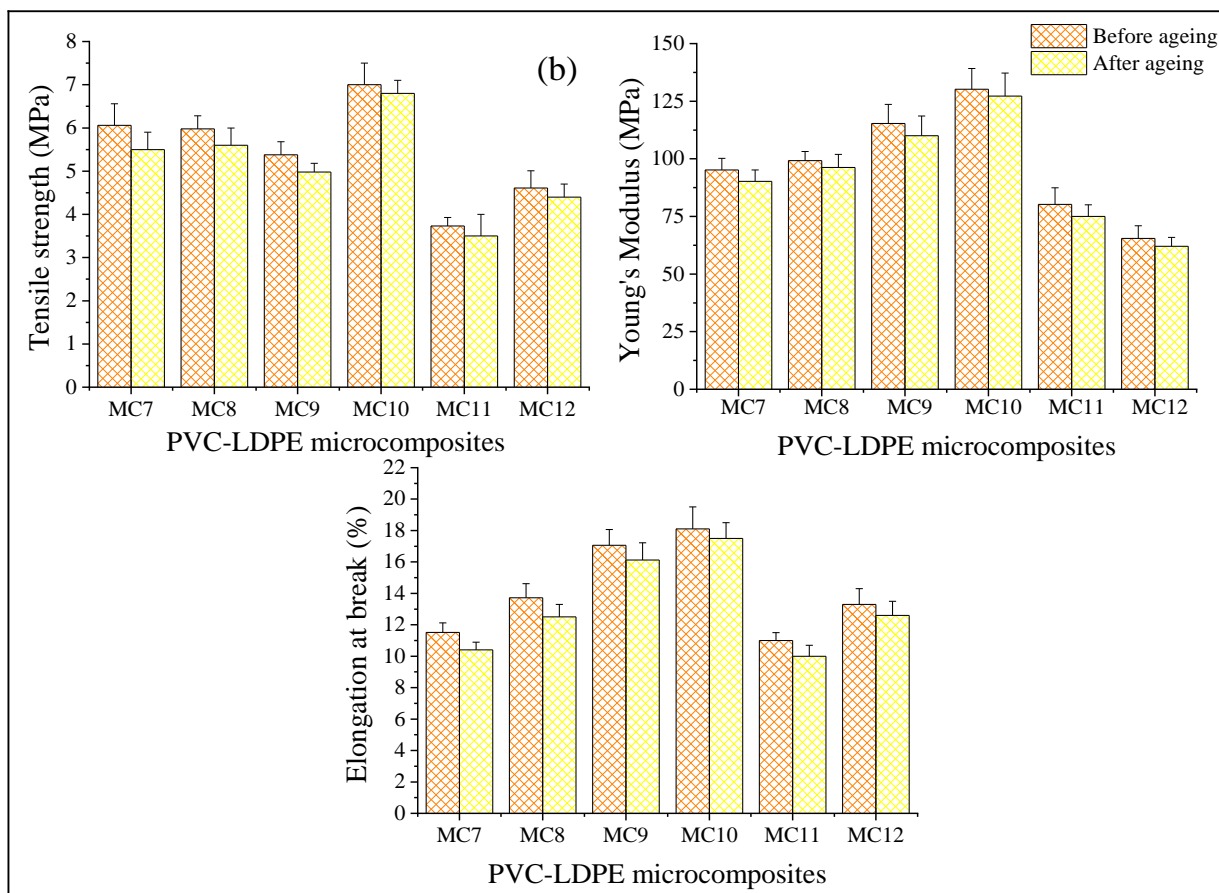


Fig 3.3(b). Evolution of the mechanical properties of PVC-LDPE microcomposites before and after heat ageing.

Figure 3.3(b) represents the influence of LDPE on the mechanical properties of the PVC microcomposites with 2, 5 and 10phr of mixed metal stabilizers. It can be observed that the incorporation of LDPE into PVC decreases the tensile strength and elongation at break when it is compared with PVC micro composites. This deterioration is due to the crystalline structure part of the macromolecular chain of LDPE polymer and which makes the PVC polymer loses partially its flexibility [33]. On the other hand, Young's Modulus values are doubly increased after addition of LDPE into PVC microcomposites. In addition, MC10 exhibits better mechanical properties than other samples, before and after ageing. In addition, it can be seen that the incorporation of LDPE enhances the mechanical stability of the PVC polymer after heat ageing. Hence, during the thermal treatment the PVC and short-chain LDPE radicals react to produce LDPE-g-PVC copolymers [22]. The mechanical properties of microcomposites based PVC become higher with increasing the content of CaSt_2 .

CHAPTER 3. APPLICATION 1

Table 3.2. The mechanical results before and after heat ageing of PVC and PVC-LDPE microcomposites.

sample	Before ageing			After ageing		
	Tensile Strength	Young's Modulus	Elongation at break	Tensile Strength	Young's Modulus	Elongation at break
	σ (MPa)	E (MPa)	ϵ (%)	σ (MPa)	E (MPa)	ϵ (%)
MC0	15,55±0,8	30,33±1,1	301,02±15	12,2±0,5	20,4±1,3	250,5±16,2
MC1	17,38±0,5	40,24±0,9	340,3±20	15,6±1	37,23±0,9	300,09±17,9
MC2	18±0,7	44,23±0,8	344,14±21	17,6±0,6	40,2±1,4	305,76±18,9
MC3	18,5±0,8	56,41±1	351,5±19,6	17,9±0,9	52,7±1,6	320±14
MC4	19,6±1	60,32±1,3	381,62±19	19±0,7	56,4±0,6	360,34±16,5
MC5	16,84±1	36,03±0,9	313,05±22	15±1,5	31,1±0,7	287,91±16,5
MC6	16,5±0,4	42,27±1,2	314,11±17	15,9±0,3	39,2±1,2	290,7±16,5
MC7	6,06±0,5	95.14±5,1	11,52±0,6	5,50±0,4	90,26±4,9	10,4±0,5
MC8	5,98±0,3	99.20±4	13,72±0,9	5,60±0,4	96,22±5,7	12,5±0,8
MC9	5,38±0,3	115.33±8,3	17,06±12	4,98±0,2	110±8,6	16,12±1,1
NC10	7.00±0,5	130.19±9	18,11±1,4	6,80±0,3	127,21±10	17,5±1
MC11	3,73±0,2	80.20±7,2	11±0,5	3,63±0,5	75,03±5	10±0,7
MC12	4,61±0,4	65.44±5,5	13,3±11	4,58±0,3	62±3,9	12,6±0,9

3.3.3. Thermal Stability of PVC and PVC-LDPE Microcomposites

Figure 3.4(a,b) shows the results of congo red tests and discoloration of three different concentrations of thermal stabilizers with (CaSt₂: ZnSt₂=9 :1 and CaSt₂: ZnSt₂=1 :9). As shown in Figure 3.4(a) , the PVC microcomposites MC4 and MC6, when the thermal stabilizer is rich in calcium, it can relatively improve the thermal stability time (t=160min)[34, 35]. Whereas, in Figure 3.4(b) thermal stability increased with increasing heat stabilizer concentrations and delayed the discoloration of PVC samples with a significant resistance to discoloration of PVC-LDPE samples MC10 and MC12 which the incorporation of LDPE into PVC showed much better antidiscoloration compared with PVC microcomposites. In addition, the samples rich in Zinc stearate MC1, MC3, MC5, MC7, MC9, and MC11 quickly turned to dark color, the reason is that ZnSt₂ can remove initial coloration by substituting labile chlorine atoms from the PVC chain [36]. However, the heat stabilizer rich in calcium stearate increases the PVC stabilization time due to the inhibition of ZnCl₂ which is responsible for dehydrochlorination process [37].

CHAPTER 3. APPLICATION 1

As is known, CaSt_2 could react with ZnCl_2 to regenerate ZnSt_2 and CaCl_2 via ester exchange reaction. On the other side, a detailed computational study is required to understand the dehydrochlorination process in presence of CaSt_2 and ZnSt_2 .

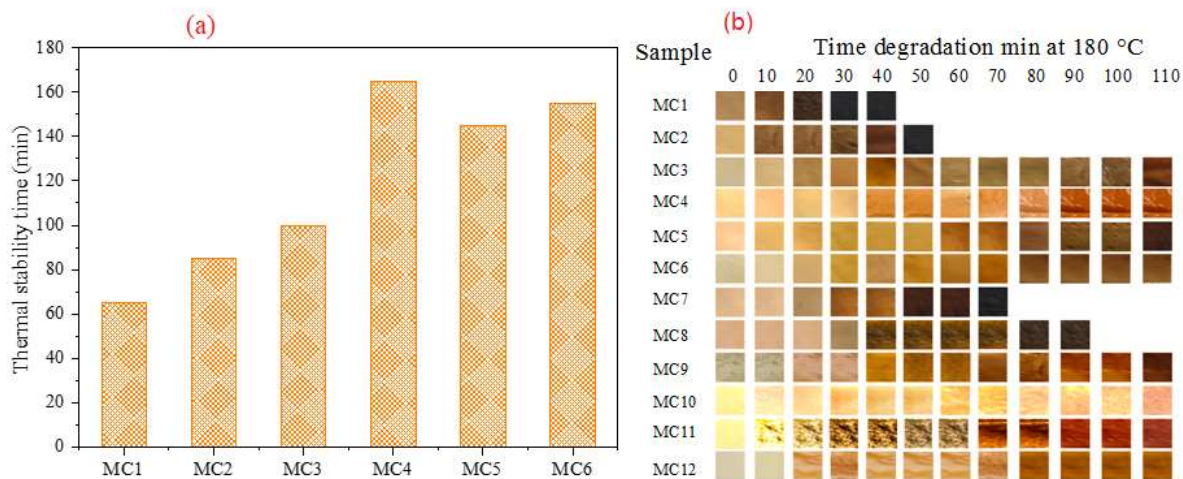


Fig 3.4. (a) Thermal stability time (Congo red test) of PVC microcomposites at 180°C.

(b) Discoloration photos of PVC and PVC-LDPE microcomposites at 180°C for 110 min.

3.3.4. Thermogravimetric Analysis (TGA, DTG)

The thermo-gravimetric curves of PVC and PVC-LDPE microcomposite with different metal mixed heat stabilizers ratios are plotted in Figures 3.5(a-d). The important temperatures and different thermal degradation levels of PVC and PVC-LDPE microcomposites are summarized in Table 3.3. As shown in the TGA graphs, thermal degradation of PVC and PVC-LDPE occurred in two major steps.

Figure 3.5(a, b) shows the first degradation of PVC begins around 277°C with remarkably lose weight which is attributed to the dehydrochlorination of PVC and the second degradation is related to the scission polyene sequences [38]. The onset degradation temperatures of PVC microcomposites are in the range of 276-290°C. It is observed that the samples MC1 and MC2 have lower decomposition temperatures as compared to any other PVC microcomposite, due to a small amount of heat stabilizer incorporated in the PVC matrix, moreover, as long as the heat stabilizer is increased, the PVC degradation is delayed significantly in the MC4, MC5 and MC6 samples, in which MC4 sample shifts to higher values. As expected, the thermal stability of samples containing high calcium concentration is much better than samples with high zinc concentration into mixed metal stabilizer, due to the ability of CaSt_2 to absorb more HCl which

CHAPTER 3. APPLICATION 1

indeed leads to much less dehydrochlorination, and more stability of PVC microcomposites [39].

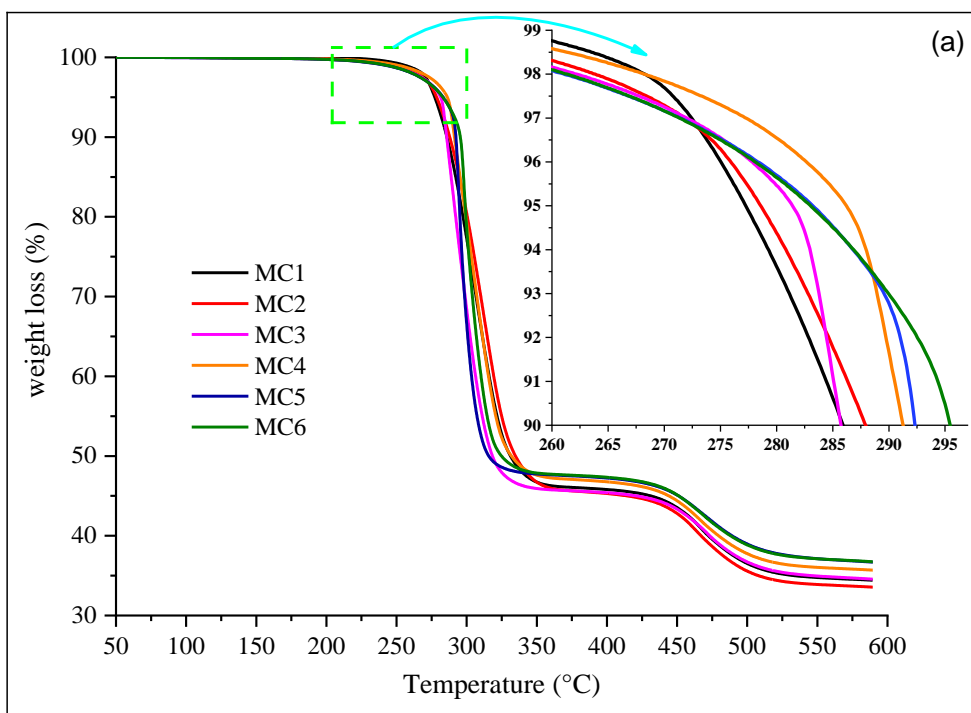


Fig 3.5(a). TGA curves of PVC microcomposites.

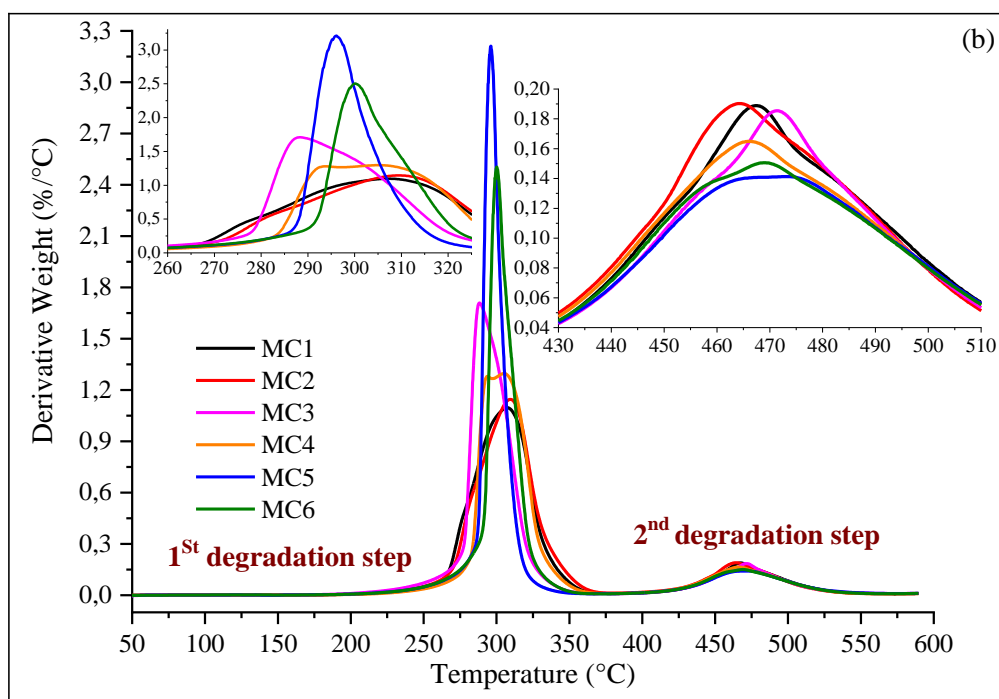


Fig 3.5(b). DTG curves of PVC microcomposites.

CHAPTER 3. APPLICATION 1

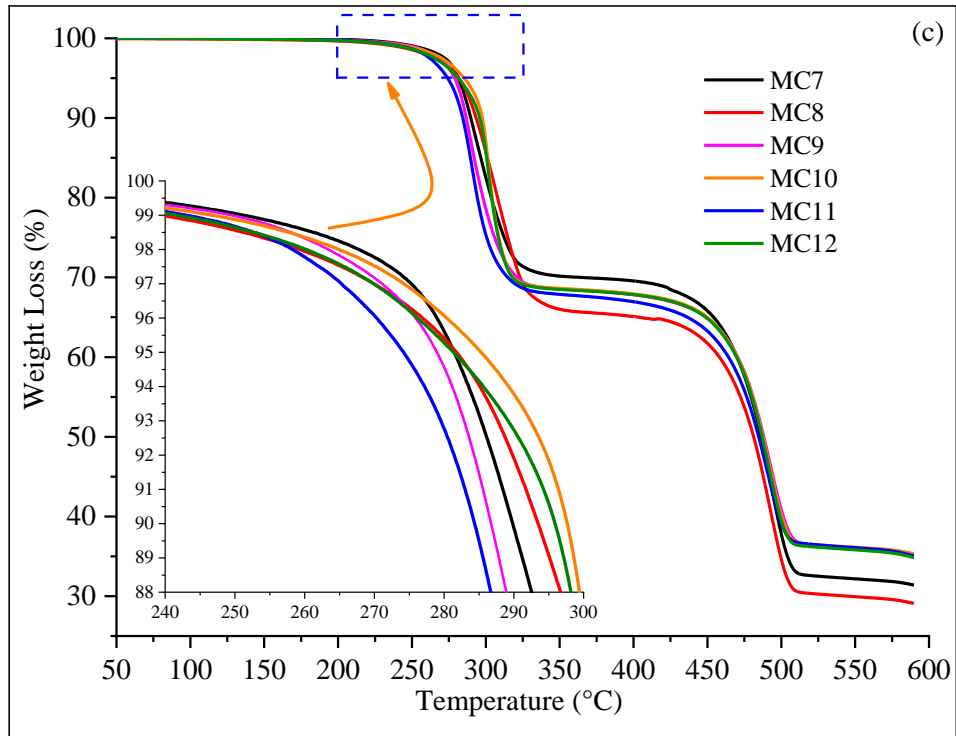


Fig 3.5(c). TGA curves of PVC-LDPE blend microcomposites.

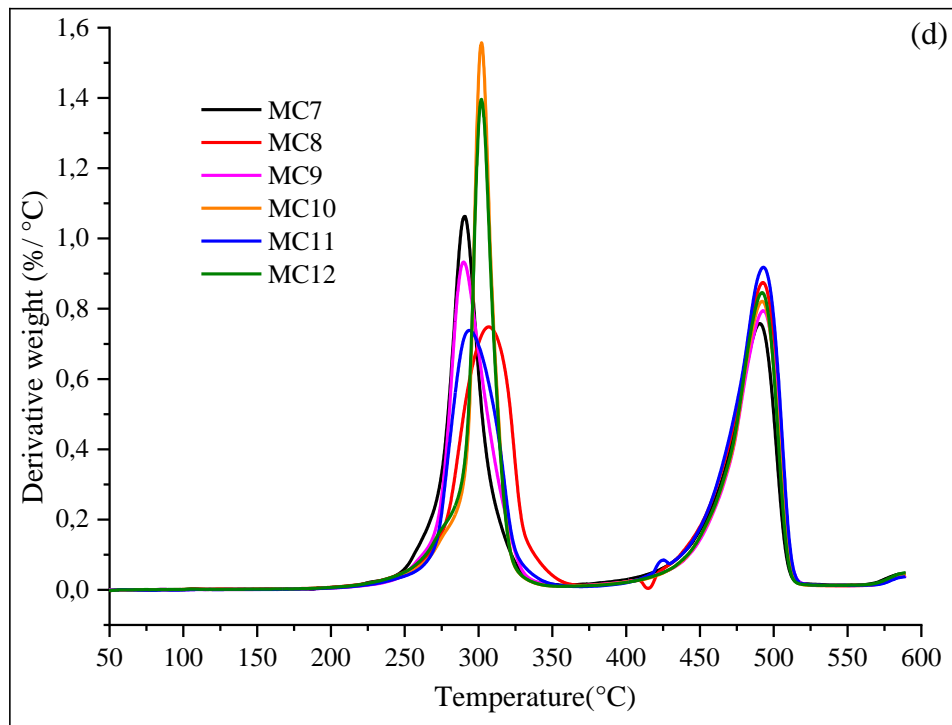


Fig 3.5(d). DTG curves of PVC-LDPE blend microcomposites.

Figures 3.5(c, d) represented the influence of LDPE on the thermal degradation of PVC, which plays the same role as heat stabilizer. Similarly to PVC degradation, it can be seen that the

CHAPTER 3. APPLICATION 1

optimum concentration of mixed stearate $\text{CaSt}_2 : \text{ZnSt}_2 = 9 : 1$ for the degradation of PVC-LDPE microcomposite is 5 phr, in addition, it can be concluded that the incorporation of LDPE into PVC enhances the values of onset degradation temperatures up to 290°C and retards the degradation process [29], accordingly to the mechanism which was proposed by Thongpin et al. [40], and Sombatsompop et al. [22], in particular through the starting of the initiation co-cross-linking process which results in macro-radical recombination reactions which lead to producing more short chains, PVC grafted with LDPE at high temperatures.

Table 3.3. Interested decomposition temperatures and weight loss levels of PVC and PVC/LDPE microcomposites.

Sample	Decomposition Temperature							
	T_{Onset} ($^\circ\text{C}$)	$T^{10\%}$ ($^\circ\text{C}$)	First stage			Second stage		
			T_{max} ($^\circ\text{C}$)	Weight Loss (%)	T_{range} /($^\circ\text{C}$)	T_{max} ($^\circ\text{C}$)	Weight Loss (%)	T_{range} /($^\circ\text{C}$)
MC1	277.28	285.36	399.54	54.07	277-343	468.30	66.50	442-490
MC2	278.72	286.43	301.22	53.10	278-350	464.63	67.50	440-493
MC3	281.13	284.10	288.00	54.00	281-335	474.49	66.30	441-494
MC4	285.55	291.29	302.91	51.09	286-355	473.75	64.21	444-498
MC5	283.30	292.24	296.23	52.51	283-330	470.27	63.00	445-502
MC6	284.61	295.56	300.32	52.23	284-339	470.02	62.10	446-501
MC7	283.52	289.83	290.20	31.00	283-315	490.6	67.40	468-505
MC8	284.48	293.53	305.80	34.00	285-317	491.01	70.50	463-508
MC9	281.00	286.72	290.03	31.45	281-323	490.55	64.60	470-509
MC10	290.20	297.72	304.82	31.35	290-325	492.51	63.50	474-511
MC11	277.22	285.44	292.65	31.90	276-322	490.06	68.55	471-508
MC12	286.42	296.06	300.19	31.50	286-324	492.23	64.85	472-510

3.3.5. Scanning Electron Microscopy (SEM) Results

Figure 3.6. Presents SEM micrographs for fracture surfaces of PVC and PVC-LDPE with CaCO_3 particles and $\text{CaSt}_2 : \text{ZnSt}_2 = 9 : 1$. (Figure 3.6(a)) and (Figure 3.6(c)) show that the hydrophilic CaCO_3 micro-particles were highly aggregated in the PVC matrix, with several voids present, leading to a decrease in the interfacial adhesion between CaCO_3 particles and PVC matrix [41]. (Figure 3.6(b)) and (Figure 3.6(d)) reveal good compatibility between

CHAPTER 3. APPLICATION 1

CaCO₃microparticles and PVC-LDPE mixtures compared with PVC matrix, due to the good distribution of CaCO₃ in the blend. As the PVC was blended with LDPE, the CaCO₃ were well dispersed in the PVC-LDPE blend, which led to a strong interfacial interaction between PVC-LDPE and CaCO₃ microparticles [42].

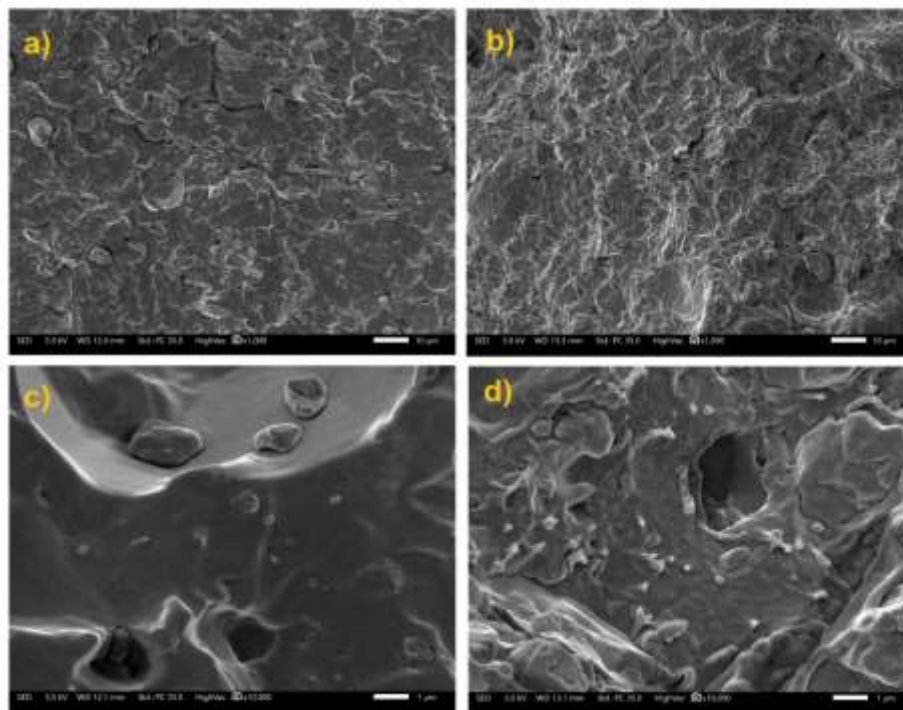


Fig 3.6. SEM images of the fracture surfaces of (a, c) MC4 and (b, d) MC10 microcomposites.

3.3.6. The Results from DFT Calculations

Geometries optimization of reactants, transitions state and products were depicted in Figure 3.7(a). PVC polymer, which may be regarded as polar, interacted with the polar part of thermal stabilizers. The strong hydrogen bond between H of PVC and O of CaSt₂ and ZnSt₂ is 2.29 and 2.35 Å, respectively, reveals the stability of reactants. In addition, Ca and Zn formed electrostatic bonds with Cl by 2.87 and 2.49 Å, respectively. The simultaneous transfer of the chlorine and the hydrogen to the thermal stabilizers leads to the formation of unsaturated groups in PVC and takes place via TS1 and TS2 which lies 29.6 and 25.0 kcal/mol, respectively, above reactants. The free energy profiles of the dehydrochlorination process are displayed in Figure 3.7(b), we found that the dehydrochlorination process can occur via a concerted mechanism with four-member ring transition state and the free activation energy with ZnSt₂ is smaller than that with CaSt₂. Our DFT results are consistent with previous theoretical and experimental results [39, 43].

CHAPTER 3. APPLICATION 1

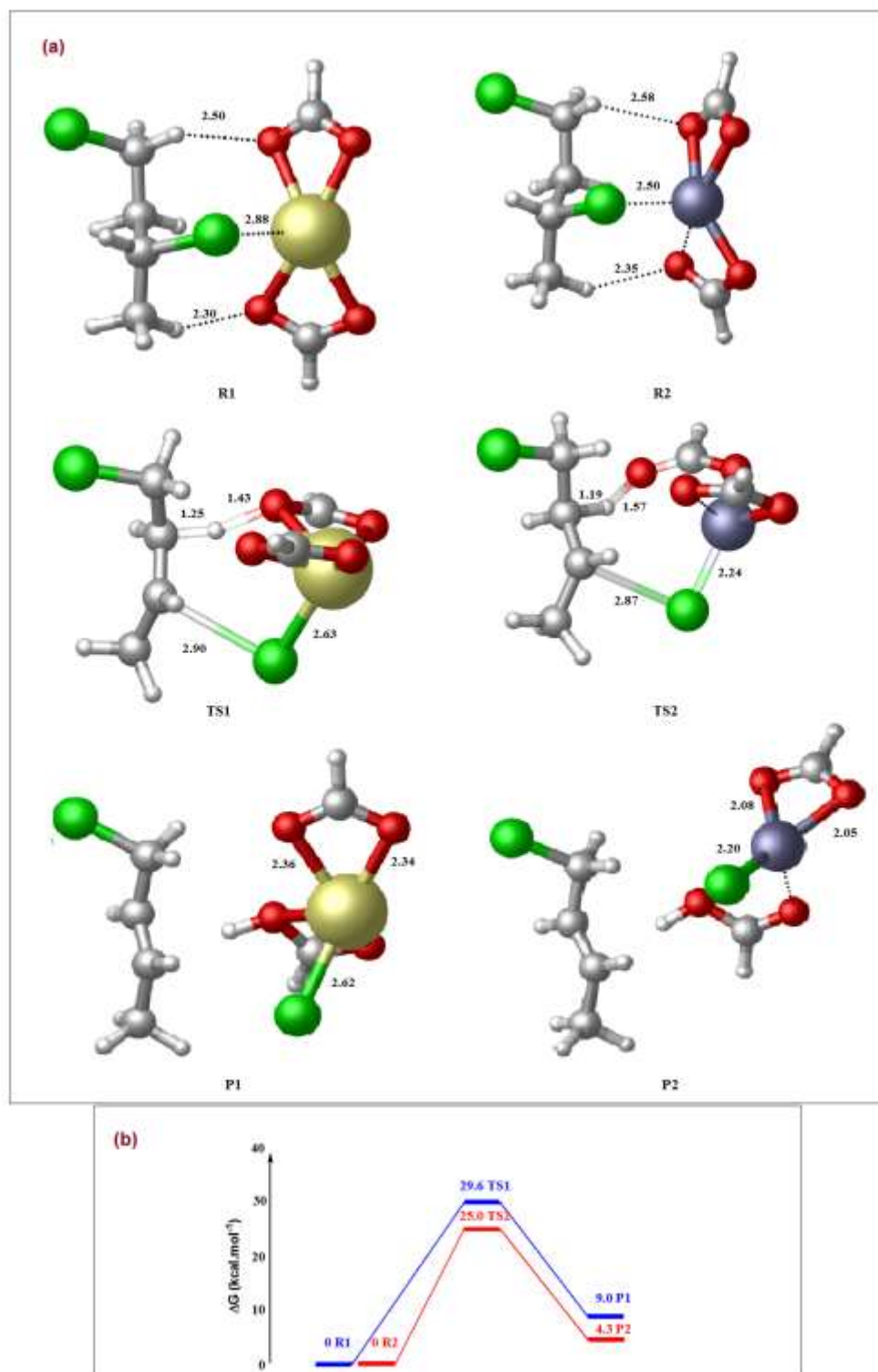


Fig 3.7. (a) Optimized geometries of reactants, transition states and products for the thermal dehydrochlorination of PVC with different thermal stabilizers. Distance given in Å. Atom color code: H in white, C in grey, Cl in green, O in red, Ca in yellow and Zn in blue and (b) Relative free energies of the dehydrochlorination process with (blue) CaSt₂ and (red) ZnSt₂ at the M06-2X/6-31++G (p, d) level.

CHAPTER 3. APPLICATION 1

3.4. CONCLUSIONS

This work highlights the importance of different additives, such as mixed metal calcium/zinc stearate, CaCO_3 particles, and LDPE with their positive effects to enhancing the polyvinylchloride (PVC) properties. The following conclusions are listed as follows.

- (1) The $\text{CaSt}_2/\text{ZnSt}_2$ stearate as heat stabilizer does not affect alone PVC degradation and mechanical properties, but the addition of LDPE in the PVC helps to upgrade the performance of the latter to be used in several fields.
- (2) The optimum ratio of ($\text{CaSt}_2: \text{ZnSt}_2 = 9:1$) was 5phr which can yield good thermal stability and high mechanical performance of PVC microcomposite before and after the heat ageing test.
- (3) LDPE as a thermoplastic polymer, with 50 phr content, exhibited the best young modulus before and after heat ageing, and confirmed the ability to be a highly effective compound to protecting the thermal stability of the PVC.
- (4) Thermal analysis revealed the excellent synergistic effects of CaCO_3 , heat stabilizer rich in calcium and LDPE for more thermal stability of PVC polymer.
- (5) SEM micrographs investigate that the CaCO_3 microparticles is well dispersed in the PVC-LDPE blend, which leads to a strong interfacial interaction between PVC and LDPE.
- (6) DFT calculation revealed that dehydrochlorination process can occur by the simultaneous transfer of the chlorine and the hydrogen to the thermal stabilizers via a concerted mechanism with four- member ring transition state with a low free energy barrier in favor of ZnSt_2 . This can help polymerists to design new thermal stabilizers for PVC.

ACKNOWLEDGEMENTS

The authors are grateful to the staff of plastic laboratory of (Entreprise des Industries du Câble ENICAB), Biskra, Algeria, for supplying the polymer materials and their additives of this work, the (Centre de Recherche Scientifique & Technique en Analyse Physico-Chimiques CRAPC), Tipaza, Algeria, for thermal analysis. The authors are also thankful acknowledgments to Dr. Antoine Kervoelen and Anthony Magueresse for supporting this experimental work by the characterization methods.

CHAPTER 3. APPLICATION 1

REFERENCES

1. Yao, J., Zhou, Z., Zhou, H.: Highway engineering composite material and its application. *Highw. Eng. Compos. Mater. Its Appl.* 1–163 (2019).
2. Grigorescu, R.M., Ghioca, P., Iancu, L., David, M.E., Andrei, E.R., Filipescu, M.I., Ion, R.M., Vuluga, Z., Anghel, I., Sofran, I.E., Nicolae, C.A., Gabor, A.R., Gheboianu, A., Bucurica, I.A.: Development of thermoplastic composites based on recycled polypropylene and waste printed circuit boards. *Waste Manag.* 118, 391–401 (2020).
3. Liu, Y., Zhou, C., Li, F., Liu, H., Yang, J.: Stocks and flows of polyvinyl chloride (PVC) in China: 1980-2050. *Resour. Conserv. Recycl.* 154, (2020).
4. Ye, L., Qi, C., Hong, J., Ma, X.: Life cycle assessment of polyvinyl chloride production and its recyclability in China. *J. Clean. Prod.* 142, 2965–2972 (2017).
5. Ali, I., Yang, W., Li, X., Ali, A., Jiao, Z., Xie, P., Dias, O.A.T., Pervaiz, M., Li, H., Sain, M.: Highly electro-responsive plasticized PVC/FMWCNTs soft composites: A novel flex actuator with functional characteristics. *Eur. Polym. J.* 126, 109556 (2020).
6. Yu, J., Sun, L., Ma, C., Qiao, Y., Yao, H.: Thermal degradation of PVC: A review. *Waste Manag.* 48, 300–314 (2016).
7. Jordan, K.J., Suib, S.L., Koberstein, J.T.: Determination of the degradation mechanism from the kinetic parameters of dehydrochlorinated poly(vinyl chloride) decomposition. *J. Phys. Chem. B.* 105, 3174–3181 (2001).
8. Balköse, D., Gökçel, H.İ., Göktepe, S.E.: Synergism of Ca/Zn soaps in poly(vinyl chloride) thermal stability. *Eur. Polym. J.* 37, 1191–1197 (2001).
9. Zhang, M., Han, W., Hu, X., Li, D., Ma, X., Liu, H., Liu, L., Lu, W., Liu, S.: Pentaerythritol p-hydroxybenzoate ester-based zinc metal alkoxides as multifunctional antimicrobial thermal stabilizer for PVC. *Polym. Degrad. Stab.* 181, 109340 (2020).
10. Liu, Y. Bin, Liu, W.Q., Hou, M.H.: Metal dicarboxylates as thermal stabilizers for PVC. *Polym. Degrad. Stab.* 92, 1565–1571 (2007).
11. Wang, M., Song, X., Jiang, J., Xia, J., Li, M.: Binary amide-containing tung-oil-based Ca/Zn stabilizers: effects on thermal stability and plasticization performance of poly(vinyl chloride) and mechanism of thermal stabilization. *Polym. Degrad. Stab.* 143,

CHAPTER 3. APPLICATION 1

- 106–117 (2017).
12. Korkusuz, Tüzüm Demir, A.P.: Evaluation of the thermal stabilization behavior of hydrotalcite against organic stabilizers for plasticized PVC films. *Polym. Bull.* 77, 4805–4831 (2020).
 13. Ye, F., Ye, Q., Zhan, H., Ge, Y., Ma, X., Xu, Y., Wang, X.: Synthesis and study of zinc orotate and its synergistic effect with commercial stabilizers for stabilizing poly(vinyl chloride). *Polymers (Basel)*. 11, (2019).
 14. Li, M., Zhang, J., Xin, J., Huang, K., Li, S., Wang, M., Xia, J.: Design of green zinc-based thermal stabilizers derived from tung oil fatty acid and study of thermal stabilization for PVC. *J. Appl. Polym. Sci.* 134, 16–20 (2017).
 15. Wang, M., Song, X., Jiang, J., Xia, J., Li, S., Li, M.: Excellent hydroxyl and nitrogen rich groups-containing tung-oil-based Ca/Zn and polyol stabilizers for enhanced thermal stability of PVC. *Thermochim. Acta.* 658, 84–92 (2017).
 16. Ye, F., Guo, X., Zhan, H., Lin, J., Lou, W., Ma, X., Wang, X.: The synergistic effect of zinc urate with calcium stearate and commercial assistant stabilizers for stabilizing poly(vinyl chloride). *Polym. Degrad. Stab.* 156, 193–201 (2018).
 17. Wang, M., Li, S., Ding, H., Xia, J., Li, M.: Construction of efficient tung-oil-based thermal stabilizers bearing imide and epoxy groups for PVC. *New J. Chem.* 44, 4538–4546 (2020).
 18. Li, X., Xiao, Y., Wang, B., Tang, Y., Lu, Y., Wang, C.: Effects of poly(1,2-propylene glycol adipate) and nano-CaCO₃ on DOP migration and mechanical properties of flexible PVC. *J. Appl. Polym. Sci.* 124, 1737–1743 (2012).
 19. Liu, P., Zhao, M., Guo, J.: Thermal stabilities of poly(vinyl chloride)/calcium carbonate (PVC/CaCO₃) composites. *J. Macromol. Sci. Part B Phys.* 45 B, 1135–1140 (2006).
 20. Ahamad, A., Patil, C.B., Gite, V. V., Hundiwale, D.G.: Evaluation of the synergistic effect of layered double hydroxides with micro- and nano-CaCO₃ on the thermal stability of polyvinyl chloride composites. *J. Thermoplast. Compos. Mater.* 26, 1249–1259 (2013).
 21. Yin, B., Hakkarainen, M.: Flexible and strong ternary blends of poly(vinyl chloride), poly(butylene adipate) and nanoparticle-plasticizers. *Mater. Chem. Phys.* 139, 734–740

CHAPTER 3. APPLICATION 1

- (2013).
22. Sombatsompop, N., Sungsanit, K., Thongpin, C.: Structural changes of PVC in PVC/LDPE melt-blends: Effects of LDPE content and number of extrusions. *Polym. Eng. Sci.* 44, 487–495 (2004).
 23. Maou, S., Meghezzi, A., Nebbache, N., Meftah, Y.: Mechanical, morphological, and thermal properties of poly(vinyl chloride)/low-density polyethylene composites filled with date palm leaf fiber. *J. Vinyl Addit. Technol.* 25, (2019).
 24. Zhao, Y., Truhlar, D.G.: Density Functionals with Broad Applicability in Chemistry. *Acc. Chem. Res.* 41, 157–167 (2008).
 25. Huang, J., He, C., Li, X., Pan, G., Tong, H.: Theoretical studies on thermal degradation reaction mechanism of model compound of bisphenol A polycarbonate. *Waste Manag.* 71, 181–191 (2018).
 26. Huang, J., Li, X., Zeng, G., Cheng, X., Tong, H., Wang, D.: Thermal decomposition mechanisms of poly(vinyl chloride): A computational study. *Waste Manag.* 76, 483–496 (2018).
 27. Huang, J., Li, X., Meng, H., Tong, H., Cai, X., Liu, J.: Studies on pyrolysis mechanisms of syndiotactic polystyrene using DFT method. *Chem. Phys. Lett.* 747, 137334 (2020).
 28. Blazsó, M., Zelei, B., Jakab, E.: Thermal decomposition of low-density polyethylene in the presence of chlorine-containing polymers. *J. Anal. Appl. Pyrolysis.* 35, 221–235 (1995).
 29. Wu, J., Chen, T., Luo, X., Han, D., Wang, Z., Wu, J.: TG/FTIR analysis on co-pyrolysis behavior of PE, PVC and PS. *Waste Manag.* 34, 676–682 (2014).
 30. Zhu, H.M., Jiang, X.G., Yan, J.H., Chi, Y., Cen, K.F.: TG-FTIR analysis of PVC thermal degradation and HCl removal. *J. Anal. Appl. Pyrolysis.* 82, 1–9 (2008).
 31. Wang, Z., Xie, T., Ning, X., Liu, Y., Wang, J.: Thermal degradation kinetics study of polyvinyl chloride (PVC) sheath for new and aged cables. *Waste Manag.* 99, 146–153 (2019).
 32. Rabinovitch, E.B., Lacatus, E., Summers, J.W.: The lubrication mechanism of calcium stearate/paraffin wax systems in PVC compounds. *J. Vinyl Technol.* 6, 98–103 (1984).

CHAPTER 3. APPLICATION 1

33. Xu, C., Fang, Z., Zhong, J.: Study on compatibilization-crosslinking synergism in PVC/LDPE blends. *Die Angew. Makromol. Chemie.* 212, 45–52 (1993).
34. Shi, Y., Chen, S., Ma, M., Wu, B., Ying, J., Xu, X., Wang, X.: Highly efficient and antibacterial zinc norfloxacin thermal stabilizer for poly(vinyl chloride). *RSC Adv.* 6, 97491–97502 (2016).
35. Wu, B., Wang, Y., Chen, S., Wang, M., Ma, M., Shi, Y., Wang, X.: Stability, mechanism and unique “zinc burning” inhibition synergistic effect of zinc dehydroacetate as thermal stabilizer for poly(vinyl chloride). *Polym. Degrad. Stab.* 152, 228–234 (2018).
36. Liu, Z., Fan, J., Feng, J., Li, M., Hu, Y., Hao, W., Feng, F.: Study on the use of rare earth stabilizer as poly(vinyl chloride) stabilizer. *J. Vinyl Addit. Technol.* 1–12 (2020).
37. Jiang, P., Song, Y., Dong, Y., Yan, C., Liu, P.: Zinc glycerolate with lanthanum stearate to inhibit the thermal degradation of poly(vinyl chloride). *J. Appl. Polym. Sci.* 127, 3681–3686 (2013).
38. Chen, J., Liu, Z., Nie, X., Zhou, Y., Jiang, J., Murray, R.E.: Plasticizers derived from cardanol: synthesis and plasticization properties for polyvinyl chloride(PVC). *J. Polym. Res.* 25, 14–16 (2018).
39. González-Ortiz, L.J., Arellano, M., Jasso, C.F., Mendizábal, E., Sánchez-Peña, M.J.: Thermal stability of plasticized poly(vinyl chloride) compounds stabilized with pre-heated mixtures of calcium and/or zinc stearates. *Polym. Degrad. Stab.* 90, 154–161 (2005).
40. Thongpin, C., Santavitee, O., Sombatsompop, N.: Degradation mechanism and mechanical properties of PVC in PVC-PE melt blends: Effects of molecular architecture, content, and MFI of PE. *J. Vinyl Addit. Technol.* 12, 115–123 (2006).
41. Sun, S., Li, C., Zhang, L., Du, H.L., Burnell-Gray, J.S.: Interfacial structures and mechanical properties of PVC composites reinforced by CaCO₃ with different particle sizes and surface treatments. *Polym. Int.* 55, 158–164 (2006).
42. Pham, H.N.T., Nguyen, V.T.: Effect of calcium carbonate on the mechanical properties of polyethylene terephthalate/polypropylene blends with styrene-ethylene/butylene-styrene. *J. Mech. Sci. Technol.* 34, (2020).
43. Wang, Y., Wang, X., Liu, L., Peng, X.: Theoretical study on the thermal

CHAPTER 3. APPLICATION 1

dehydrochlorination of model compounds for poly(vinyl chloride). J. Mol. Struct. THEOCHEM. 896, 34–37 (2009).

CHAPTER 4. APPLICATION 2

MECHANICAL, MORPHOLOGICAL, AND THERMAL PROPERTIES OF POLYVINYL CHLORIDE / LOW DENSITY POLYETHYLENE COMPOSITES FILLED WITH DATE PALM LEAF FIBER

ABSTRACT

This chapter investigates the mechanical, morphological, and thermal properties of polyvinyl chloride (PVC) and low-density polyethylene (LDPE) blends, at three different concentrations: 20, 50, and 80 wt.% of LDPE. Besides, composite samples that were prepared from PVC-LDPE blend reinforced with different date palm leaf fiber (DPLF) content, 10, 20, and 30 wt.%, were also studied and characterized using mechanical tests, thermal analysis and scanning electron microscopy (SEM). The sample in which PVC-LDPE (20 wt.%/80 wt.%) had the greatest tensile strength, elongation at break, and modulus. The good thermal stability of this sample can be seen that T10% and T20% occurred at higher temperatures compared to others blends. DPLF slightly improved the tensile strength of the polymer blend matrix at 10 wt.% (C10). The modulus of the composites increased significantly with increasing filler content. Ageing conditions at 80 °C for 168 h slightly improved the mechanical properties of composites. Scanning electron microscopic micrographs showed that morphological properties of tensile fracture surfaces are in accordance with the tensile properties of these blends and composites. Thermogravimetric analysis and derivative thermogravimetry show that the thermal degradation of PVC-LDPE (20 wt.%/ 80 wt.%) blend and PVC-LDPE-DPLF (10 and 30 wt.%) composites took place in two steps: in the first step, the blend was more stable than the composites. In the second step, the composites showed a slightly better stability than the PVC-LDPE (20 wt.%/ 80 wt.%) blend. Based on the above investigation, these new green composites (PVC-LDPE-DPLF) can be used in several applications.

Keywords: Polymer blend, Polyvinyl chloride, Low density polyethylene, Composite, Date palm fiber, Mechanical properties.

CHAPTER 4. APPLICATION 2

4.1. INTRODUCTION

Date palm (*Phoenix dactylifera* L) is a widespread plant cultivated in all Saharan countries. Date palm is the basis of Algerian Saharan oasis agriculture, and the valorization of date palm fiber in material engineering is an important economic activity in northern Africa. Lignocellulosic fibers obtained from palm date trees have received increasing attention in composite processing. Wood fibers are among the most frequently used natural materials because of their low weight, high performance, low cost, renewable character, high specific modulus, availability, and biodegradability [1–3]. The replacement of glass fiber with cheaper natural fiber is an ongoing quest in academia and industry [4,5]. Over the last decade, much effort has been devoted to preparing polymeric matrices from date palm fibers [6–12]. Several researchers have studied the mechanical and thermal properties of thermoplastic composites reinforced with date palm fiber [13–15]. Natural fiber reinforced polymer composites are already being used extensively in different fields [16]. Poly (vinyl chloride) (PVC) is a widely used base material in the industry [17,18]. PVC is a polymer with low thermal stability, so easily degradable by dehydrochlorination around 100°C as a result of the formation of conjugated double bonds and polyene sequences [19]. Naghmouchi et al. studied PVC filled with olive stone flour [20]. Blending polymers is an effective way to prepare new polymeric materials with better properties than virgin polymers [21,22]. In particular, the addition of low-density polyethylene (LDPE) into PVC was shown to improve certain blend properties [23], but the incompatibility between PVC and LDPE can decrease the mechanical properties of resulting blends [24]. It was reported that chlorinated polyethylene, poly (methyl methacrylate-co-butyl acrylate), and poly (ethylene-co-meth- acrylate) significantly improved the compatibility of the PVC-LDPE blend [25]. To enhance the compatibility between wood fibers and PVC-LDPE blends, chemical treatments were applied to fibers with Maleic anhydride-grafted- polyethylene and Silane A-137 or Silane A-1100 [26]. Using the untreated natural fiber as reinforcement in composites is more convenient than using treated natural fiber, because synthetic fibers are not always produced using “Green Chemistry” methods: (1) using polluting; (2) producing hazardous chemicals; (3) posing a risk to the environment [27]. The Algerian palm grove, the pivot of the oasis ecosystem, generates significant amounts of waste. Our work aims to recover this waste in the production of green composites. In this chapter, we investigate the mechanical, morphological, and thermal properties of composites based on PVC-LDPE; moreover, we used cheap and biodegradable waste material abundantly present in Saharan countries, in particular, the afore mentioned date palm leaf fiber (DPLF), as a reinforcement of the new composites.

CHAPTER 4. APPLICATION 2

4.2. EXPERIMENTAL DETAILS

4.2.1. Materials

This study concerns two fundamentally different thermoplastics as matrix: an amorphous PVC and a semi crystalline LDPE. PVC type 4000M and LDPE (melting point = 129 °C; the specific enthalpy of melting=106 J/g) produced by the Algerian Company named “Enterprise National des Industries Pétro-chimiques” ENIP’ in Skikda on the Eastern Coast of Algeria. PVC has the following physical characteristics according to table 4.1 and with commercial grade additives according to Table 4.2.

Table 4.1. properties of PVC

Properties	Values
K value	67- 72
Degree of polymerization	1250 – 1450
Bulk density without compacting	0,43 - 0,50
Apparent density after compaction	0,53 - 0,63
Free flow	≥ 10g/S
Moisture content	≤ 0,3%
Thermal stability	60 min at 180°C

Table 4.2. Additives of PVC

Additives	PVC resin	Stabilizer (Ca/Zn)	Plasticizer (DOP)
Weight %	65	05	30

4.2.2. Date Palm Leaves Fibers Preparation

DPLFs were obtained from the date farm’s agricultural waste in Biskra, Algeria. DPLF washed ground and sieved to achieve a uniform particle size. The sieved wood was dried in a laboratory oven at 50°C to a final moisture content of 3% to 4% and stored in plastic bags for further compounding.

CHAPTER 4. APPLICATION 2

4.2.3. Blend and Composite Preparation.

DPLF was dried in an oven under vacuum at 80 °C overnight, to reduce the humidity content. A Gelimat thermo-kinetic mixer (a high-intensity turbine mixer) was used to mix the DPLF filler with the polymer matrix. PVC-LDPE blends (80/20, 50/50, and 20/80 wt.%) and composites PVC-LDPE (20/80 wt.%) filled with DPLFs (10, 20, and 30 wt.%) were prepared by a Brabender mono- screw extruder, the processing temperature ranged from 135 °C to 170 °C and compression molding press at 150 °C for 2 min at a mechanical pressure of 300 bar. The temperature was varied and optimized not only to obtain an easily processable homogeneous mixture but also to avoid the degradation of all composites. The different samples are shown in Table 4.3. The samples were machined by a hot hydraulic press after the extrusion process. Figure 4.1. shows the geometry of the specimens for mechanical testing.

Table 4.3. Different compositions and codes of the composite samples.

Samples	Date palm leaves	Polyvinyl chloride	Low density polyethylene
Codes	DPLFs %	PVC %	LDPE %
C0	0	20	80
C10	10	18	72
C20	20	16	64
C30	30	14	56

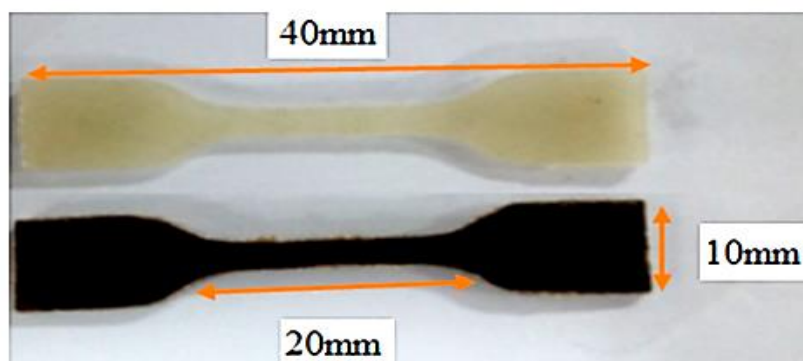


Fig 4.1. The geometry of the notched specimens for mechanical test.

4.2.4. Ageing Conditions

composites were subjected to heat ageing at 80°C for 168hr.

CHAPTER 4. APPLICATION 2

4.2.5. Characterization

4.2.5.1. Mechanical Characteristics

The mechanical properties mechanical in the tensile mode were measured at $25\text{ }^{\circ}\text{C} \pm 2\text{ }^{\circ}\text{C}$ using a many). Each tensile specimen was placed between two disks, and then subjected to tensile strength. As the specimen stretches, the software recorded provides the graph as well as all the desired of the specimen fractures. The various properties determined include tensile strength, elongation at break, and modulus. Tensile tests were performed at room temperature on samples with a length of 40 mm, a width of 10 mm, and a thickness of 2.0 mm, five samples were tested and an average value was reported.

4.2.5.2. Morphological Analysis

The morphology of the polymeric blends and the composites were studied using a Philips XL-30 scanning electron microscope (SEM).

4.2.5.3. Thermal Properties

The thermograms of the polymeric blends and the composites were recorded by using SDT Q600 (thermogravimetric analysis/derivative thermogravimetry [TGA/DSC] simultaneous thermogravimetric analyzer and differential scanning calorimeter) from TA Instruments under N_2 atmosphere from room temperature up to $600\text{ }^{\circ}\text{C}$ using a heating rate of $10\text{ }^{\circ}\text{C}/\text{min}$.

4.3. RESULTS AND DISCUSSION

4.3.1. Mechanical Results

4.3.1.1. Influence of LDPE Content on Mechanical Properties of Blends

Mechanical measurements were carried out to study the tensile properties of LDPE-PVC with different LDPE contents. Tensile strength, elongation at break, and modulus values in PVC-LDPE blends are shown in Figure 4.2.

It is obvious that the tensile strength, elongation at break, and modulus vary noticeably and attain the optimum values (9.53 MPa, 86%, 193 N/cm²), respectively, at about 80 wt.% of LDPE. Thongpin et al. [30] studied PVC-PE mixtures with different contents of PE which the contents of PE in PVC were varied from 0 to 30 wt.% of PVC resin and suggested that as the PE was increased, the mechanical characteristics of PVC-PE mixtures progressively deteriorated due to the thermodynamic incompatibility, but our experimental results indicate that mechanical properties of the blend improved significantly by increasing the LDPE content

CHAPTER 4. APPLICATION 2

to values above 50 wt.% in accordance with Bataille et al. [31] who studied a PE-PVC mixture for which the loadings of PE were varied from 0 to 100 wt.%. The matrix with LDPE (80 wt.%) content showed a significant improvement in the mechanical properties, this improvement can be attributed to the good adhesion between LDPE and PVC, this result was further confirmed by SEM micrographs (see below).

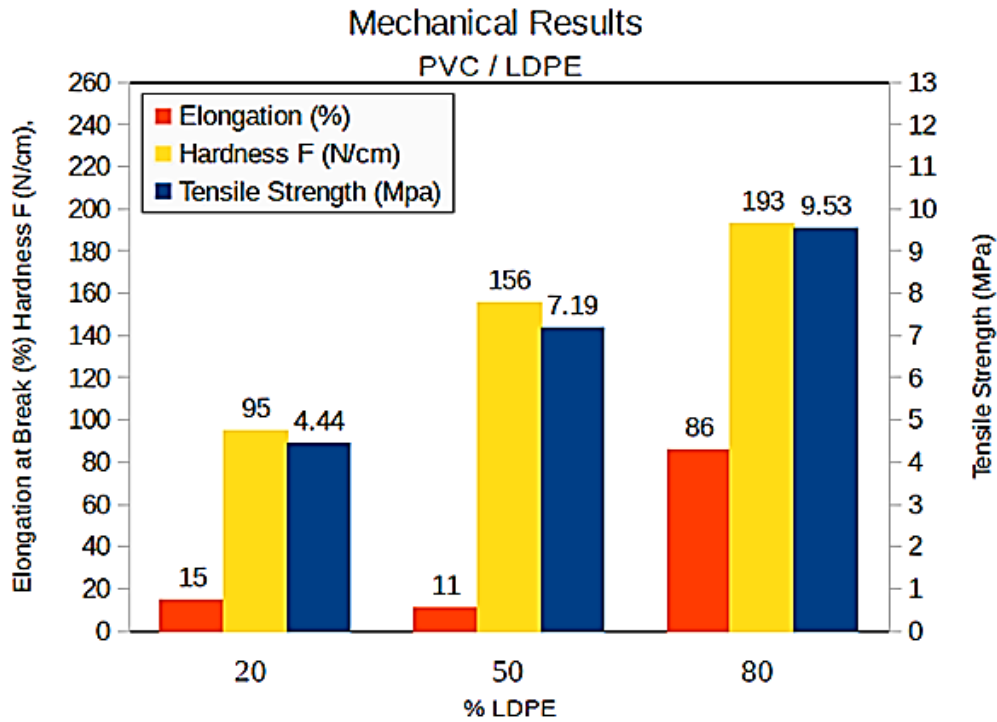


Fig 4.2. Evolution of the tensile strength, the elongation at break, and the modulus of PVC-LDPE with various LDPE content.

4.3.1.2. The Mechanical Properties of the Composites

In this subsection we characterize the mechanical properties of the composites tested in the tensile mode at room temperature (25 °C). The tensile strength (TS), elongation at break and modulus of PVC-LDPE (C0) matrix and PVC-LDPE-DPLF (C10, C20 and C30) composites before and after ageing are presented in Figure 4.3.

The sample (C0) tensile strength increased by 0.16 MPa after reinforcement with 10 wt.% of date palm fiber (C10). The Addition of 20 and 30 wt.% DPLF (C20, C30) decreased the tensile strength of the composites by 1.36, 1.17 MPa respectively, due to reduction in the interfacial bonding between matrix and DPLF [32].

CHAPTER 4. APPLICATION 2

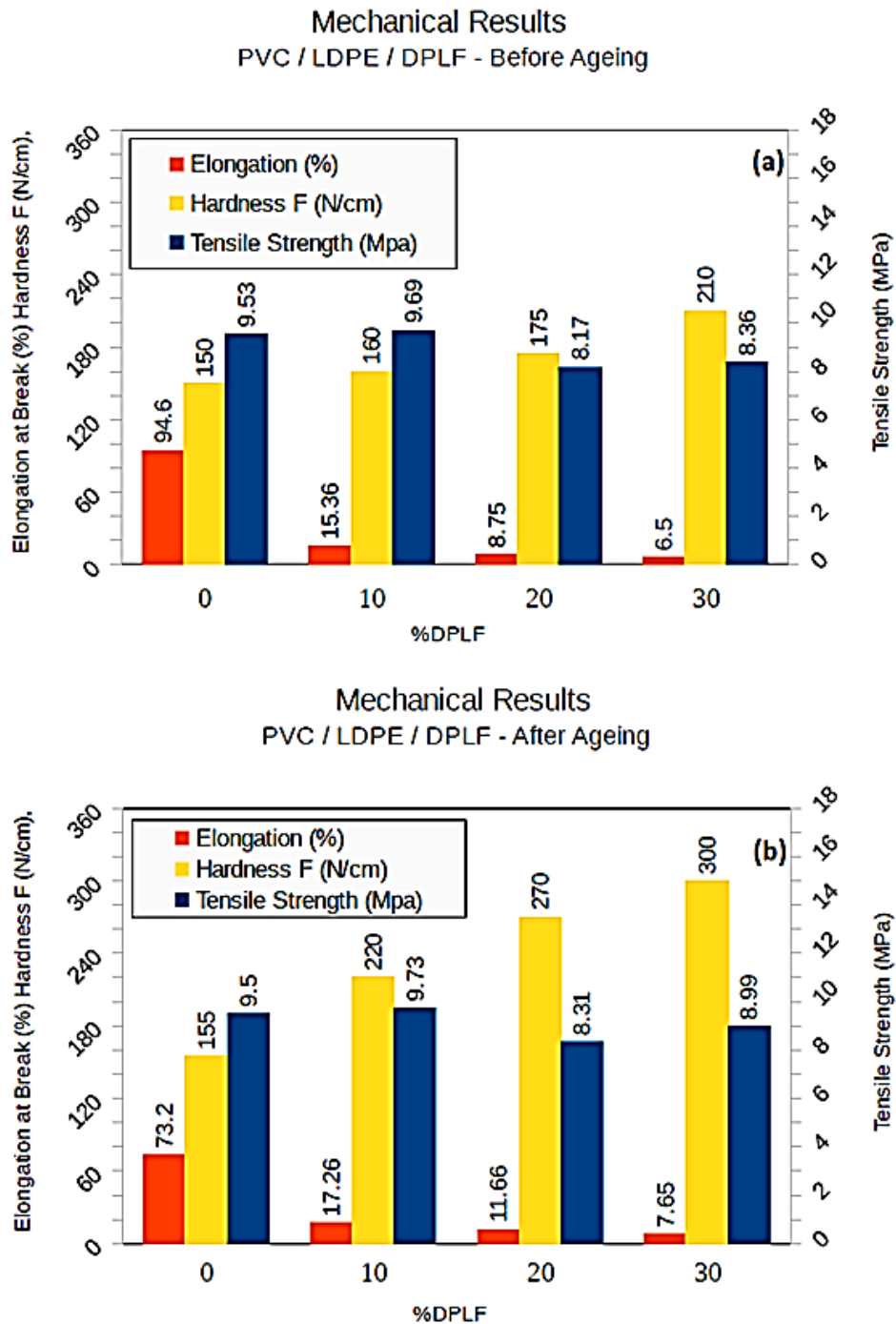


Fig 4.3. Evolution of the tensile strength, the elongation at break, and the modulus of PVC-LDPE (20/80) with various DPLF content (a) before and (b) after ageing.

Pure blend matrices (C0) showed very high elongation values. When date palm fibers were added to the polymer matrices, the % elongation at break decreased as visualized in Figure 4.3. Addition of DPLF to the blend matrix decreased the flexibility of the polymer matrix, due to the poor interfacial fiber-matrix adhesion [33], leading to quicker fracture than observed in pure

CHAPTER 4. APPLICATION 2

LDPE-PVC blend. Modulus is among the most important mechanical properties of polymers, which is evident in different applications [34]. The modulus increases noticeably when DPLF is added, due to the distribution of fillers in the matrix that makes the composites more rigid. The ageing process improved tensile strength, % elongation at break and modulus of all composites. Ultimately, this is due to moisture evaporation during the ageing process.

4.3.2. Morphological Results

Figure 4.4(a–c) shows SEM micrographs for fracture surfaces of the PVC-LDPE blends at three different concentrations 20, 50, and 80 wt.% of LDPE. The phase separation between PVC and LDPE is clearly observed in the blends containing low LDPE and becomes homogeneous at higher concentrations, for the morphology of the C10, a homogeneous surface and good dispersion of the DPLF were observed. Then, the miscibility became poor, and an agglomeration of the DPLF was seen in C20 and C30 as shown in Figure 4.4(d–f). All the SEM micrographs are in accordance with the tensile properties of these blends and composites.

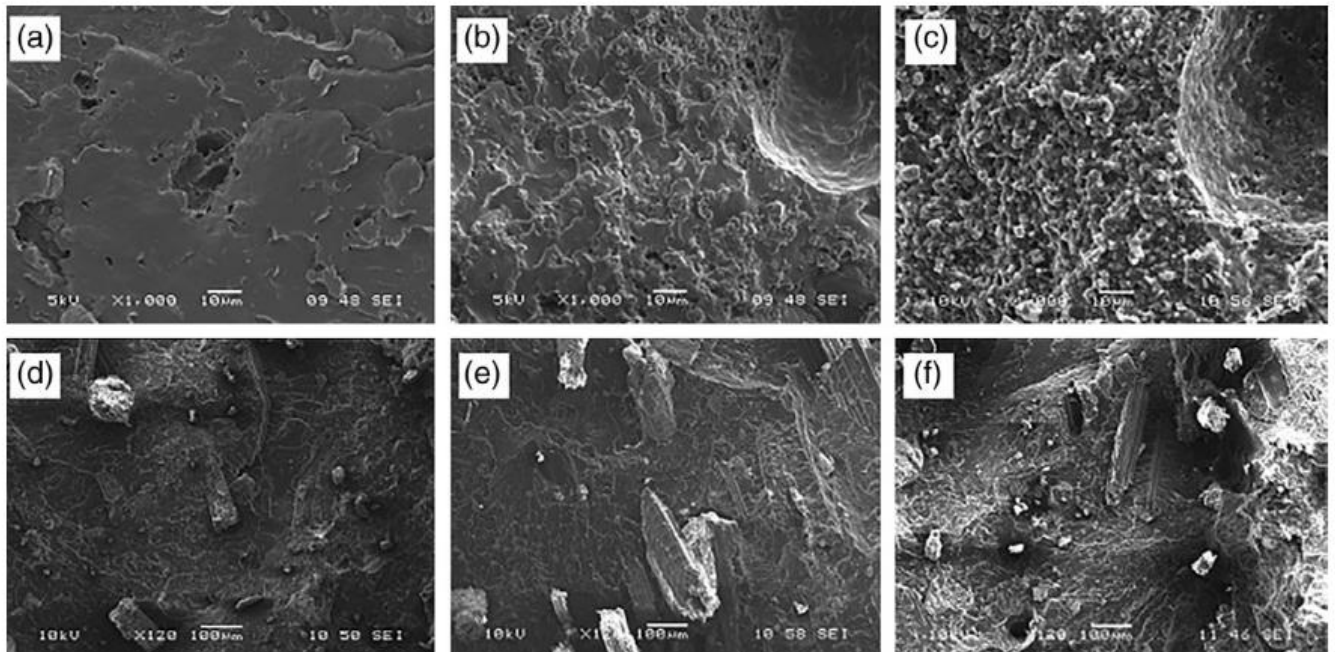


Fig 4.4. SEM photo micrographs of (a) PVC-LDPE (20/80) C0, (b) PVC-LDPE (50/50), (c) PVC-LDPE (80/20), (d) PVC-LDPE-DPLF (C10), (e) PVC-LDPE-DPLF (C20), and (f) PVC-LDPE-DPLF (C30).

4.3.3. Thermal Analysis

4.3.3.1. Thermal Analysis of Matrices.

First, (TGA, DTG) analysis was performed on PVC/LDPE blend with different LDPE contents as shown in Figure 4.5.

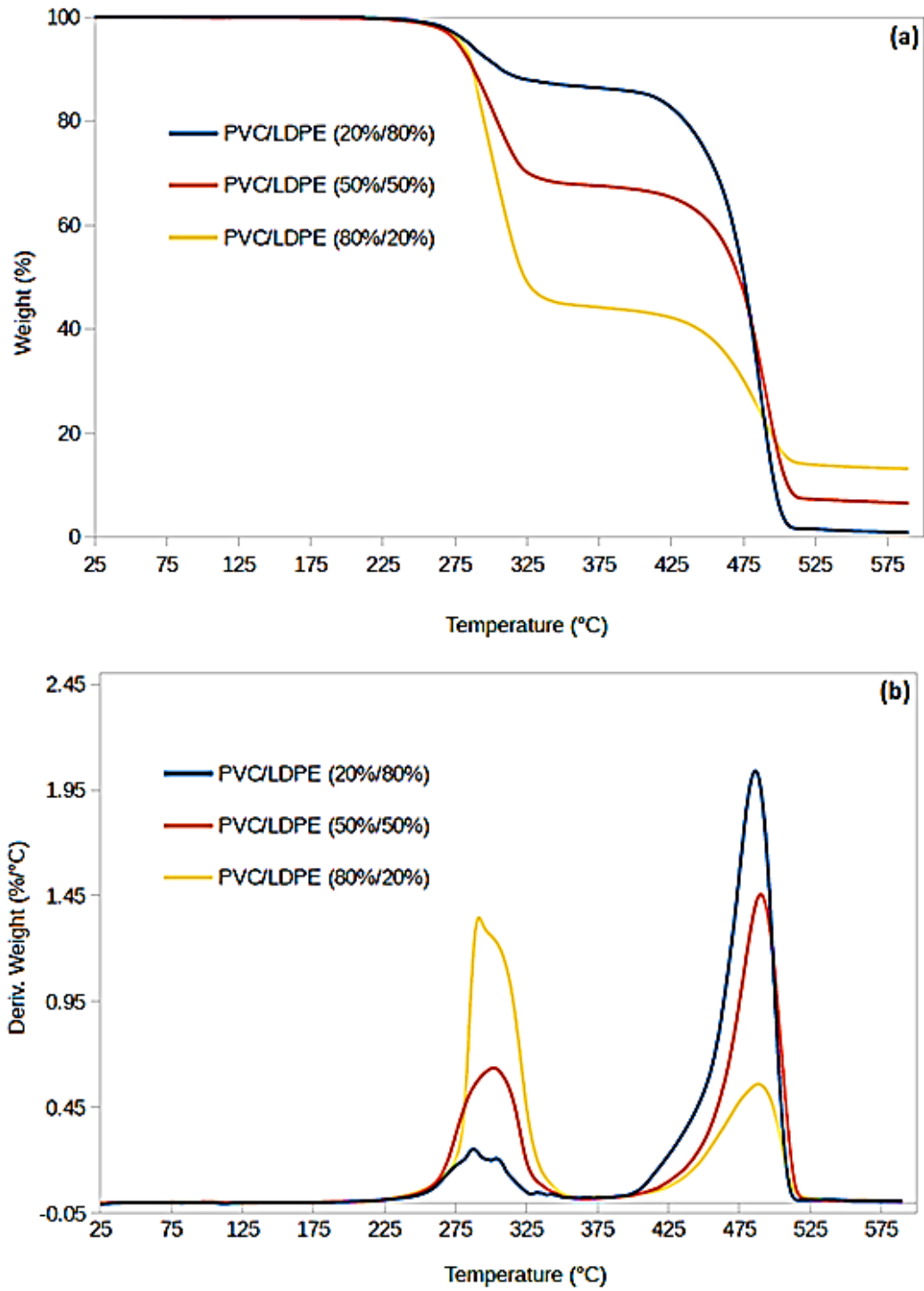


Fig 4.5. Effect of LDPE content on (a) TGA and (b) DTG (b) of PVC-LDPE blend.

CHAPTER 4. APPLICATION 2

The degradation of the blend occurred in two steps, the first step is probably related to the dehydrochlorination of small amounts of PVC, this process generating PVC macroradicals and dehydrogenation of LDPE, in turn generating LDPE macro-radicals. The second step probably associated with the thermal degradation of the LDPE by scission of bonds along the long chain, producing shorter-chain LDPE and more degradation of PVC, followed by the formation of long conjugated double bonds or polyene sequences. This is in line with the mechanism of macro-radical generation and the macro-radical cross- recombination of PVC and LDPE proposed by Thongpin et al. [30] and Sombatsompop et al. [35].

The decomposition temperatures are presented in Table 4.4. It is clear that by addition of LDPE to PVC, the decomposition temperatures T10% and T20% shift to higher values. The largest shifts of T10% and T20% were attributed to the sample containing 80 wt.% of LDPE.

Table 4.4. The temperature of decomposition of PVC-LDPE Samples with different ratio.

Sample	T _{10%} (°C)	T _{max} (°C) first step	T _{max} (°C) second step
PVC-LDPE (20%/80%)	306.51	280.89	486.24
PVC-LDPE (50%/50%)	290	302.18	490.45
PVC-LDPE (80%/20%)	286.82	291.75	488.34

4.3.3.2. Thermal Analysis of Composites

To investigate the effect of the reinforcing date palm fiber in thermal performance of the composites, TG and DTG for the pure PVC-LDPE, PVC-LDPE-DPLF 10, and 30 wt.% fiber content are shown in Figure 4.6 (a: TGA, b: DTG thermograms). The decomposition temperatures of matrix and the two fiber loading composites are summarized in Table 4.5. From Figure 4.6(a), (C30) 30 wt.% fiber loading curve in the range 25 °C-180 °C indicates a weight loss of about 4%, which is attributed to water evaporation. However, the samples (C0) and (C10) 10 wt.% fiber loading are stable in that range. In the second range, from 180 °C to 525 °C, the thermal degradation of all composites can be divided into two steps. The first step starts at 244 °C and continues up to 435 °C with a weight loss of about 20%. This step is related to the degradation of small amounts of PVC-LDPE blend (dehydrochlorination of PVC,

CHAPTER 4. APPLICATION 2

dehydrogenation of LDPE) and thermal decomposition of hemicelluloses and cellulose [36]. A weight loss in the PVC-LDPE composites is observed in the range of 253.9 °C-375 °C. The second step is much faster than the first one and the thermal degradation of composites ranging from 435 °C to 489 °C is as a result of pyrolysis of polymer matrix and non-cellulosic materials in the fiber [37].

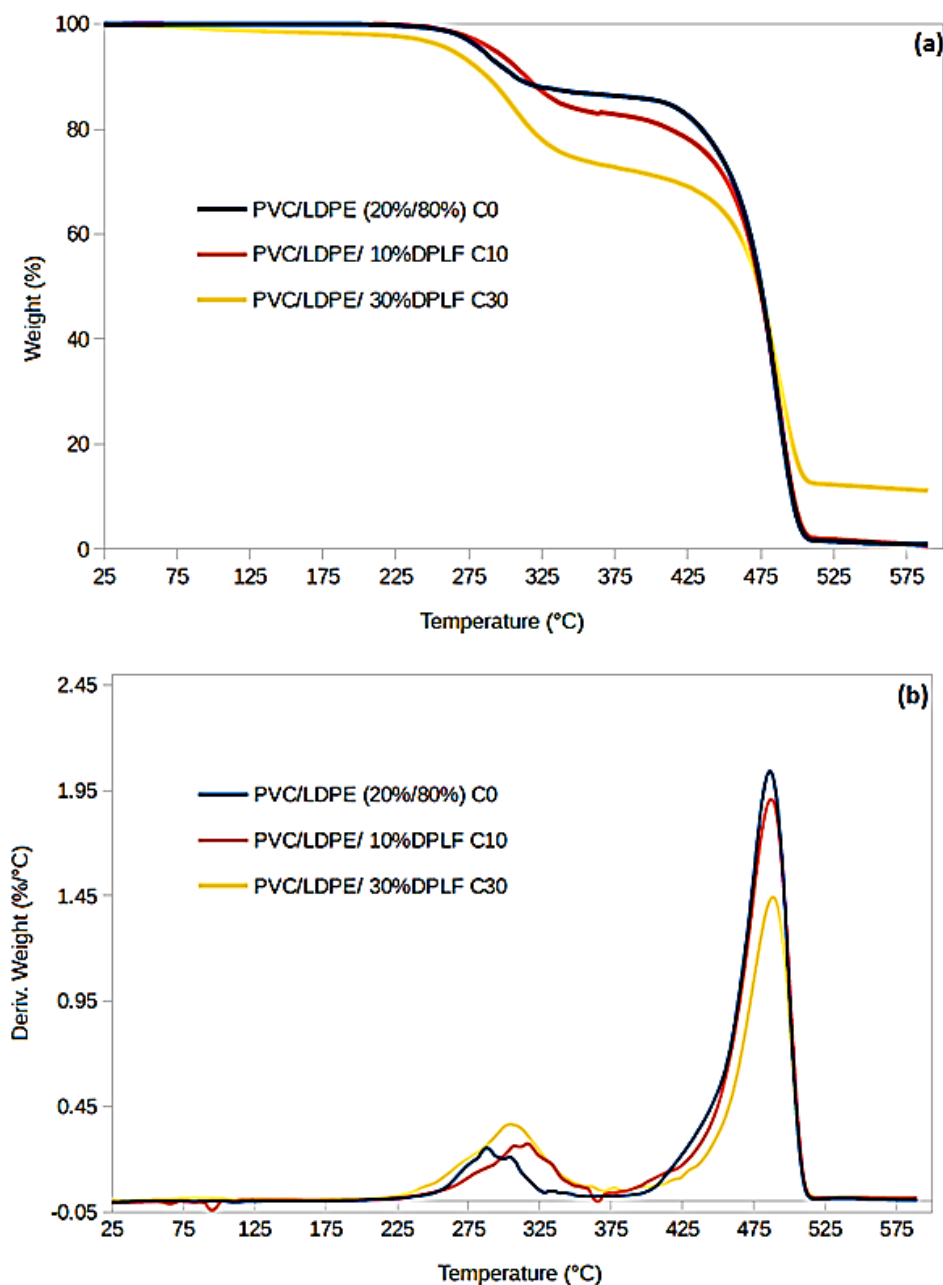


Fig 4.6. Effect of fiber loading on (a) TGA and (b) DTG of PVC-LDPE-DPLF composite.

(C0) was thermally stable at 320 °C up until 410 °C, and then started to degrade rapidly in the second step, with maximum weight loss rate occurring at 486 °C in the DTG curves in Figure

CHAPTER 4. APPLICATION 2

4.6(b), showing that the maximum peak of degradation increased after introducing DPLF to PVC-LDPE from 486 °C for (C0) to 489 °C (C10, C30) composites. This shows that DPLFs slightly enhanced the thermal stability of the composites at higher temperatures.

Table 4.5. The temperature of decomposition of PVC-LDPE-DPLF samples with different ratio.

Samples	T _{max.20%}	Onset temperature	Rapidest temperature
C0	433.25	280.84	486.24
C10	422.98	276.12	487.88
C30	316.45	270.69	489.50

CHAPTER 4. APPLICATION 2

4.4. CONCLUSIONS

PVC was blended with LDPE to prepare compositions in which the concentration of LDPE varied from 20, 50, and 80 wt.%. It was found that:

1. The sample in which PVC-LDPE (20 wt.%/80 wt.%) had good mechanical and thermal properties. The following conclusions from the study of LDPE-PVC-DPLF composites are summarized as below:
2. Adding 10 wt.% DPLF improved the tensile strength. The modulus of the composites significantly increased with an increase in the filler content in the entire concentration range. The maximum value of 210 and 300 N/cm², respectively, attributed to the composite filled with DPLF 30 wt.%. This result indicates that the filler has a strong reinforcing effect and that the filler is distributed homogeneously within the sample. Furthermore, when date palm fibers were added to the polymer matrices, the percentage elongation at break before and after ageing decreased. The material becomes brittle if filled with more than 10 wt.% of the date palm fiber. The presence of the filler also improved the tensile strength before and after ageing, the maximum value of 9.69 and 9.73 MPa, respectively, for the composite filled with DPLF 10 wt.%.
3. SEM micrographs showed that morphological properties of tensile fracture surface are in accordance with the tensile properties of these blends and composites.
4. The thermal degradation of PVC-LDPE (20wt.%/80wt.%) blend and PVC-LDPE-DPLF (10 wt.%, 30 wt.%) composites took place in two steps: in the first step, the blend was more stable than the composites. In the second step, the composites showed slightly greater stability than the PVC-LDPE (20 wt.%/80 wt.%) blend.

Overall, the application of green composites PVC-LDPE-DPLF is feasible, and can be used in several applications.

ACKNOWLEDGEMENTS

The authors wish to thank the staff of Plastic Laboratory of Enterprise des Industries du Câble ENICAB, Biskra, Algeria, where the samples were prepared, and the Centre de Recherche Scientifique & Technique en Analyse Physico-Chimiques, Tipaza, Algeria, for thermal analysis, and the authors express their gratitude to Sigismund Melissen for English revision.

CHAPTER 4. APPLICATION 2

REFERENCES

1. P. Gatenholm and J. Felix, "Methods for Improvement of Properties of Cellulose-Polymer Composites," in *Wood Fiber/ Polymer Composites: Fundamental Concepts, Process, Material Options*, Forest Product Society, Madison, WI, 57 (1993).
2. P. Xi, F. Mizi, H. John, and A.Z. Majeed, *J. Compos. Mater.*, 46, 237 (2012).
3. A.V. Ratna Prasad and K. Mohan Rao, *Mater. Des.*, 32, 508 (2011).
4. I. Van de Weyenberg, J. Ivens, A. De Coster, B. Kinob, E. Baetens, and I. Verpoesta, *Compos. Sci. Technol.*, 63, 1241 (2003).
5. B. Dahlke, H. Larbig, H.D. Scherzer, and R. Poltrock, *J. Cell. Plast.*, 34, 361 (1998).
6. B. Agoudjil, A. Benchabane, A. Boudenne, L. Ibos, and M. Fois, *Energ. Buildings*, 43, 491 (2011).
7. F.D. Alsewailem and Y.A. Binkhder, *J. Reinf. Plast. Comp.*, 29, 1743 (2010).
8. T. Alsaeed, B. Yousif, and H. Ku, *Mater. Des.*, 43, 177 (2012).
9. A. Abdal-hay, N.P.G. Suardana, D.Y. Jung, K.S. Choi, and J. K. Lim, *Int. J. Precis. Eng. Manuf.*, 13, 1199 (2012).
10. M.A. AlMaadeed, R. Kahraman, P.N. Khanam, and N. Madi, *Mater. Des.*, 42, 289 (2012).
11. M.A. AlMaadeed, R. Kahraman, P.N. Khanam, and S. Al-Maadeed, *Mater. Des.*, 43, 526 (2013).
12. S. Mahdavi, H. Kermanian, and A. Varshoei, *Bio-Res.*, 5, 2391 (2010).
13. J.R. Mohanty, S.N. Das, H.C. Das, and S.K. Swain, *Fiber. Polym.*, 15, 1062 (2014).
14. K.M. Zadeh, I.M. Inuwa, R. Arjmandi, A. Hassan, M. Almaadeed, Z. Mohamad, and P.N. Khanam, *Fiber. Polym.*, 18, 1330 (2017).
15. M.A. AlMaadeed, Z. Nógellová, I. Janigová, and I. Krupa, *Mater. Des.*, 58, 209 (2014).

CHAPTER 4. APPLICATION 2

16. M. García, J. Hidalgo, I. Garmendia, and J. García-Jaca, *Compos. A. Appl. Sci. Manuf.*, 40, 1772 (2009).
17. A. Avila, E.I. Sánchez, and M.I. Gutiérrez, *Chemom. Intell. Lab. Syst.*, 77, 247 (2005).
18. E. Santamaría, M. Edge, N.S. Allen, H.B. Harvey, M. Mellor, and J. Orchison, *J. Appl. Polym. Sci.*, 93, 2744 (2004).
19. M. Saeedi, I. Ghasemi, and M. Karrabi, *Iran. Polym. J.*, 20, 424 (2011).
20. I. Naghmouchi, P. Mutjé, and S. Boufi, *J. Appl. Polym. Sci.*, 131, 41083 (2014).
21. N. Wang, N. Gao, Q. Fang, and E. Chen, *Mater. Des.*, 34, 1222 (2011).
22. C. Albano, J. González, M. Ichazo, C. Rosales Urbina de Navarro, and C. Parra, *Compos. Struct.*, 48, 49 (2000).
23. N. Sombatsompop, K. Sungsanit, and C. Thongpin, *Polym. Eng. Sci.*, 44, 487 (2004).
24. O. Olabisi, L.M. Roberson, and M.T. Shaw, *Polymer miscibility*, Academic Press, New York, (1979).
25. J. Prachayawarakorn, J. Khamsri, K. Chaochanchaikul, and N. Sombatsompop, *J. Appl. Polym. Sci.*, 102, 598 (2006).
26. J. Prachayawarakorn, S. Khunsumled, C. Thongpin, A. Kositchaiyong, and N. Sombatsompop, *J. Appl. Polym. Sci.*, 108, 3523 (2008).
27. Y. Zhang, B. Wen, L. Cao, X. Li, and J. Zhang, *J. Wuhan. Univ. Technol. Mat. Sci. Ed.*, 30, 198 (2015).
28. S. Nedjma, H. Djidjelli, A. Boukerrou, Y. Grohens, N. Chibani, D. Benachour, and I. Pillin, *J. Vinyl Addit. Technol.*, 22, 173 (2014).
29. S.M. Mirmehdi, F. Zeinaly, and F. Dabbagh, *Compos. Part B Eng.*, 56, 137 (2014).
30. C. Thongpin and O. Santavitee, *J. Vinyl Addit. Technol.*, 12, 115115 (2006).
31. P. Bataille, C. Jolicoeur, and H.P. Schreiber, *J. Vinyl Addit. Technol.*, 2, 218 (1980).

CHAPTER 4. APPLICATION 2

32. I. Ahmad, P.Y. Wong, and I. Abdullah, *Polym. Compos.*, 27, 395 (2006).
33. B.D. Park and J.J. Balatinecz, *J. Polym. Compos.*, 18,79 (1997).
34. Y.A. El-Shekeil, S.M. Sapuan, M. Jawaid, and O.M. Al- Shuja'a, *Mater. Des.*, 58, 130 (2014).
35. N. Sombatsompop, K. Sangsanit, and C. Thongpin, *J. Appl. Polym. Sci.*, 92, 3167 (2004).
36. Z.N. Azwa, B.F. Yousif, A.C. Manalo, and W. Karunasena, *Mater. Des.*, 47, 424 (2013).
37. M.S. Huda, L.T. Drzal, M. Misra, A.K. Mohanty, K. Williams, and D.F. Mielewski, *Ind. Eng. Chem. Res.*, 44, 593 (2005).

CHAPTER 5. APPLICATION 3

EFFECT OF VARIOUS CHEMICAL MODIFICATIONS ON DATE PALM FIBERS (DPFs)-PVC-HDPE BLEND COMPOSITES: STRUCTURAL, MORPHOLOGICAL, THERMAL, MECHANICAL, MECHANICAL DYNAMICAL, AND RHEOLOGICAL PROPERTIES

ABSTRACT

To avoid garbage accumulation and guarantee the degradation of the thermoplastic wastes with high-level safety. Polyvinylchloride (PVC) and polyethylene high density (HDPE) are attracting more attention in the process of recycling and biodegradability in which exhibits great performance and potential application in several industrial fields. Leaflets and rachis fibers (DPFs) from the natural waste of the date palm tree pruning were used as an eco-friendly effective filler to reinforce PVC-HDPE (20:80) blend composites. Composites with untreated and treated DPFs loading of 30 wt.% were prepared using twin screw extruder and then compression molding. A comfortable and low cost and high safety processes to investigate modified fiber surfaces from DPFs using various treatments as alkali (NaOH), 3-aminopropyltriethoxysilane (APTES), combined alkali-silane, bleaching (NaClO₂), and peroxide hydrogen plus nitric acid (H₂O₂+HNO₃). The development of successful surface modification of DPFs from delignification to the extraction of cellulose microcrystals (CMCs) has been confirmed by infrared spectroscopy (FTIR), scanning electron microscopy (SEM) and thermogravimetric analysis (TGA). Additionally, the results revealed an improvement of structural, morphological, thermal, mechanical, dynamic-mechanical, rheological and water uptake performances of the composites as a function of the modified DPFs. Hence, the PVC-HDPE-HNO₃F composite can be a good potential candidate for several structural applications.

Keywords: PVC-HDPE, DPFs, Surface treatment, Cellulose microcrystals, Water Uptake, Rheological properties.

CHAPTER 5. APPLICATION 3

5.1. INTRODUCTION

Recently, green polymer composites are attracting more attention from both fundamental and applied research for improving sustainable eco-friendly products as an alternative to synthetic fibers [1,2]. In addition, Natural fibers are among the most commonly used in polymer composite technology due to their low price and high performance [3,4]. Poly vinyl chloride (PVC) is one of the most used thermoplastic polymers [5,6]. The main drawback of PVC to enhancing their performances in different industrial applications is mainly low thermal stability, so it's easy to degrade by dehydrochlorination process around 100°C [7]. To solve this limitation, resistant blends have been produced by the incorporation of different thermoplastic polymers in PVC [8–10]. Among the natural waste reinforcements, a new type of lignocellulosic biomass is derived from the leaflets and rachis of a desert date palm tree (*Phoenix dactylifera* L), which is a member of the *Arecaceae* family [11,12]. This tree is widely abundant in all Saharan countries, especially Algeria and it represents an excellent source of natural waste reinforcing composites [13,14]. While, some experimental studies have been performed on the characterization and chemical extraction of date palm fibers [15,16]. Their use as a green filler to reinforce thermoplastic and thermoset materials, especially in polymer blends, is very limited except a few reports mentioned the use of date palm fiber as a reinforcement in polymeric blends [17].

The characteristics and efficiency of technology materials produced from date palm fiber depend not only on the properties of their individual components, but also on their interfacial adhesion behavior between matrix and fiber [18,19]. Unfortunately, there is an important drawback in the use of natural fiber in composite materials technologies due to the water uptake effect, in which the hydroxyl groups present in natural fiber are responsible for the hydrophilic character [20,21]. It appears hard to guarantee the uniform distribution of these lignocellulosic fibers in the polymer matrix during the extrusion process. The physical properties of green fillers can be enhanced by improving the compatibility between the fiber and the polymer matrix by different chemical modifications such as alkaline and silane treatments [22,23]. Neat cellulose fibers can be extracted from natural fibers using various chemical treatments. In this context, the target is to eliminate lignin and hemicellulose, and to concentrate on reaching the higher yield of crystalline cellulose [24,25]. From an environmental point of view, Plastic garbage accumulated in landfill sites which standard waste disposed into the environment can take many years to degrade due to its poor degradability. Date palm fiber reinforced PVC-HDPE blends are able to decrease environmental pollution by incorporating biodegradable products. It is also an easier way to dispose of PVC and HDPE plastic wastes,

CHAPTER 5. APPLICATION 3

which are abundantly available in nature. Recently, natural wastes as DPFs and polymeric materials have been the focus of attention of many researchers. Among these studies on the raw and modified date palm fibers, reinforced polymer composites are plotted in Table 5.1. Our study aims to recover these wastes by exploring the influence of date palm fiber surface treatment, such as alkaline treatment, silane treatment, hybrid alkaline-silane treatment, sodium chlorite bleaching treatment and hydrogen peroxide plus nitric acid treatment, on the morphological, thermal, mechanical, rheological and dynamical mechanical properties of PVC-HDPE-DPFs green composites reinforced with 30 wt.% of date palm fiber.

5.2. EXPERIMENTAL

5.2.1. Raw Materials Used

Polyvinyl chloride PVC 4000 M (K value 67-72, Bulk density 0.43-0.50 g/cm³) was provided by the "Entreprise Nationale de Pétrochimie (ENIP)" in Skikda, Algeria. High-density polyethylene (HDPE) Rigidex HD5226EA (Bulk density 0.95 g/cm³, melt flow index 0.18 g/10min) was provided by INEOS Polyolefins (Barcelona, Spain). Ca/Zn stearate was obtained from Nanjing OMYA Fine Chemical Ind. Co. Ltd. (Nanjing China). Bis (2-ethylhexyl) terephthalate (DOP) was supplied from Shanxi Sanwei Group Co., Ltd. Date palm fibers (DPFs) were obtained from leaflets and rachis of date palm tree. DPFs were collected from the region of Sidi Okba, Biskra, in Algeria. Various chemicals used in this study like sodium hydroxide (NaOH), glacial acetic acid (CH₃COOH), 3-aminopropyltriethoxysilane (APTES), sodium chlorite (NaClO₂), hydrogen peroxide (H₂O₂) and nitric acid (HNO₃) were purchased from Sigma Aldrich. France.

Table 5.1. Some published research studies on treated date palm fibers reinforced polymer composites.

Date Palm Fibers (DPFs)	Polymer Matrix	Ref
CH ₃ COOH /H ₂ O ₂ treated three parts of DPFs	HDPE	[20]
The natural treatment process	LLDPE	[26]
Alkali treated DPF	Polyurethane	[21]
untreated leaves fibers	Epoxy Resin	[27]
Alkali, Bleaching NaClO ₂ and H ₂ SO ₄ treated Midrib part of date palm tree	NR	[15]
Untreated date palm fibers	R LDPE-RHDPE- RPP	[18]

CHAPTER 5. APPLICATION 3

Alkali, silane and alkali-silane treatments of DPFs	UP	[28]
DPFs	PLA	[19]
Bleached date palm leaf fiber	LDPE/PP	[29]
Alkali treated of date palm leaves	RLDPE, RHDPE and RPP	[1]

Note: Low density polyethylene-(LDPE), Polypropylene-(PP), Poly (lactic acid)-(PLA), High density polyethylene-(HDPE) Natural rubber-(NR), Unsaturated polyester-(UP), Low density polyethylene-(LLDPE), Recycled-(R).

5.2.2. Extraction Procedure of the Date Palm Fibers (DPFs)

In this experiment, the collected date palm fibers (leaflets and rachis) were washed several times with tap water to remove dust. After that, the fibers were immersed in a glass beaker (2L) filled with deionized water at 80°C for 2 hours under mechanical stirring for removing waxes and impurities. After this step, the fibers were dried in the air oven at 65 ° C for 4 days. The dried fibers were then crushed to fine powder with a Moulinex coffee grinder (MoulinexAR11, France) and powders were sieved into different particle sizes (< 450 µm).

5.2.3. Chemical Composition of the Date Palm Fibers (DPFs)

The chemical composition of DPFs was determined in experimental method reported by other work [15,17]. The chemical composition of DPFs is: cellulose 42%, lignin 29%, hemicellulose 20%, Ash 9% and a density of 1.19 g/cm³ similar to those reported in literature review [30].

5.2.4. Surface Treatment of the Date Palm fibers (DPFs)

In order to increase the loading of the cellulose in DPFs and to enhance the compatibility between fiber and matrix, table 2 displays chemical composition of DPFs obtained before and after the five different chemical treatments.

5.2.4.1. Alkali Treatment of DPFs

Alkaline extraction of DPFs was done in order to remove residual lignin, and partially remove the other alkali soluble compounds from DPFs surface, in line with the method mentioned in the literature [31,32]. The pre-treatment was conducted by soaking the DPFs in a glass beaker (2L) filled with NaOH solution (5 wt.%) for 24 hours at room temperature. Finally, the sample was fully washing by water and then neutralized by immersion in 2% glacial acetic acid solution. Then, the modified fibers were collected by filtration and dried at 65 ° C for 48 h.

CHAPTER 5. APPLICATION 3

5.2.4.2. Silane Treatment of DPFs

Silane treatment of date palm fibers was done to improve the interaction between fiber and matrix using 3-aminopropyltriethoxysilane (APTES) [33]. In brief, a solution of 90/10 (v / v) ethanol / water was prepared and stirred for 30 min, the silane (3.5 wt.% based on the DPFs content) was introduced slightly and gradually to guarantee a good distribution, the pH solution was regulated with glacial acetic acid, while the aqueous solution was stirred, hydrolysis was then conducted at room temperature for 3 hours, during that time, DPFs were introduced to the solution and placed at room temperature for 3 h. After silanization treatment, the fibers were washed several times with 90/10 (v / v) ethanol / water solution, this step requires the removal of unreacted excess silane molecules. Finally, the treated fibers were filtered and then dried in an oven at 65 ° C for 48 h.

5.2.4.3. Combined Alkali-Silane Treatment of DPFs

The combined Alkali-silanization treatment was applied to DPFs; the fibers treated with NaOH were followed by the silane chemical modification. Alkali and silane modification procedures were the same used at above [34,35].

5.2.4.4. Sodium Chlorite Treatment of DPFs

Initially, the delignified DPFs were immersed in a solution prepared of equal volume (v : v) of 2% (w/v) sodium chlorite solution in deionized water and buffer solution at temperature of 70°C for 2 h [36]. Finally, the bleached fibers were washed with deionized water and dried at room temperature for 72 h to obtain cellulose microfibrils (CMFs).

5.2.4.5. Hydrogen Peroxide +Nitric Acid Treatment of DPFs

Obtained cellulose microfibrils (CMFs) from the previous treatment was hydrolyzed by treating with mixed 65 wt.% HNO₃ and 30 wt.% H₂O₂ solution (1 :2, v:v) at 50 °C for 30 minutes under continuous stirring at 300 rpm, as reported in literature[37]. To stop the reaction, solution was quenched by adding ice cubes. The final product (hydrogels) was washed several times with deionized water and centrifuged to collect the suspension, which was dialyzed against deionized water for several days to eliminate all residual acids and carbohydrates.

CHAPTER 5. APPLICATION 3

Table 5.2. Amount of various chemical compounds in untreated and various chemically treated date palm fibers (leaflets and rachis)

Date palm fibers	Lignin (%)	Hemicellulose (%)	Cellulose (%)	Ash (%)
Untreated fibers UntF	29± 7.5	20 ± 2	42±5.1	9±1.4
Alkali treated fibers AIF	16± 3.9	13 ± 3.06	65 ±7.03	6±0.9
Silane treated fibers SiF	19± 2.7	14 ± 4	62 ±4.3	5±0.32
Alkali-silane treated fibers (Al-Si) F	12± 1.9	8 ± 0.8	77 ±8	4±0.9
Bleaching treated fibers NaClO ₂ F	-	4± 1.02	93 ±6.1	3±0.5
Nitric hydrolysis treatment (H ₂ O ₂ +HNO ₃) F	-	-	98±6	1 ±0.1

5.2.5. Processing of The Composites

The steps of fabrication process of DPFs fibers reinforced PVC-HDPE composites are depicted in Figure 5. 1.

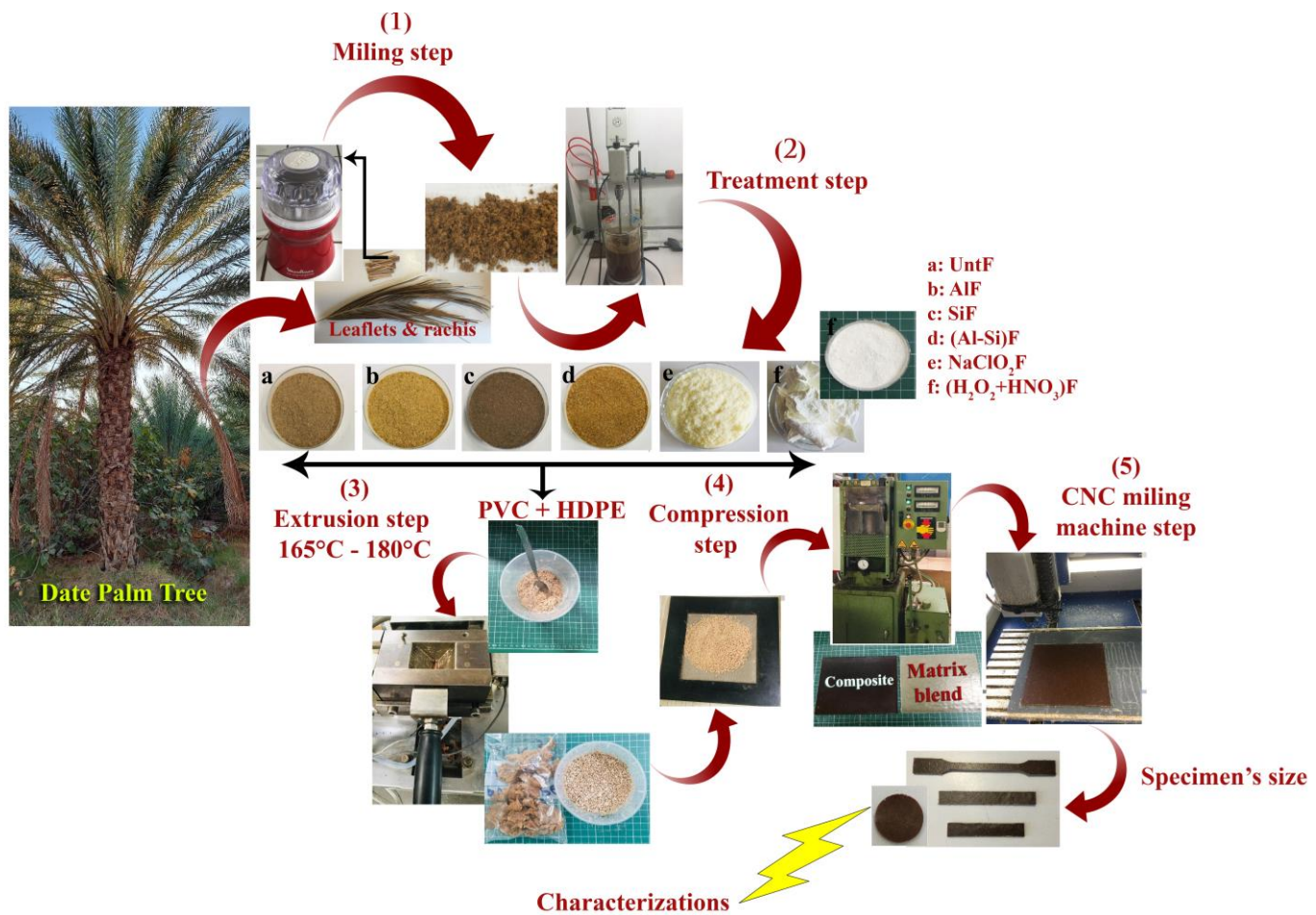


Fig 5.1. The steps of fabrication process of DPFs fibers reinforced PVC-HDPE composites.

CHAPTER 5. APPLICATION 3

PVC and their additives, HDPE, and DPFs were placed in a vacuum oven at 65°C overnight to remove the moisture content. All compounds were manually blended in a plastic beaker. Composites PVC-HDPE-DPFs reinforced with untreated and treated DPFs (30wt. %) were fabricated by a laboratory twin screw extruder, the processing temperature ranged from 165°C to 180°C and speed of 60 rpm, followed by compression molding at 170°C for 5 min at a mechanical pressure of 200 bar. This temperature average was varied and adjusted to obtain an easily processable homogeneous mixture and prevent the thermal deterioration of all ingredients. The code and composition of the composite samples are shown in Table 5.3.

Table 5.3. The sample code and composition of PVC-HDPE-DPFs composites.

Sample Code	PVC-HDPE (phr)	DPFs (phr)	Composition
MC1 (PVC -HDPE)	20/80	-	Matrix blend
MC2 (PVC -HDPE -UntF)	20/80	30	PVC - HDPE - Untreated fiber
MC3 (PVC -HDPE -AIF)	20/80	30	PVC - HDPE - alkali treated DPFs
MC4 (PVC -HDPE -SiF)	20/80	30	PVC - HDPE - silane treated DPFs
MC5 (PVC -HDPE -(Al-Si) F)	20/80	30	PVC – HDPE - combined alkali-silane treated DPFs
MC6 (PVC -HDPE -NaClO ₂ F)	20/80	30	PVC - HDPE - NaClO ₂ treated DPFs
MC7 (PVC -HDPE -HNO ₃ F)	20/80	30	PVC - HDPE - H ₂ O ₂ + HNO ₃ treated DPFs

5.2.6. Characterizations

5.2.6.1. Morphological Properties

Morphology of the fracture surface of the DPFs and composite samples are broken into liquid nitrogen and were examined by using a Jeol JSM-6031 scanning electron microscope (SEM) at an accelerated voltage of 10 kV. The fracture surface was sputter-coated with a thin gold layer before the observation.

5.2.6.2. Fourier Transform Infrared Spectroscopy (FTIR)

FTIR analysis of the untreated and treated DPFs with different chemical treatments, were carried out using a Fourier Transform Infrared Spectroscopy Vertex 70v FTIR (Bruker

CHAPTER 5. APPLICATION 3

Company, Billerica, MA, USA). All spectra were measured in the transmission mode in the range of 4000 - 500 cm^{-1} with a 4 cm^{-1} spectrum resolution.

5.2.6.3 Thermogravimetric Analysis (TGA)

TGA measurements of DPFs and composites were performed in a thermal analyzer (Setaram TG/DTA 92-10) at 10 $^{\circ}\text{C}/\text{min}$ heating rate under nitrogen atmosphere in the temperature range of 20 to 600 $^{\circ}\text{C}$.

5.2.6.4 Diffraction Analysis (DRX)

The crystallinity index (CrI) of raw and modified date palm fibers with various treatment were calculated from an X-ray diffractograms using a Rigaku MiniFlex 600 diffractometer with a $\text{Cu K}\alpha$ radiation and $\lambda = 1,5406 \text{ \AA}$. The (2θ) angular region from 0 $^{\circ}$ to 60 $^{\circ}$ was scanned at a rate of 0.05 $^{\circ}$ step and a step time of 10 s. Crystallinity index was determined by Segal method (Segal et al., 1959) :

$$\text{CrI}_{\%} = \frac{I_{200} - I_{am}}{I_{200}} \times 100\%$$

Where I_{200} represents maximum intensity of the crystalline peak at a 2θ between 21 $^{\circ}$ and 23 $^{\circ}$ and I_{am} represents minimum intensity of the amorphous peak at a 2θ between 16 $^{\circ}$ and 18 $^{\circ}$.

5.2.6.5. Mechanical Properties

5.2.6.5.1. Tensile Properties

Tensile experiments were conducted to determine the force needed to fracture and the elongation degree of the specimen before the breaking point. The tensile behaviors of the matrix and the composites were determined using MTS synergy RT1000 testing with a load cell of 5KN and displacement rate of 10 mm/min at ambient temperature according to ISO: 527-2. The sample dimensions were (120 \times 5 \times 2 mm^3). Five specimens were tested and the average value was recorded.

CHAPTER 5. APPLICATION 3

5.2.6.5.2. Flexural Properties

Three-point bending flexural tests of the matrix and the composites were performed using MTS synergy RT1000 at room temperature (23°C) and crosshead displacement speed of 1.5 mm/min with load cell 10KN up to break the specimen according to ISO: 14125. The sample dimensions were (75 × 10 × 2 mm³). Five specimens were tested and the average value was reported.

5.2.6.6. Dynamical Mechanical Analysis (DMA)

Dynamical mechanical properties of the matrix and the composites were evaluated using DMA Q800 model of TA instruments using a heating rate of 5 °C/min in the temperature range -50 - 120°C at fixed frequency of 1 Hz. The specimen having the dimensions of (60 mm x 10 mm x 2 mm).

5.2.6.7. Rheological Measurements

The complex shear viscosities were studied by using an Anton Paar MCR301 rheometer. the measurement was conducted using a gap size of 1.5 mm between parallel-plate geometry (25 mm diameter) The instrument calibrated and programmed to perform the frequency sweep analysis at 170°C and the frequency varied from 0.01 to 100 Hz with oscillation strain of 0.5% were used in which related to the linear viscoelastic region. Disk specimens for rheology tests are manufactured by using a circular mold (25 mm diameter and 2 mm thickness) and a laboratory hot press machine at 170°C with 200 bar pressure.

5.2.6.8. Water Uptake Test

Water absorption test was conducted for each sample, with dimensions of (15 mm × 15 mm × 2 mm), according to ASTM D 570-98 [38]. The composite samples were dried in a vacuum oven at temperature 65 °C for 24h to reduce humidity and then cooled in desiccator. The initial weight of the test specimen (W_0) was weighted and registered before immersion in sea water. Then, the weight of the test specimen (W_1) was weighted again and registered every 24 h at room temperature for 40 days. All the samples were weighted with a precision of 0.001 g and the results were analyzed.

The values of the water uptake in percentage were calculated using Equation:

$$W_A (\%) = \left(\frac{W_1 - W_0}{W_0} \right) \times 100$$

CHAPTER 5. APPLICATION 3

Where W_A is the water uptake (%), W_1 is the weight of the composite sample after immersion into sea water and W_0 is the oven-dry weight of the composite sample before immersion.

5.3. RESULTS AND DISCUSSIONS

5.3.1. Date Palm Fibers (DPFs) Characterization

5.3.1.1. Morphological Properties of DPFs

Scanning electron microscopy is one of the most important characterization techniques for determining the effect of surface modification on fiber morphology. Figure 5.2(a, b) displayed SEM micrographs of untreated and alkali treated DPFs. It is obviously shown that alkali treatment enhanced the surface performance of DPFs, due to the partial removal of lignin and other residues, which can be obviously shown on the surface of the untreated fiber. In addition, the alkali modification made the hydroxyl groups of the fiber surface more reactive in which can easily interact with polymer matrix [39,40]. SEM micrograph of silane treated DPFs is displayed in Figure 5.2(c), it is obviously that some irregular-shaped voids are presented by modifying the structure of fibers due to the partial removal of unnecessary compounds linked DPFs [41,42].

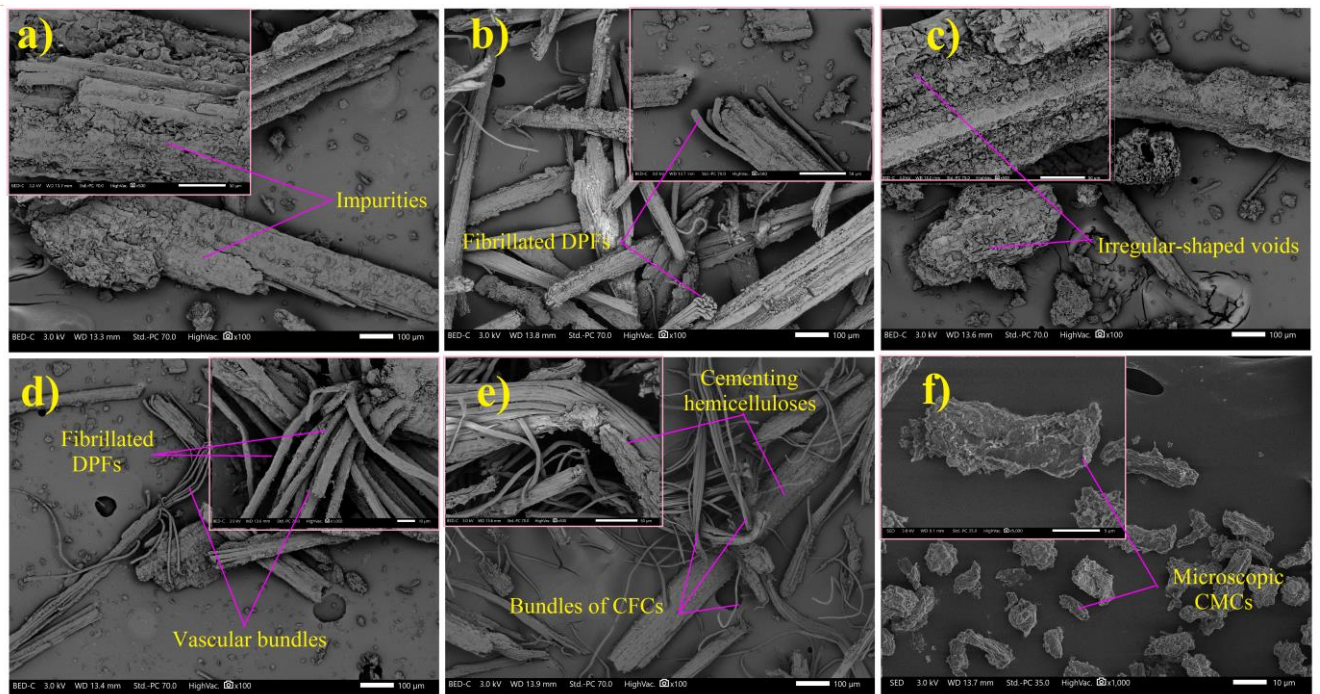


Fig 5.2. SEM micrograph of (a) raw DPFs, (b) NaOH treated DPFs (c) Silane treated DPFs (d) alkali-Silane treated DPFs (e) Cellulose microfibrils (CMFs) (f) Cellulose microcrystals (CMCs).

CHAPTER 5. APPLICATION 3

The combined alkali-silane treatment of DPFs in Figure 5.2(d) changed the surface quality of the fibers. Consequently, the surface of the fibers appeared more “rougher” compared with that of the fibers treated with alkaline solution. In addition, the alkali-silanization process partially fibrillated the surface of the fibers resulting vascular bundles.

The micrograph of DPFs treated with NaClO_2 in Figure 5.2(e) showed the cementing hemicelluloses around single cellulose bundles [43], leading to a more homogenous fiber surface with less void space due to the extraction of the majority of lignin from the DPFs by defibrillation processes. Figure 5.2(d) showed SEM micrograph obtained for cellulose microcrystals resulting from $\text{H}_2\text{O}_2+\text{HNO}_3$ treatment of purified CMFs. After acid hydrolysis, defibrillation process occurred preferentially in the amorphous domain and transformed the crystalline domain from cellulose microfibrils to cellulose microcrystals, with microscopic CMCs ranging from 5 μm to 15 μm . Generally, these modifications have benefits in several applications when the DPFs are used as reinforcing materials [17].

5.3.1.2. FTIR Analysis of DPFs

The FTIR spectrum registered for untreated and treated DPFs with different treatments are represented in Figure 5.3. In fact, all fibers showed the stretching vibration bands of various chemical functional groups of lignin, hemicelluloses, and cellulose, thus the acid treatment had not affected the chemical structure of the modified fibers. The strong and large band centered around 3395- 3420 cm^{-1} is attributed to the O-H stretch and hydrogen bond of the hydroxyl groups [21]. The double peak appeared at 2942 and 2861 cm^{-1} are assigned to CH_2 stretching vibrations, the peak at 1755 cm^{-1} in the FTIR spectrum of the UntF may be assigned to the C=O stretch of the ester group in both hemicelluloses and lignin [44,45].

Three peaks are characteristic of lignin: at 1638 cm^{-1} , 1514 cm^{-1} and 1484 cm^{-1} are attributed to the C-C Stretching , C=C stretching , and C-H deformation vibrations, respectively [46], these peaks were gradually weakened in all the samples except for untreated DPFs, indicating the decrease of the relative proportion of non-cellulosic components in DPFs after various chemical treatments. New weak peaks appeared at 1171 cm^{-1} and 1332 cm^{-1} in both spectrums of SiF and (Al-Si)F which are associated to Si-O-fiber stretching vibration of fibers treated with silane [47].

Moreover, the weak peak at 690 cm^{-1} assigned to the asymmetric Si-O-Si vibration due to dehydration-condensation reaction [35]. The band at 1157 cm^{-1} attributed to the symmetric C-O-C stretching vibration of cellulose. The peak appeared at 1061 cm^{-1} is associated to the C-O stretching ring in hemi- celluloses. Two new peaks observed at 1383 cm^{-1} and 664 cm^{-1} are

CHAPTER 5. APPLICATION 3

associated with CH_2 stretching vibration and C-OH out of plane deformation in cellulose, respectively [48]. The peak at 2861 cm^{-1} disappeared in NaClO_2F and $(\text{H}_2\text{O}_2+\text{HNO}_3)\text{F}$ spectrums, due to the non-cellulosic part was removed partially and also the purity of extracted CMFs and CMCs respectively.

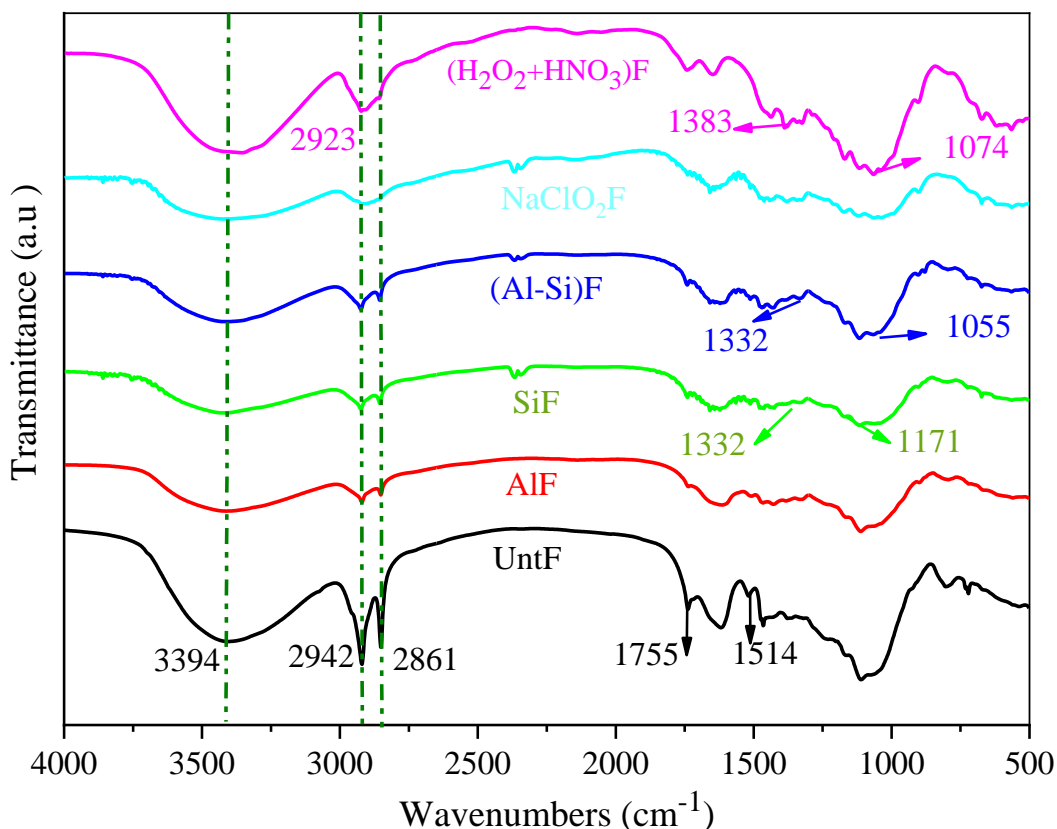


Fig 5.3. FTIR spectra of DPFs before and after various surface fiber modifications.

5.3.1.3. Thermogravimetric Analysis of DPFs

Thermogravimetric analysis was used to investigate the influence of various treatments on the thermal behaviors of the DPFs. The TGA and DTG graphs of five samples modified with different treatments (alkaline, silane, alkali-silane, bleaching and acid hydrolysis) and an untreated sample are presented in Figure 5.4(a-b), and its decomposition temperatures with the percentage of char yield were listed in Table 5.3.

The DTG graph of the raw fiber appeared four decomposition stages. The first stage at temperature range $30\text{--}135^\circ\text{C}$ is attributed to the moisture evaporation with a weight loss of around 4wt.% (drying zone). The second stage at temperature range $200\text{--}350^\circ\text{C}$ is related to the hemicellulose pyrolysis. The third stage showed a 65% weight loss from $340\text{--}420^\circ\text{C}$ due to loss of the cellulose compound.

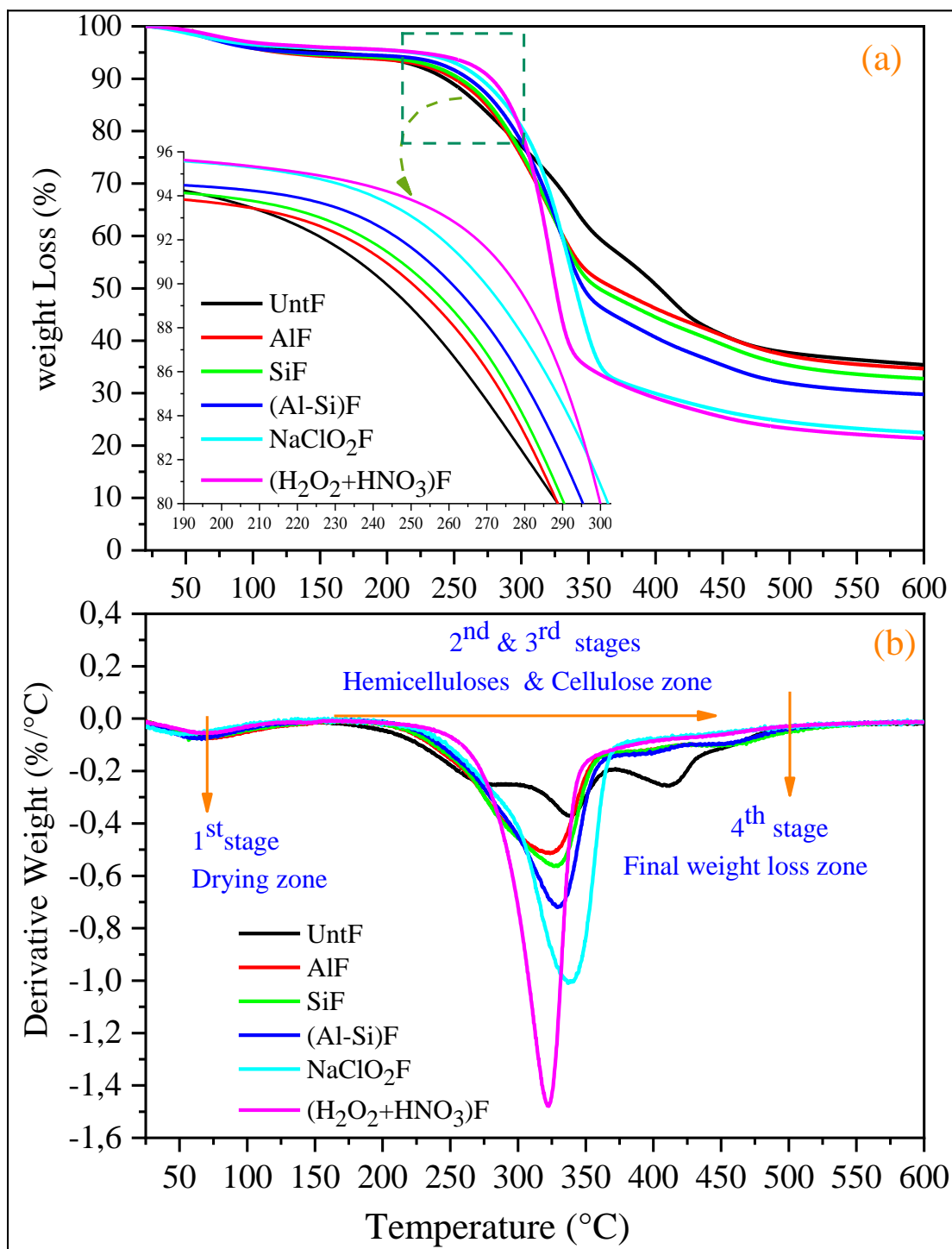


Fig 5.4. Thermal stability of DPFs before and after various surface fiber modifications determined by (a) TGA, (b) DTG.

The fourth stage at temperature range 400–550 °C is attached to the degradation of lignin and residual carbon (final weight loss zone). TGA graph showed the onset temperature of alkali treated, silane treated, alkali-silane treated, bleached, and acid treated DPFs were 188.76 °C,

CHAPTER 5. APPLICATION 3

194.72 °C, 202.47 °C, 214.04 °C, and 230.33 °C respectively which all assign to the initial deterioration of cellulose and also due to the removal of lignin, and hemicelluloses contents after DPFs treatments. Silane and alkali-silane modifications increased the initial degradation temperatures of the DPFs, this might be owing to the formation of siloxane bridges on the DPFs surface between silanol groups of the silane coupling agents and the cellulose hydroxyls [49], which revealed that silane and combined alkali-silane modifications reduced the thermal degradation of DPFs by increasing crystalline domain.

The thermal pyrolysis investigations of DPFs extracted by different treatments were compared, and it was found that the CMCs exhibited the highest thermal stability, a similar result reported by several researchers [25, 37, 46, 50]. The char yield was maximum for raw DPFs which (36.12 %) due to the unfinished degradation of lignin.

Table 5.4. Values of T_{onset} , $T_{10\%}$, $T_{20\%}$, $T_{\text{MAX}1, 2, 3}$, and % char yield (CY) of DPFs surface modifications.

Fiber	Decomposition Temperature (°C)						CY (wt.%)
	T_{Onset}	$T_{10\%}$	$T_{20\%}$	$T_{\text{MAX}1}$	$T_{\text{MAX}2}$	$T_{\text{MAX}3}$	
UntF	178.42	243.33	288.43	270.33	340.97	412.47	36.12
AlF	188.76	250.31	288.9	324.71	394.91	457.25	35.21
SiF	194.72	254.35	290.69	328.69	397.53	461.21	33.08
(Al-Si) F	202.47	260.88	295.46	330.41	398.17	462.9	30.04
NaClO ₂ F	214.04	269.89	302.01	332.33	432.57	-	22.73
(H ₂ O ₂ +HNO ₃) F	230.33	277.75	300.07	322.52	438.92	-	21.52

5.3.1.4. X-ray Diffraction Analysis of DPFs

X-ray diffraction tests were carried out on raw date palm fibers, Alkali treated fibers, silane treated fibers, Alkali-silane treated fibers, bleached fibers, and cellulose microfibrils to determine the effect of different treatments on the crystallinity of the final date palm fibers. The XRD profiles of raw and treated date palm fibers are shown in Fig 5. 5.

XRD experiments indicate two distinct peaks which are close to $2\theta=16^\circ$ and 23° in accordance with (Amroune et al., 2019; Bendahou et al., 2009). The existence of these two peaks (cellulose crystallographic planes I_{101} and I_{002}) suggests that the cellulose's chemical structure was not modified during the surface modifications. There was a significant improvement in crystallinity from 47.17 % for raw DPFs, 54.31 % for Alkali treated fiber, 54.06 % for Silane treated fiber

CHAPTER 5. APPLICATION 3

56.85 % for Alkali-Silane treated fiber, 59.85 % for bleached fiber, and 67.46 % for cellulose microcrystals. The removal of amorphous materials after different chemical treatments was certainly responsible for the increase in crystallinity.

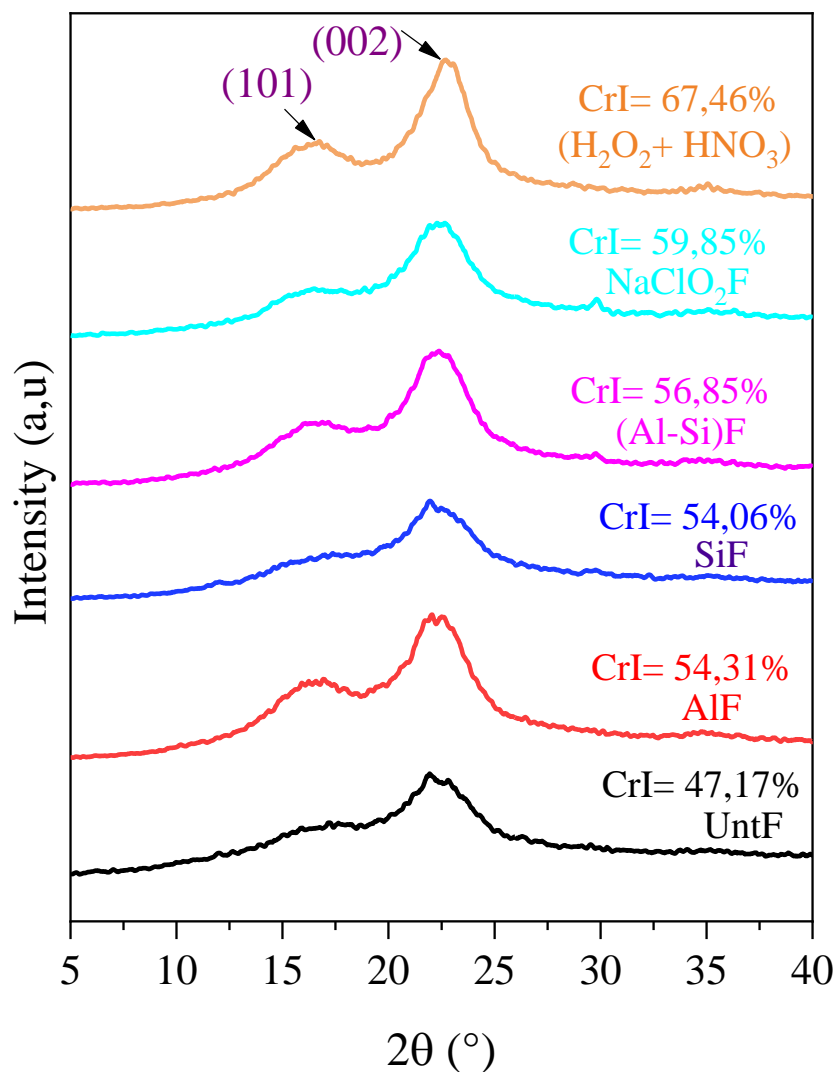


Fig 5.5. X-ray diffraction patterns of DPFs before and after various surface modifications of fibers.

5.3.2. Characterization of PVC-HDPE-DPFs Composites

5.3.2.1. Morphological Investigation of the PVC-HDPE-DPFs Composites

Figure 5.6 (A-G) displayed fracture surfaces of PVC-HDPE blend and various PVC-HDPE-DPFs composites. In Figure 5.6(A), the fracture surface of PVC-HDPE blend is slightly homogeneous, but some cracks are clearly observed between PVC and HDPE, which are attributed to the incompatibility between PVC and HDPE. For PVC-HDPE-UntF composite

CHAPTER 5. APPLICATION 3

shown in Figure 5.6(B), it is obviously observed large fiber breaks, due to the reactive surface of cellulose in DPFs covered by lignin and impurities resulting in weak interfacial adhesion between untreated fiber and matrix [51]. Whereas, interfacial adhesion performs an important role in evaluating the composite mechanical characteristics.

Figure 5.6(C) shows a slightly poor interfacial fiber-matrix bonding with small gaps and pulled out in the PVC-HDPE-AIF composite, due to the presence of a small part of lignin and hemicelluloses on the DPFs surface. Figure 5.6(D, E) appeared SEM micrographs of both PVC-HDPE-SiF and PVC-HDPE-(Al-Si)F composites. It can be seen a better fiber-matrix interfacial adhesion compared with PVC-HDPE-AIF composite because the silane coupling agents have the capability to create chemical bonds as bridges between the DPFs and PVC-HDPE blend matrix [42].

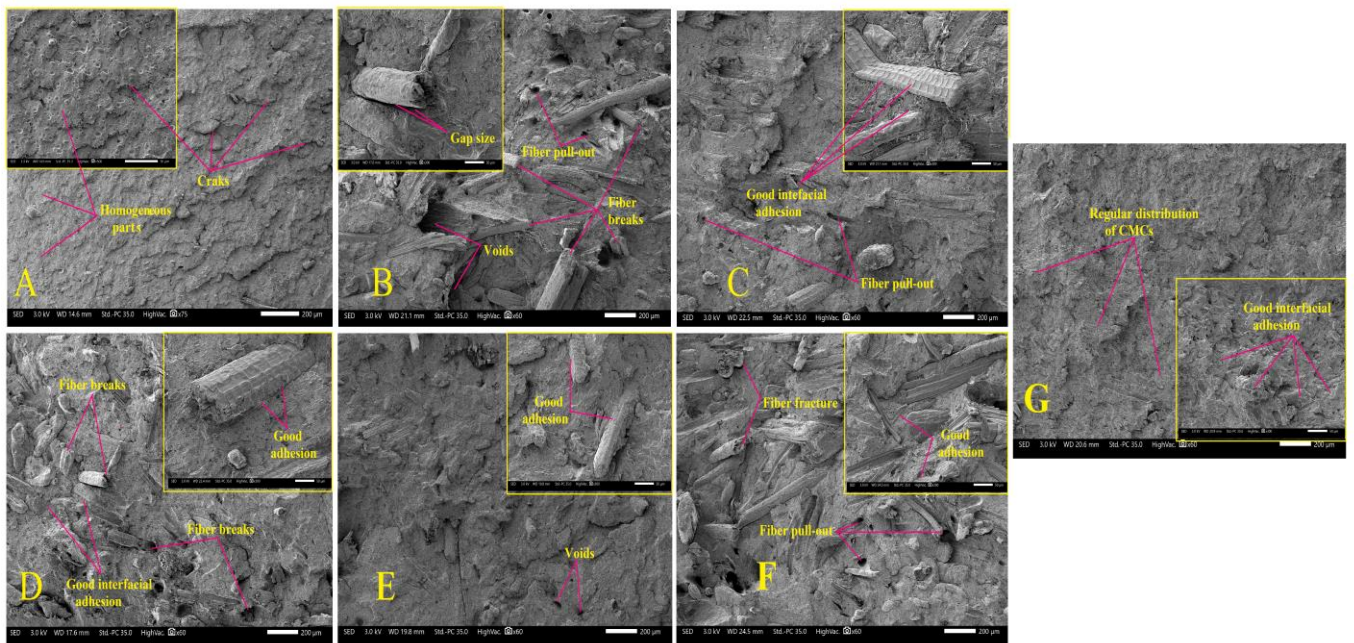


Fig 5.6. Scanning electron micrographs of (A) HDPE-PVC, (B) HDPE-PVC-UntF, (C) HDPE-PVC-AIF (D) HDPE-PVC-SiF (E) HDPE-PVC-(Al-Si) F, (F) HDPE-PVC-NaClO₂F, and (G) HDPE-PVC-HNO₃F.

In addition, the existence of (ethanol/water) mixture in the silane solution, leads to the removal of lignin and part of the hemicelluloses on the DPFs surface resulting in an increase of cellulose concentration in the DPFs. Several other experiments reported that alkali, silane, and even the combination of alkali-silane chemical modifications can strengthen the intrfacial bonding of the fiber-matrix and enhanced the mechanical and physical properties of green composites [52–54].

CHAPTER 5. APPLICATION 3

Moreover, Figure 5.6(F) shows that the delignified fibers treated with NaClO_2 are indeed efficient in increasing the compatibility of PVC-HDPE-DPFs composites.

As a result, compatibility is verified to be enhanced by missing voids in fractured surfaces and reducing gaps or/and pull-out fibers between the CMFs and the PVC-HDPE matrix. In addition, the increase in the surface crystalline region of the cellulose fibers enhances interfacial adhesion in PVC-HDPE-CMFs composites through the elimination of the lignin and hemicellulose components. As shown in Figure 5.6(G), the PVC-HDPE blend matrix reinforced by $(\text{H}_2\text{O}_2 + \text{HNO}_3)\text{F}$ showed a regular distribution of CMCs on the surface of the PVC/HDPE blends, resulting in good interfacial adhesion [55].

5.3.2.2. Thermal Properties of the PVC-HDPE-DPFs Composites

The thermal decomposition behavior of PVC-HDPE matrix, PVC-HDPE-untreated DPFs and PVC-HDPE-DPFs composites with various surface treatments of DPFs are evaluated by thermogravimetric analysis Figure 5.7 (a) and (b). TGA and DTG curves are used for determining the weight loss from 25 °C to 600 °C. The decomposition temperatures with the percentage of char yield were listed in Table 5.5. It was found that PVC-HDPE matrix showed two steps degradations with onset temperature around 250 °C, while their composites showed three steps degradation as displayed in Figure 5.7(a). This was due to the moisture evaporation with a weight loss of around 4 wt.%. The onset temperature (T_{onset}) of PVC-HDPE-DPFs composites increases based on DPFs modifications according to the order PVC-HDPE-UntF < PVC-HDPE-AIF < PVC-HDPE-SiF < PVC-HDPE-(Al-Si)F < PVC-HDPE- NaClO_2F < PVC-HDPE- HNO_3F [56,57]. If we compare the onset temperatures in composites, PVC-HDPE- HNO_3F shows the highest T_{onset} value (285.72°C) and PVC-HDPE-UntF shows the lowest value (247.59°C). The higher T_{onset} in composite implies that CMCs increase the interfacial interactions between the matrix and the cellulose microcrystals.

Moreover, the pyrolysis temperatures $T_{10\%}$, $T_{50\%}$, T_{Max1} and T_{Max2} of PVC-HDPE- HNO_3F composite shift to higher values resulting in an increase of thermal stability. In the temperature range of 260 °C to 300 °C, there was a loss in the mass of PVC-HDPE-DPFs composites, resulting in the release of small amounts of PVC-HDPE blend via PVC dehydrochlorination, HDPE dehydrogenation processes [10], and also thermal degradation of holocellulose compounds. The thermal degradation of composites ranging from 420 °C to 550 °C is much faster than the previous step as a result of complete degradation of polymer matrix and lignin [58].

CHAPTER 5. APPLICATION 3

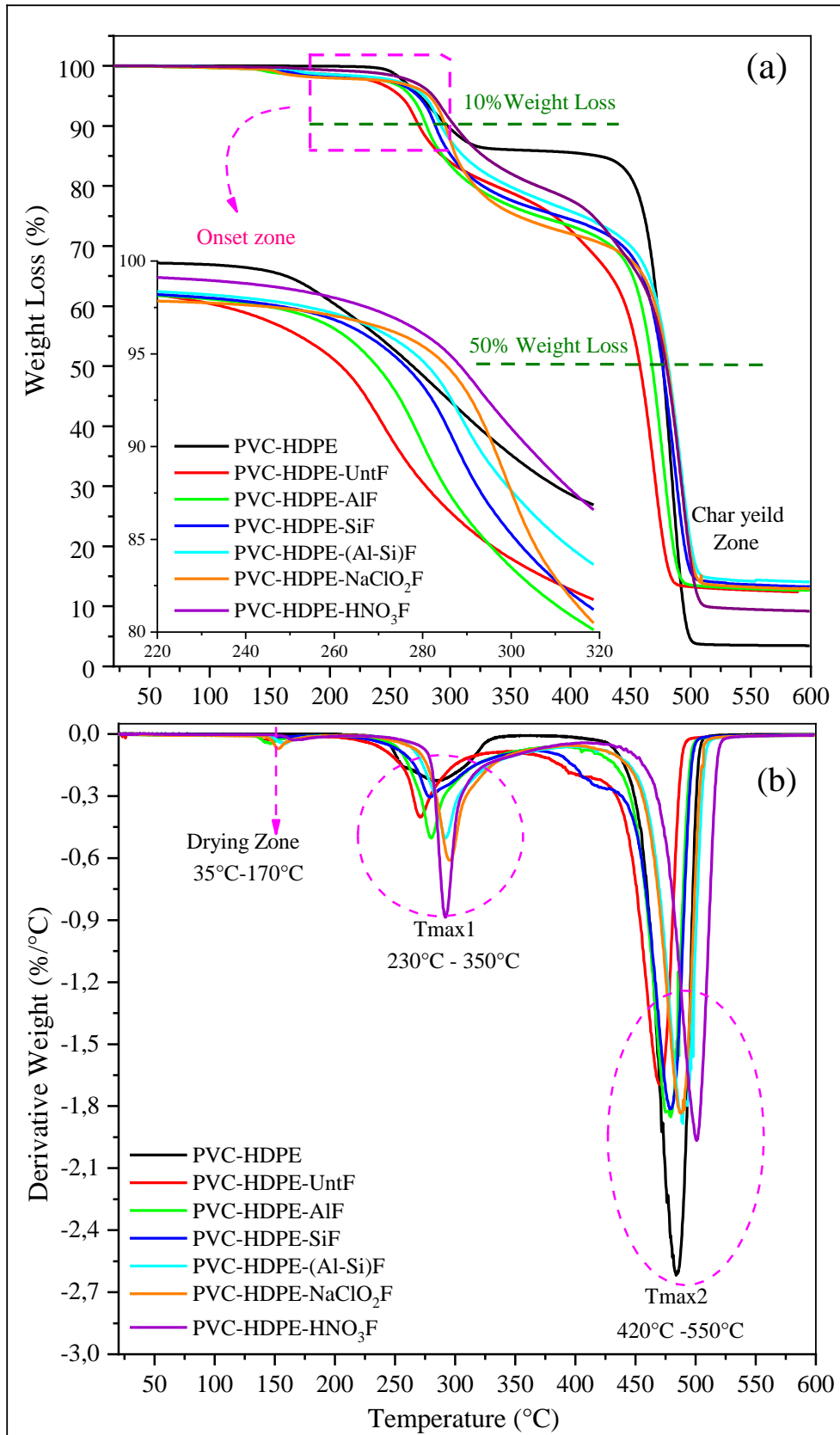


Fig 5.7. Thermal stability of PVC-HDPE and PVC-HDPE-DPFs composites determined by (a) TGA, (b) DTG.

CHAPTER 5. APPLICATION 3

The addition of the DPFs to the matrix increased the composite char yield. The residues were also lower for the PVC-HDPE-HNO₃F composites than for the others because the CMCs had lower residue than the other DPFs fibers.

Table 5.5. Thermal degradation temperatures, T_{onset} (°C), T_{10%}, T_{50%}, T_{MAX1,2}, and % char yield of PVC-HDPE and its composites.

Sample	Decomposition Temperature (°C)					Char Yield (%)
	T _{Onset}	T _{10%}	T _{50%}	T _{MAX1}	T _{MAX2}	
PVC-HDPE	250.14	297.20	475.57	260.82	484.60	03.33
PVC-HDPE-UntF	247.59	274.37	457.63	271.73	468.92	12.44
PVC-HDPE-AIF	269.54	280.89	469.04	278.90	475.44	13.22
PVC-HDPE-SiF	275.73	287.42	477.20	280.89	478.06	12.50
PVC-HDPE - (Al-Si) F	278.42	292.31	482.01	290.89	487.90	12.64
PVC-HDPE-NaClO ₂ F	282.23	295.57	482.10	293.81	488.49	12.84
PVC-HDPE-HNO ₃ F	285.72	303.72	480.64	291.66	500.90	09.04

5.3.2.3. Mechanical Properties of the PVC-HDPE- DPFs Composites

The tensile and flexural properties of the PVC-HDPE blend and PVC-HDPE-DPFs composites with different chemical treatments are shown in Figure 5.8(a,b). It can be observed that tensile and flexural modulus of composites improved owing to different chemical treatments of DPFs surface, while the opposite effect obviously observed for the tensile strength properties compared to PVC-HDPE matrix blend. These two effects were linked to an increase in the hardness of the composites and the low compatibility of the PVC-HDPE polymer blend in the composite samples, respectively.

The tensile and flexural behaviors of PVC-HDPE-DPFs composites increased in the following order: MC2 < MC3 < MC4 < MC5 < MC6 < MC7 (as shown in Table 5.6), this result was due to increasing interfacial interactions between each fiber surface and PVC-HDPE blend. On the other hand, the PVC-HDPE-HNO₃F (MC7) sample showed the highest tensile and flexural values, due to increasing crystalline cellulose concentration of the composite leading to efficient stress transfer [59].

In addition, MC2 sample filled with untreated DPFs showed a decrease in the mechanical behaviors compared with others. This might be due to the low cellulose content of the untreated natural fibers. Moreover, treated DPFs reinforced PVC-HDPE ameliorate and also increase

CHAPTER 5. APPLICATION 3

mechanical properties of composites. These results obtained were similar to those reported by many researchers, who used various treatments fibers reinforced composites [60–62].

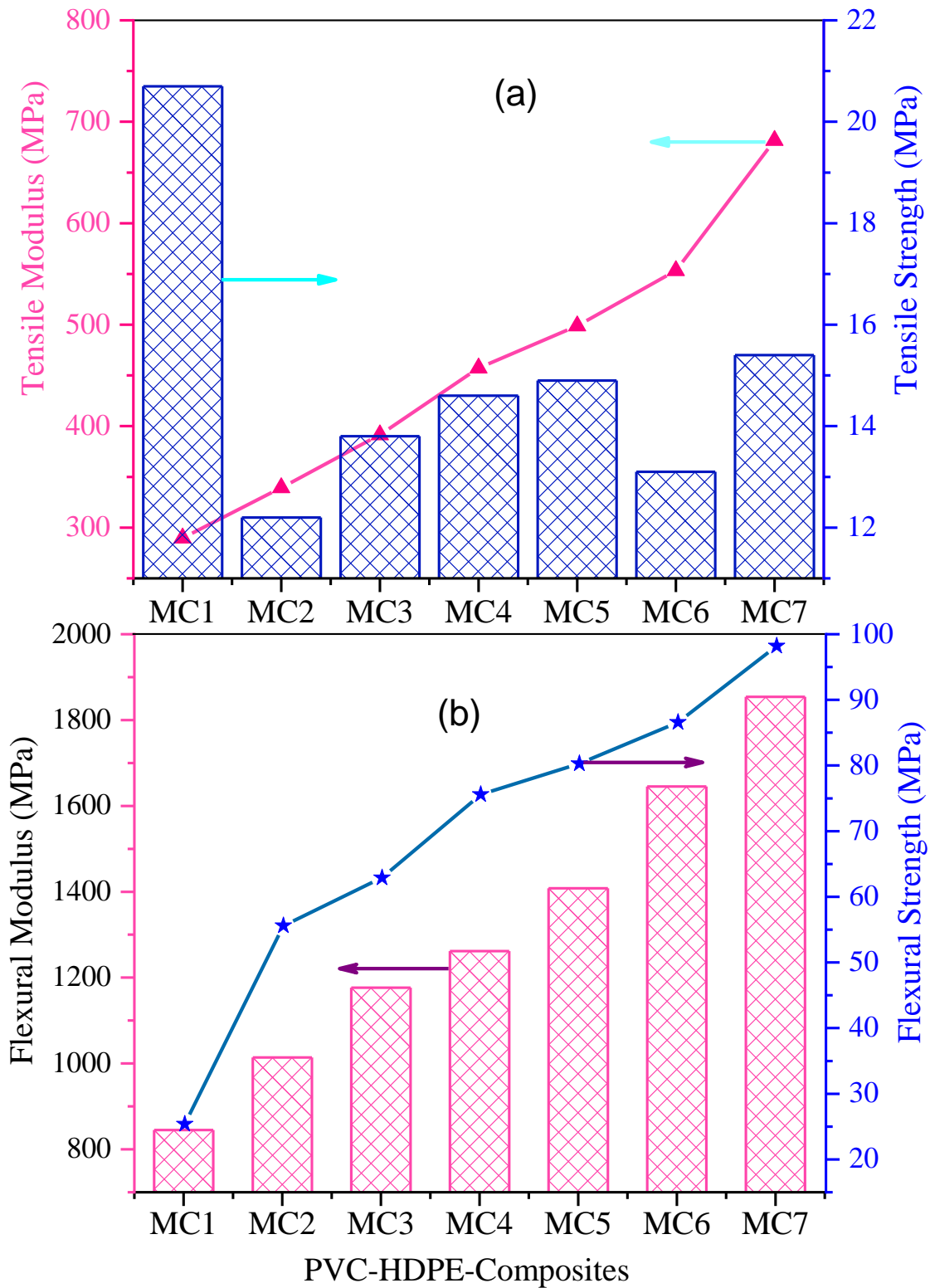


Fig 5.8. (a) Tensile results, (b) Flexural results of PVC-HDPE and PVC-HDPE-DPFs composites.

CHAPTER 5. APPLICATION 3

Table 5.6. Mechanical properties of PVC-HDPE and its composites.

Sample	Tensile results (MPa)		Flexural results (MPa)	
	Tensile Strength	Tensile Modulus	Flexural Strength	Flexural Modulus
MC1	20,73±5,17	289,83±58,34	25,4±19,22	845,01±189,67
MC2	12,22±2,30	339,29±86,54	55,6±10,50	1014,12±201,92
MC3	13,80±1,05	391,43±98,78	62,9±14,45	1176,65±201,09
MC4	14,62±3,25	457,4±100,09	75,6±19,33	1261,58±268,51
MC5	14,91±3,54	498,93±103,87	80,3±16,65	1408,13±358,35
MC6	14,50±2,68	553,29±110,90	86,6±10,23	1645,02±360,21
MC7	15,4±6,21	681,65±107,43	98,2±12,41	1854,29±394,11

5.3.2.4. Rheological Measurements of the PVC-HDPE- DPFs Composites

Clearly, different treatments of DPFs (alkaline, silane, alkaline-silane, bleaching and acid hydrolysis) demonstrate various constituent distribution systems in PVC-HDPE blend, with various adhesion degrees with PVC-HDPE chains. Consequently, investigating the rheological behavior of their composites is interesting [63]. Figures 5. (9-11) provide respectively the complex viscosity (η^*), storage modulus(G') and loss modulus (G'') at different frequencies for PVC-HDPE matrix and PVC-HDPE-DPFs composites before and after fiber surface modifications. From Figure 5.9 the complex viscosity (η^*) for both untreated and treated DPFs have obvious hindering effect on the motion of PVC-HDPE chain [64].

It is also shown that (η^*) ranking of the composites based on the increase of the low-frequency responses is the following: PVC-HDPE-UntF < PVC-HDPE-AIF < PVC-HDPE-SiF < PVC-HDPE-(Al-Si) F < PVC-HDPE-NaClO₂F < PVC-HDPE-HNO₃F. As shown in Figures 5.10 and 5.11 both G' and G'' increase linearly with an increase in frequency due to the presence of Newtonian behavior. However, at low frequency, PVC-HDPE-CMCs shows higher (η^*) (168000Pa.s) and (G') (8130Pa) than others. This is attributed to the better distribution of CMCs in PVC-HDPE matrix system and the solid-like behavior in PVC-HDPE blend filled with 30% of DPFs [65].

CHAPTER 5. APPLICATION 3

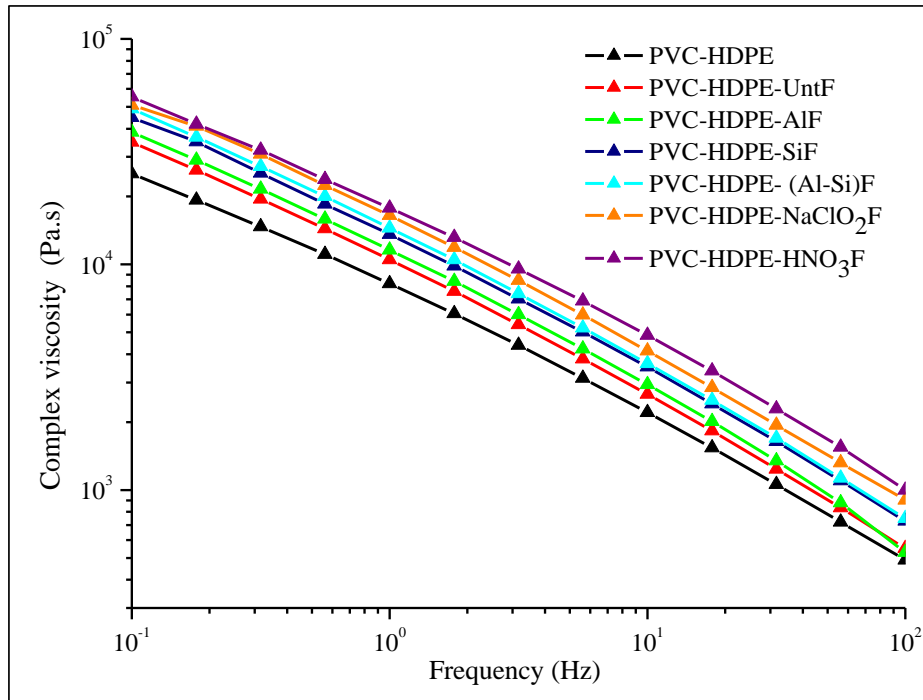


Fig 5.9. Complex viscosity, η^* vs frequency, curves of PVC-HDPE and PVC-HDPE-DPFs composites at 170 °C.

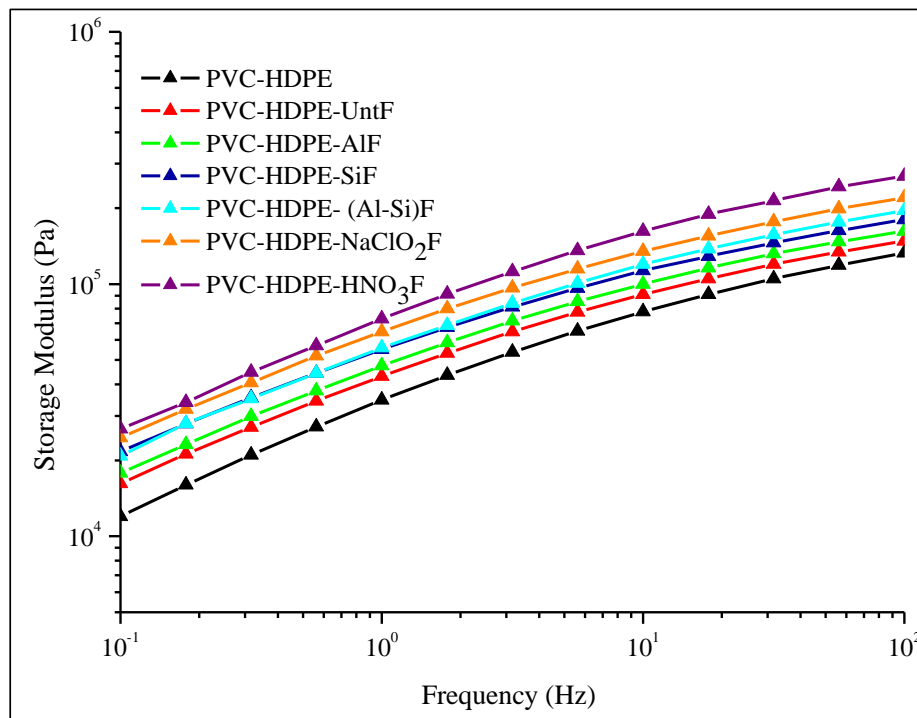


Fig 5.10. Storage moduli G' vs frequency, curves of PVC-HDPE and PVC-HDPE-DPFs composites at 170 °C.

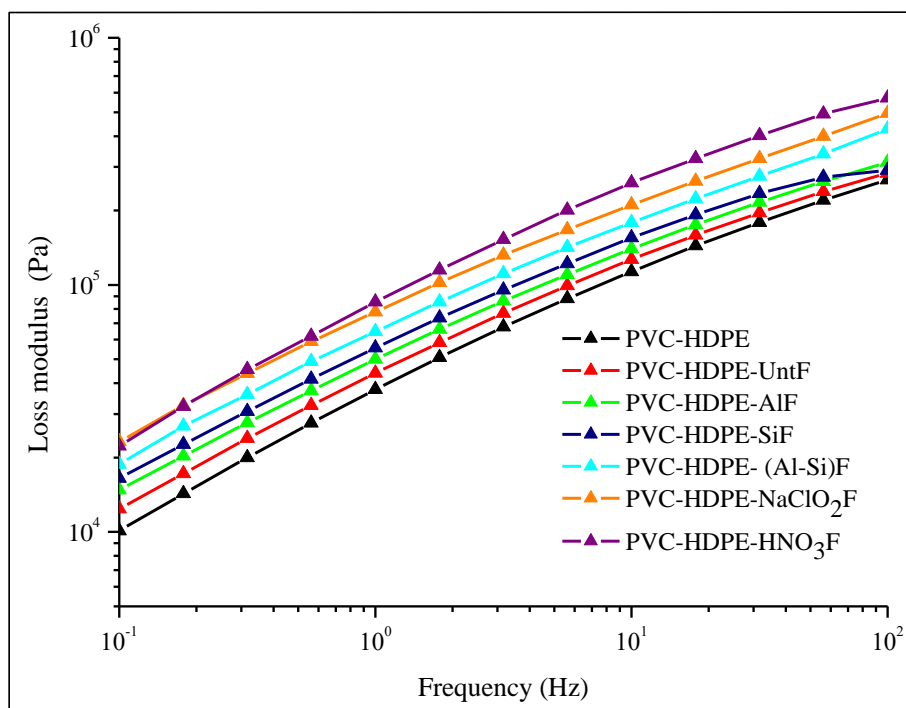


Fig 5.11. Loss moduli G'' vs frequency, curves of PVC-HDPE and PVC-HDPE- DPFs composites at 170 °C.

In addition, CMCs (with High cellulose concentration) exhibited stronger fluid dynamic interactions among DPFs (CMC–matrix interactions) [66] than those at low concentration of cellulose. Similar ‘viscosity behavior’ has also be observed on the polypropylene (PP) based various treated coir [67]. In summary, the CMCs have well distribution attributed to the improved compatibility (good interaction with PVC-HDPE chains) and thus reduce the interactions between DPFs.

5.3.2.5. Dynamic Mechanical Analysis (DMA) of the PVC-HDPE- DPFs Composites

Dynamical mechanical analysis was conducted on PVC-HDPE-DPFs composites to evaluate the storage modulus (E'), Loss modulus (E''), and damping factor ($\tan \delta$), which are related to the dynamic behavior of fiber-reinforced composites [23]. The DMA results of composites are presented in Figure 5.12 (a-c) and table 5.8. As shown in Figure 5.12(a), storage modulus (E') of PVC-HDPE-UntF displayed a positive impact due to the existence of cellulose in the DPFs, but was not as efficient as other modified fibers making significant compatibility with the PVC-HDPE blend after surface modifications.

Storage modulus (E') increased with increasing cellulose concentration of treated fibers, indicating an enhancement in the stiffness of the PVC-HDPE-DPFs composites, thus, then the

CHAPTER 5. APPLICATION 3

storage values were: (PVC-HDPE-UntF: 2997.07 MPa, PVC-HDPE-AIF: 3139.84 MPa, PVC-HDPE-SiF: 3215.91 MPa, PVC-HDPE-(Al-Si) F: 3385.60 MPa, PVC-HDPE-NaClO₂F : 3431.24 MPa, PVC-HDPE-HNO₃F : 3552.95 MPa). It was clearly, that the PVC-HDPE-HNO₃F sample exhibits the highest storage modulus, due to better bonding between hydroxyl groups on cellulose microcrystals and PVC-HDPE blend matrix, and also is due to the development in the part of the cellulose region in DPFs after chemical treatments [68]. From the graph in Figure 5.12(b), the loss modulus of PVC-HDPE-DPFs composites enhances more than a blend of PVC-HDPE attributed to the increase of internal friction, which leads to energy dissipation. In the glassy polymeric domain, there is a small variation in the loss modulus of all composites.

Moreover, the results appear α -relaxation temperature in the range from 45°C to 54°C. Thus, the PVC-HDPE-DPFs samples with various treatments, were recorded the higher values of α -relaxation temperature (T_g from E'') compared to PVC-HDPE-UntF sample, due to the surface of the fiber became more rougher, toothed and etched after the chemical modification and also the removal of the lignin and different residues that protects the surface of the fiber.

In addition, the PVC-HDPE-UntF sample exhibited the maximum loss modulus, due to the high thermal energy dissipation. In addition, the molecular disturbance at the bonding surface between fiber/blend matrix was reduced via the frictional resistance of the interfacial dynamic [69].

Figure 5.12(c) shows the damping factor ($\tan \delta$). It can be observed that the $\tan \delta$ increased with increasing the temperature for all composites, and showed a T_g in the range from 79°C to 97 °C. The PVC-HDPE-DPFs composites with various treatments revealed higher glass temperature values and lower magnitude of the relaxation along compared to the PVC-HDPE-UntF and PVC-HDPE samples [41,70], as summarized in table 5.7.

In addition, it was found that maximum $\tan \delta$ values of PVC-HDPE-AIF, PVC-HDPE-SiF, and PVC-HDPE-(Al-Si) F composites are (0.247, 0.237 and 0.235) respectively, and T_g values of PVC-HDPE-(Al-Si) F, PVC-HDPE-NaClO₂F, and PVC-HDPE-HNO₃F composites are (89.48°C, 93.70°C and 96.91 °C) respectively. For H₂O₂+HNO₃ treated DPFs composite was showed the highest T_g value (96.91 °C) which indicates the better interfacial adhesion in PVC-HDPE-HNO₃F composite, and shows a high limitation of the interfacial mobility in the fiber-matrix interface systems [71].

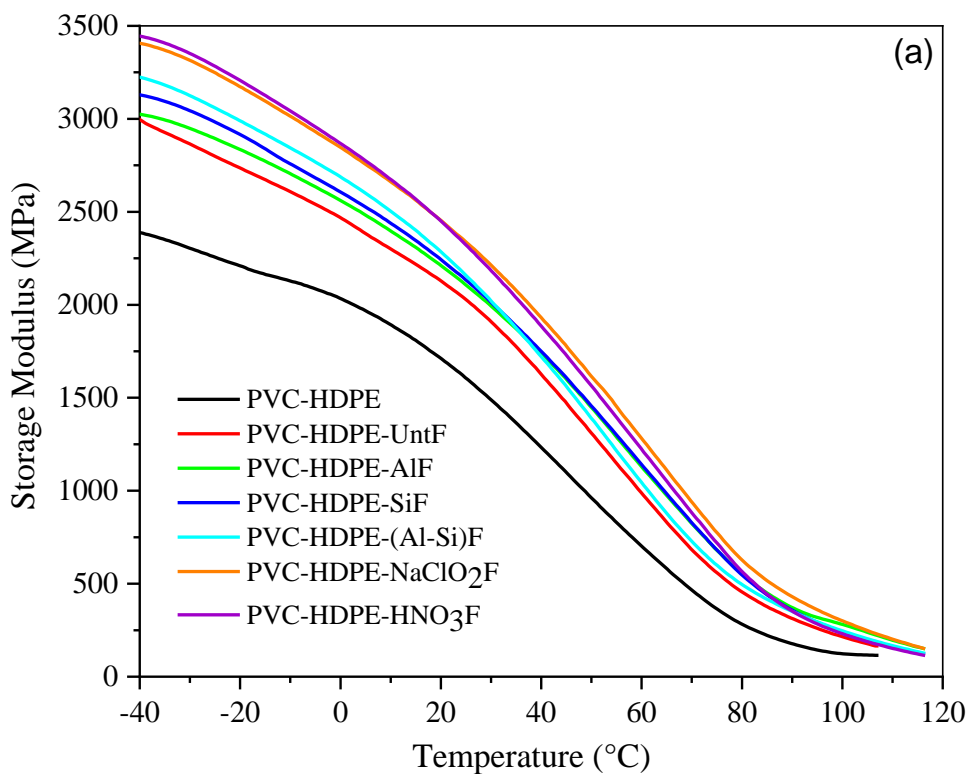


Fig 5.12. (a) Storage modulus (E') curves of PVC-HDPE and PVC-HDPE-DPFs composites as a function of temperature.

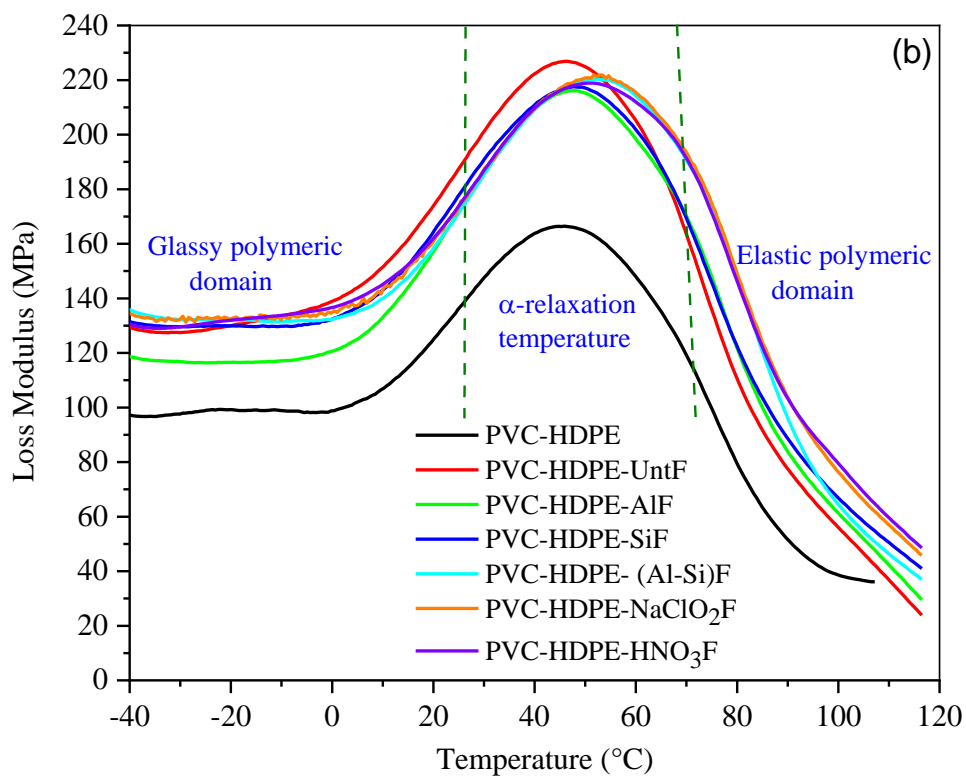


Fig 5.12. (b) Loss modulus (E'') curves of PVC-HDPE and PVC-HDPE-DPFs composites as a function of temperature.

CHAPTER 5. APPLICATION 3

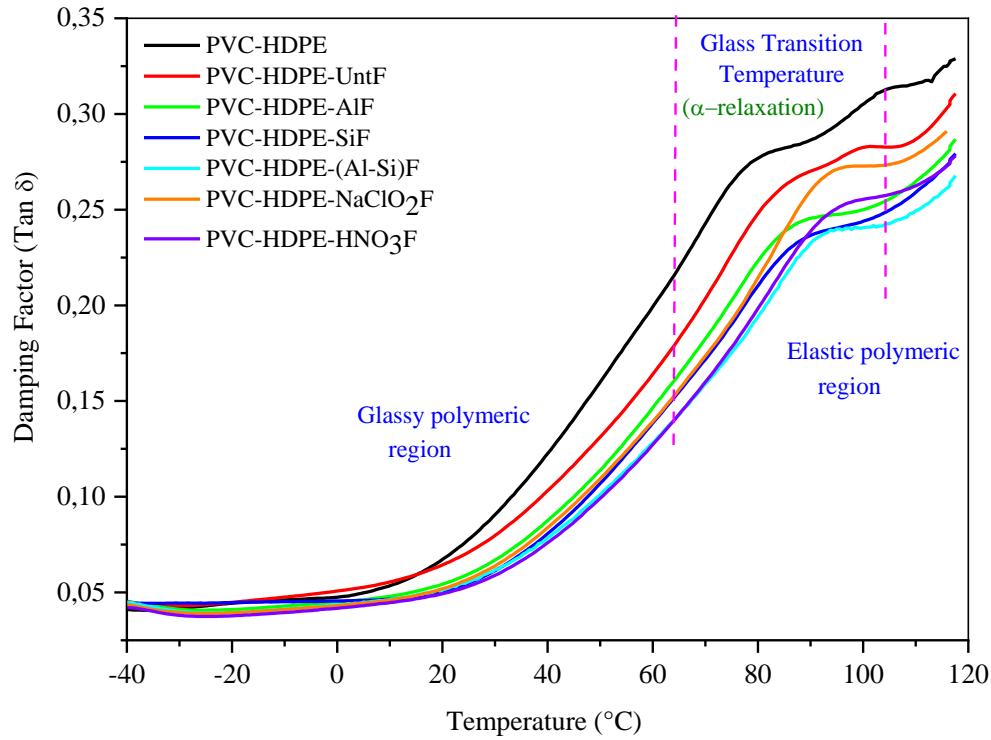


Fig 5.12. (c) Damping factor (Tan δ) curves of PVC-HDPE and PVC-HDPE-DPFs composites as a function of temperature.

Table 5.7. Dynamical mechanical properties of PVC-HDPE and its composites.

Sample	Tg from Tan δ (°C)	Tg from E'' (°C)	Peak of Tan δ (MPa)	Peak of E'' (MPa)	Peak of E' (MPa)
PVC-HDPE	78.81	44.91	0.278	166.76	2002.34
PVC-HDPE -UntF	83.65	45.50	0.266	220.19	2997.07
PVC-HDPE -AlF	86.23	47.71	0.247	215.63	3139.84
PVC-HDPE -SiF	89.48	50.24	0.237	217.46	3215.91
PVC-HDPE- (Al-Si)F	90.33	51.66	0.235	221.05	3385.60
PVC-HDPE -NaClO ₂ F	93.70	52.76	0.270	222.02	3431.24
PVC-HDPE -HNO ₃ F	96.91	53.59	0.253	218.37	3552.95

5.3.2.6. Water Uptake behavior of the PVC-HDPE- DPFs Composites

The effects of water uptake as a function of immersion time (t) for each sample soaked in seawater at room temperature (23°C) for 40 days are shown in Figure 5.13. One of the key drawbacks of fiber materials is its high hydrophilicity due to its hydrophilic hydroxyl groups, which make it polar and thus susceptible to water absorption. In addition, the high salinity of sea water means in high concentration metal ions, such as Na⁺, K⁺, Ca⁺⁺ and Mg⁺⁺ which allows

CHAPTER 5. APPLICATION 3

this latter to sediment on fiber surface leading to higher water absorption (fibers swelling) [72]. Firstly, it can clearly observe that, PVC-HDPE polymer blend seems lesser water uptake (<0.5 %) which revealed their hydrophobic nature. Additionally, it was shown in the first stage of the curves that the percentage of water uptake for both untreated and treated DPFs composites with various treatments increases rapidly from first day to fifteen days (24 hours *15= 360 hours) and then increases slowly until saturation point with immersion time [73].

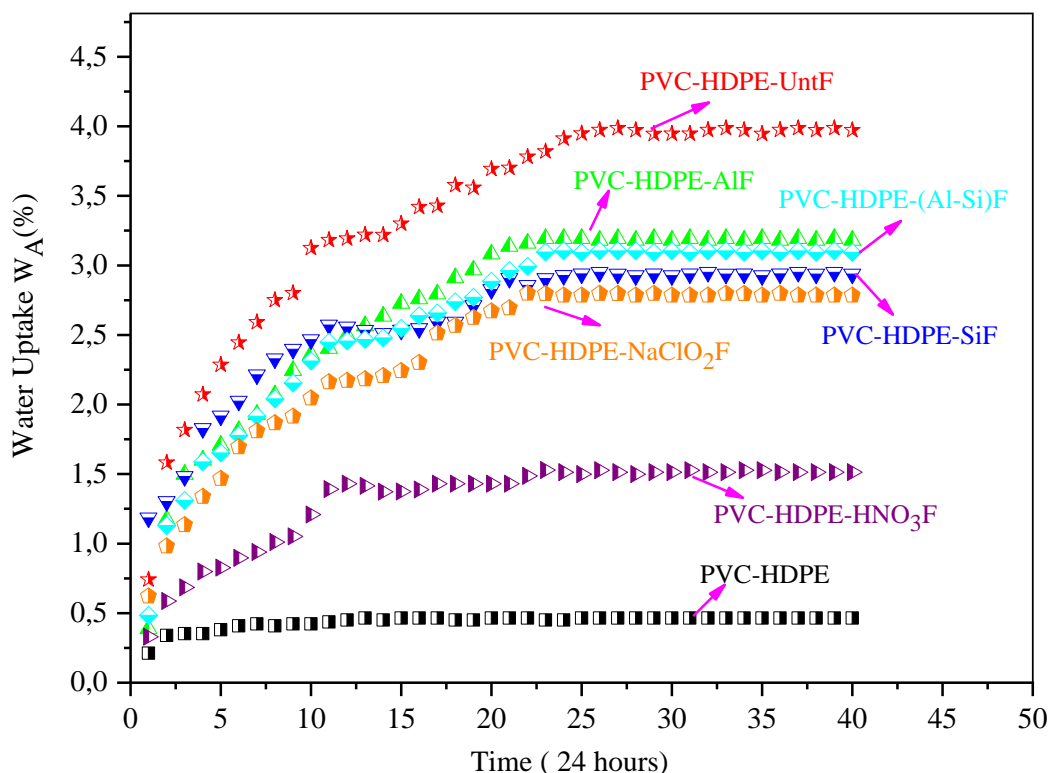


Fig 5.13. Water uptake properties of pure blend matrix and DPFs reinforced composites with and without various treatments.

Moreover, the highest water absorption is showed for untreated DPFs composite at (3.97 %), due to hydroxyl and oxygen groups of lignin and hemicelluloses which are responsible for absorbing water molecules [74]. The water uptake of the PVC-HDPE-AIF (3.18 %), PVC-HDPE-(Al-Si)F (3.09 %), PVC-HDPE-SiF (2.93 %), and PVC-HDPE-NaClO₂F (2.78 %), composites significantly decreased by various treatments, this is due to reduced hydrophilic nature of the DPFs resulting good interfacial adhesion between fiber and matrix.

Furthermore, addition of CMCs to the PVC-HDPE reduced the water absorption ability at 1.5 %. However, the PVC-HDPE-CMCs composite treated with H₂O₂+HNO₃ exhibits the lowest water uptake due to higher degree of crystallinity and hydrophilic nature of CMCs [75]. Moreover, the mechanical behavior and T_g of PVC-HDPE-CMCs are improved by the addition

CHAPTER 5. APPLICATION 3

of CMCs particles, which decreases the mobility of the polymer chains, thus decreasing the absorption of moisture.

CHAPTER 5. APPLICATION 3

5.4. CONCLUSIONS

The opportunity for the use of waste lignocellulosic fibers as reinforcement materials is focused on the interfacial bonding between the fibers and the polymeric matrix to design ecofriendly composites. For this cause, the chemical treatment of DPFs is important to enhancing the performance characteristics of the PVC-HDPE-DPFs composites. The alkali, silane, combined alkali-silane treated DPFs composites improved thermal, mechanical, mechanical dynamical and rheological properties compared with raw DPFs composite, whereas, the bleached and hydrolyzed DPFs composites exhibited the optimum properties. In addition, PVC-HDPE-CMCs composite had the lower water uptake rate. The findings from this study are very helpful in selecting type of the fiber surface treatment. Further enhancement of compatibility between fiber and matrix was then obtained by the addition of CMCs to PVC-HDPE blend composites, which serve as a new category of eco-friendly materials. In view of their efficiency and the use of PVC-HDPE waste as matrix, it can be revealed that the development of such composites can be an attractive and useful way for development of PVC-HDPE-DPFs composite applications which according to their high industrial performance in construction materials.

ACKNOWLEDGEMENTS

The authors are grateful to the staff of plastic laboratory of (Entreprise des Industries du Câble ENICAB), Biskra, Algeria, for supplying the polymer materials and their additives of this work, the authors are also thankful acknowledgments to Dr Françoise PERESSE for supporting this experimental work by the characterization methods.

CHAPTER 5. APPLICATION 3

REFERENCES

1. Zadeh, K. M., Ponnamma, D. & Al Ali Al-Maadeed, M. Date palm fibre filled recycled ternary polymer blend composites with enhanced flame retardancy. *Polym. Test.* 61, 341–348 (2017).
2. Boubekour, B., Belhaneche-Bensemra, N. & Massardier, V. Low-Density Polyethylene/Poly(Lactic Acid) Blends Reinforced by Waste Wood Flour. *J. Vinyl Addit. Technol.* 1–9 (2020).
3. El Achaby, M., Kassab, Z., Barakat, A. & Aboulkas, A. Alfa fibers as viable sustainable source for cellulose nanocrystals extraction: Application for improving the tensile properties of biopolymer nanocomposite films. *Ind. Crops Prod.* 112, 499–510 (2018).
4. Chaudhary, V. & Ahmad, F. A review on plant fiber reinforced thermoset polymers for structural and frictional composites. *Polym. Test.* 91, 106792 (2020).
5. Yu, J., Sun, L., Ma, C., Qiao, Y. & Yao, H. Thermal degradation of PVC: A review. *Waste Manag.* 48, 300–314 (2016).
6. Liu, Y., Zhou, C., Li, F., Liu, H. & Yang, J. Stocks and flows of polyvinyl chloride (PVC) in China: 1980-2050. *Resour. Conserv. Recycl.* 154, (2020).
7. Korkusuz & Tüzüm Demir, A. P. Evaluation of the thermal stabilization behavior of hydrotalcite against organic stabilizers for plasticized PVC films. *Polym. Bull.* 77, 4805–4831 (2020).
8. Wu, J. *et al.* TG/FTIR analysis on co-pyrolysis behavior of PE, PVC and PS. *Waste Manag.* 34, 676–682 (2014).
9. Maou, S., Meghezzi, A., Nebbache, N. & Meftah, Y. Mechanical, morphological, and thermal properties of poly(vinyl chloride)/low-density polyethylene composites filled with date palm leaf fiber. *J. Vinyl Addit. Technol.* 25, (2019).
10. Bittencourt, P. R. S. & Scremin, F. R. Evolved Gas Analysis of PE:PVC Systems Thermodegradation Under Inert and Oxidizing Atmosphere. *J. Polym. Environ.* 27, 612–617 (2019).

CHAPTER 5. APPLICATION 3

11. Almi, K., Benchabane, A., Lakel, S. & Kriker, A. Potential utilization of date palm wood as composite reinforcement. *J. Reinf. Plast. Compos.* 34, 1231–1240 (2015).
12. Alotaibi, M. D. *et al.* Characterization of natural fiber obtained from different parts of date palm tree (*Phoenix dactylifera L.*). *Int. J. Biol. Macromol.* 135, 69–76 (2019).
13. Chikhi, M. Young's modulus and thermophysical performances of bio-sourced materials based on date palm fibers. *Energy Build.* 129, 589–597 (2016).
14. Meftah, Y. *et al.* Influence of Alkali Treatment and Dune Sand Content on the Properties of Date Palm Fiber Reinforced Unsaturated Polyester Hybrid Composites. *Rev. des Compos. des matériaux avancés* 30, 161–167 (2020).
15. Bendahou, A., Habibi, Y., Kaddami, H. & Dufresne, A. Physico-chemical characterization of palm from *Phoenix Dactylifera-L*, preparation of cellulose whiskers and natural rubber-based nanocomposites. *J. Biobased Mater. Bioenergy* 3, 81–90 (2009).
16. Al-Oqla, F. M. & Sapuan, S. M. Natural fiber reinforced polymer composites in industrial applications: Feasibility of date palm fibers for sustainable automotive industry. *J. Clean. Prod.* 66, 347–354 (2014).
17. Awad, S., Zhou, Y., Katsou, E., Li, Y. & Fan, M. *A Critical Review on Date Palm Tree (Phoenix dactylifera L.) Fibres and Their Uses in Bio-composites. Waste and Biomass Valorization* (Springer Netherlands, 2020). doi:10.1007/s12649-020-01105-2.
18. Noorunnisa Khanam, P. & AlMaadeed, M. A. Improvement of ternary recycled polymer blend reinforced with date palm fibre. *Mater. Des.* 60, 532–539 (2014).
19. Kharrat, F. *et al.* Minimally processed date palm (*Phoenix dactylifera L.*) leaves as natural fillers and processing aids in poly(lactic acid) composites designed for the extrusion film blowing of thin packages. *Ind. Crops Prod.* 154, 112637 (2020).
20. Mahdavi, S., Kermanian, H. & Varshoei, A. Comparison of mechanical properties of date palm fiber- polyethylene composite. *BioResources* 5, 2391–2403 (2010).
21. Oushabi, A. *et al.* The effect of alkali treatment on mechanical, morphological and

CHAPTER 5. APPLICATION 3

- thermal properties of date palm fibers (DPFs): Study of the interface of DPF–Polyurethane composite. *South African J. Chem. Eng.* 23, 116–123 (2017).
22. Prachayawarakorn, J., Khunsumled, S., Thongpin, C., Kositchaiyong, A. & Sombatsompop, N. Effects of silane and MAPE coupling agents on the properties and interfacial adhesion of wood-filled PVC/LDPE blend. *J. Appl. Polym. Sci.* 108, 3523–3530 (2008).
 23. De Fátima V. Marques, M., Melo, R. P., Da S. Araujo, R., Do N. Lunz, J. & De O. Aguiar, V. Improvement of mechanical properties of natural fiber-polypropylene composites using successive alkaline treatments. *J. Appl. Polym. Sci.* 132, 1–12 (2015).
 24. Amel, B. A., Paridah, M. T., Sudin, R., Anwar, U. M. K. & Hussein, A. S. Effect of fiber extraction methods on some properties of kenaf bast fiber. *Ind. Crops Prod.* 46, 117–123 (2013).
 25. El Achaby, M., Kassab, Z., Barakat, A. & Aboukhas, A. Alfa fibers as viable sustainable source for cellulose nanocrystals extraction: Application for improving the tensile properties of biopolymer nanocomposite films. *Ind. Crops Prod.* 112, 499–510 (2018).
 26. Alshabanat, M. Morphological, thermal, and biodegradation properties of LLDPE/treated date palm waste composite buried in a soil environment. *J. Saudi Chem. Soc.* 23, 355–364 (2019).
 27. Djoudi, T., Hecini, M., Scida, D., Djebbloun, Y. & Djemai, H. Physico-Mechanical Characterization of Composite Materials Based on Date Palm Tree Fibers. *J. Nat. Fibers* 0, 1–14 (2019).
 28. Wazzan, A. A. The Effect of Surface Treatment on the Strength and Adhesion Characteristics of Phoenix dactylifera-L (Date Palm) Fibers. 4037, (2007).
 29. Bendahou, A. *et al.* Short palm tree fibers poly olefin composites: Effect of filler content and coupling agent on physical properties. *Macromol. Mater. Eng.* 293, 140–148 (2008).
 30. Ghori, W., Saba, N., Jawaid, M. & Asim, M. A review on date palm (phoenix dactylifera) fibers and its polymer composites. *IOP Conf. Ser. Mater. Sci. Eng.* 368, (2018).

CHAPTER 5. APPLICATION 3

31. Tran, T. P. T., Bénézet, J. C. & Bergeret, A. Rice and Einkorn wheat husks reinforced poly(lactic acid) (PLA) biocomposites: Effects of alkaline and silane surface treatments of husks. *Ind. Crops Prod.* 58, 111–124 (2014).
32. Lassoued, M., Mnasri, T., Hidouri, A. & Ben Younes, R. Thermomechanical behavior of Tunisian palm fibers before and after alkalization. *Constr. Build. Mater.* 170, 121–128 (2018).
33. Oushabi, A. *et al.* Improvement of the interface bonding between date palm fibers and polymeric matrices using alkali-silane treatments. *Int. J. Ind. Chem.* 9, 335–343 (2018).
34. Odera, R. S., Onukwuli, O. D. & Aigbodion, V. S. Effect of alkali-silane chemical treatment on the tensile properties of raffia palm fibre. *Aust. J. Multi-Disciplinary Eng.* 15, 91–99 (2019).
35. Puglia, D. *et al.* Effect of alkali and silane treatments on mechanical and thermal behavior of Phormium tenax fibers. *Fibers Polym.* 14, 423–427 (2013).
36. Boufi, S. & Chaker, A. Easy production of cellulose nanofibrils from corn stalk by a conventional high speed blender. *Ind. Crops Prod.* 93, 39–47 (2016).
37. Cao, Y. *et al.* Combined bleaching and hydrolysis for isolation of cellulose nanofibrils from waste sackcloth. *Carbohydr. Polym.* 131, 152–158 (2015).
38. Patel, V. K. & Dhanola, A. Influence of CaCO₃, Al₂O₃, and TiO₂ microfillers on physico-mechanical properties of Luffa cylindrica/polyester composites. *Eng. Sci. Technol. an Int. J.* 19, 676–683 (2016).
39. Johar, N., Ahmad, I. & Dufresne, A. Extraction, preparation and characterization of cellulose fibres and nanocrystals from rice husk. *Ind. Crops Prod.* 37, 93–99 (2012).
40. Alila, S., Besbes, I., Vilar, M. R., Mutjé, P. & Boufi, S. Non-woody plants as raw materials for production of microfibrillated cellulose (MFC): A comparative study. *Ind. Crops Prod.* 41, 250–259 (2013).
41. Gharbi, A., Hassen, R. B. & Boufi, S. Composite materials from unsaturated polyester resin and olive nuts residue: The effect of silane treatment. *Ind. Crops Prod.* 62, 491–

CHAPTER 5. APPLICATION 3

- 498 (2014).
42. Liu, Y. *et al.* Characterization of silane treated and untreated natural cellulosic fibre from corn stalk waste as potential reinforcement in polymer composites. *Carbohydr. Polym.* 218, 179–187 (2019).
 43. Pelissari, F. M., Jose, P. & Menegalli, F. C. Isolation and characterization of cellulose nanofibers from banana peels. 417–432 (2014) doi:10.1007/s10570-013-0138-6.
 44. Uma Maheswari, C., Obi Reddy, K., Muzenda, E., Guduri, B. R. & Varada Rajulu, A. Extraction and characterization of cellulose microfibrils from agricultural residue - *Cocos nucifera* L. *Biomass and Bioenergy* 46, 555–563 (2012).
 45. Reddy, K. O. *et al.* Extraction and characterization of cellulose single fibers from native african napier grass. *Carbohydr. Polym.* 188, 85–91 (2018).
 46. Morán, J. I., Alvarez, V. A., Cyras, V. P. & Vázquez, A. Extraction of cellulose and preparation of nanocellulose from sisal fibers. *Cellulose* 15, 149–159 (2008).
 47. Zhou, F., Cheng, G. & Jiang, B. Effect of silane treatment on microstructure of sisal fibers. *Appl. Surf. Sci.* 292, 806–812 (2014).
 48. Kabir, M. M., Wang, H., Lau, K. T. & Cardona, F. Effects of chemical treatments on hemp fibre structure. *Appl. Surf. Sci.* 276, 13–23 (2013).
 49. Al-Maharma, A. & Al-Huniti, N. Critical Review of the Parameters Affecting the Effectiveness of Moisture Absorption Treatments Used for Natural Composites. *J. Compos. Sci.* 3, 27 (2019).
 50. Nuruddin, M., Tcherbi-Narteh, A., Hosur, M. & Jeelani, S. Effect of chemical treatments on morphology, crystalline and thermal properties of kenaf fiber. *CAMX 2014 - Compos. Adv. Mater. Expo Comb. Strength. Unsurpassed Innov.* (2014).
 51. Atiqah, A., Jawaid, M., Ishak, M. R. & Sapuan, S. M. Effect of Alkali and Silane Treatments on Mechanical and Interfacial Bonding Strength of Sugar Palm Fibers with Thermoplastic Polyurethane. *J. Nat. Fibers* 15, 251–261 (2018).

CHAPTER 5. APPLICATION 3

52. Singh, T. *et al.* Fabrication of waste bagasse fiber-reinforced epoxy composites: Study of physical, mechanical, and erosion properties. *Polym. Compos.* 40, 3777–3786 (2019).
53. Surya Rajan, B., Balaji, M. A. S. & Saravanakumar, S. S. Effect of chemical treatment and fiber loading on physico-mechanical properties of *Prosopis juliflora* fiber reinforced hybrid friction composite. *Mater. Res. Express* 6, (2019).
54. Sgriccia, N., Hawley, M. C. & Misra, M. Characterization of natural fiber surfaces and natural fiber composites. *Compos. Part A Appl. Sci. Manuf.* 39, 1632–1637 (2008).
55. Bhasney, S. M., Mondal, K., Kumar, A. & Katiyar, V. Effect of microcrystalline cellulose [MCC] fibres on the morphological and crystalline behaviour of high density polyethylene [HDPE]/ polylactic acid [PLA] blends. *Compos. Sci. Technol.* 187, 107941 (2020).
56. Yu, T., Ren, J., Li, S., Yuan, H. & Li, Y. Effect of fiber surface-treatments on the properties of poly(lactic acid)/ramie composites. *Compos. Part A Appl. Sci. Manuf.* 41, 499–505 (2010).
57. Asim, M., Jawaid, M., Abdan, K. & Ishak, M. R. Effect of Alkali and Silane Treatments on Mechanical and Fibre-matrix Bond Strength of Kenaf and Pineapple Leaf Fibres. *J. Bionic Eng.* 13, 426–435 (2016).
58. Omid, N., Sujan, D., Teh, J. Y., Willey, Y. H. L. & Ian, J. D. Influence of alkali treatment and nanoclay content on the properties of rice husk filled polyester composites. *Mater. Sci. Forum* 882, 89–100 (2017).
59. Šturcová, A., Davies, G. R. & Eichhorn, S. J. Elastic modulus and stress-transfer properties of tunicate cellulose whiskers. *Biomacromolecules* 6, 1055–1061 (2005).
60. Soatthiyanon, N., Aumnate, C. & Srikulkit, K. Rheological, tensile, and thermal properties of poly(butylene succinate) composites filled with two types of cellulose (kenaf cellulose fiber and commercial cellulose). *Polym. Compos.* 41, 2777–2791 (2020).
61. Ku, H., Wang, H., Pattarachaiyakoop, N. & Trada, M. A review on the tensile properties of natural fiber reinforced polymer composites. *Compos. Part B Eng.* 42, 856–873

CHAPTER 5. APPLICATION 3

- (2011).
62. Arrakhiz, F. Z. *et al.* Mechanical properties of high density polyethylene reinforced with chemically modified coir fibers: Impact of chemical treatments. *Mater. Des.* 37, 379–383 (2012).
 63. Dehouche, N., Idres, C., Kaci, M., Zembouai, I. & Bruzard, S. Effects of various surface treatments on Aloe Vera fibers used as reinforcement in poly(3-hydroxybutyrate-co-3-hydroxyhexanoate) (PHBHHx) biocomposites. *Polym. Degrad. Stab.* 175, (2020).
 64. Nayak, S. & Mohanty, J. R. Study of Mechanical, Thermal, and Rheological Properties of Areca Fiber-Reinforced Polyvinyl Alcohol Composite. *J. Nat. Fibers* 16, 688–701 (2019).
 65. Zhu, X., Kong, M., Lv, Y., Huang, Y. & Li, G. Selective distribution of nanoparticles in immiscible blends : Effects on the morphology evolution and rheology in quiescent annealing , shear and extensional flow. 1357, (2020).
 66. Ying, Z. *et al.* Rheological and mechanical properties of polylactide nanocomposites reinforced with the cellulose nanofibers with various surface treatments. *Cellulose* 25, 3955–3971 (2018).
 67. Raji, M., Essabir, H., Bouhfid, R. & El Kacem Qaiss, A. Impact of chemical treatment and the manufacturing process on mechanical, thermal, and rheological properties of natural fibers-based composites. *Handb. Compos. from Renew. Mater.* 1–8, 225–252 (2017).
 68. Kim, S. H. *et al.* Rheological and mechanical properties of polypropylene composites containing microfibrillated cellulose (MFC) with improved compatibility through surface silylation. *Cellulose* 26, 1085–1097 (2019).
 69. Goriparthi, B. K., Suman, K. N. S. & Mohan, N. Composites : Part A Effect of fiber surface treatments on mechanical and abrasive wear performance of polylactide / jute composites. *Compos. Part A* 43, 1800–1808 (2012).
 70. Negawo, T. A. *et al.* Mechanical, morphological, structural and dynamic mechanical properties of alkali treated Ensete stem fibers reinforced unsaturated polyester

CHAPTER 5. APPLICATION 3

- composites. *Compos. Struct.* 207, 589–597 (2019).
71. Zhang, Q. *et al.* Improvement on the properties of microcrystalline cellulose/polylactic acid composites by using activated biochar. *J. Clean. Prod.* 252, 119898 (2020).
 72. Kazemi Najafi, S. & Younesi Kordkheili, H. Effect of sea water on water absorption and flexural properties of wood-polypropylene composites. *Eur. J. Wood Wood Prod.* 69, 553–556 (2011).
 73. Nayak, S. & Mohanty, J. R. Influence of chemical treatment on tensile strength, water absorption, surface morphology, and thermal analysis of areca sheath fibers. *J. Nat. Fibers* 16, 589–599 (2019).
 74. Hamidon, M. H., Sultan, M. T. H., Ariffin, A. H. & Shah, A. U. M. Effects of fibre treatment on mechanical properties of kenaf fibre reinforced composites: A review. *J. Mater. Res. Technol.* 8, 3327–3337 (2019).
 75. Rico, M., Rodríguez-Llamazares, S., Barral, L., Bouza, R. & Montero, B. Processing and characterization of polyols plasticized-starch reinforced with microcrystalline cellulose. *Carbohydr. Polym.* 149, 83–93 (2016).